

THE USE OF THE ELECTROMAGNETIC INDUCTION METHOD
ON ENVIRONMENTAL PROBLEMS IN NEW MEXICO

INDEPENDENT STUDY
BY CHRISTOPHER DOMINICK GRANDE
NEW MEXICO INSTITUTE OF MINING AND TECHNOLOGY
GEOSCIENCE DEPARTMENT
SUBMITTED FEBRUARY 14, 1995

ACKNOWLEDGEMENTS

I would like to thank the following people for their involvement with my independent study:

Jan Hendrickx, Ph D. for his patience, mentorship, research efforts and support; Peter Mozley, Ph D. for his academic advisement and scholarly input; James Smoake, Ph D. for his advisement and confidence; David Johnson, Ph D. for career direction and moral support; Robert Bretz, Ph D. who supported part of my research efforts; Anton Budding, Ph D. provided field assistance for the fissure measurements as well as research input; Bill Haneberg, Ph D. for his academic and research advisement.

Victor Pujals, P.E. for his strong support for me to finish this project; Mary Andleman for her friendship, understanding, technical editing and management skills.

Michael Yao, M.S., Ph D. candidate, provided me with friendship, research advisement, and academic assistance. Geoscience and Hydrology secretaries which provided administrative and moral support. I am especially grateful to my family (**Anna Grande, Joseph Grande and Glenn Grande**) for their patience, understanding and unconditional support. Without my family's support I would not have completed this independent study. Lastly, to someone who is dear to my heart **Malissa Weimer**, I would not have been able to complete my Master's degree. Malissa was understanding, loving, and gave unconditional support.

Table of Contents

<u>Section</u>	<u>Page</u>
ABSTRACT	i
I. INTRODUCTION	1
II. ELECTROMAGNETIC INDUCTION METHOD	5
III. CASE STUDY 1: DETECTION OF SALINE BRINES FROM EVAPORATION PITS	7
1. INTRODUCTION	7
2. SITE DESCRIPTIONS AND EM SURVEYS	9
A. EM Surveys	10
B. Geology of the Site	11
3. RESULTS AND DISCUSSION	11
4. CONCLUSIONS	13
IV. CASE STUDY 2: THE USE OF THE EM METHOD IN DETECTING THE SAN MARCIAL FISSURE	14
1. INTRODUCTION	14
2. SITE DESCRIPTIONS AND EM SURVEYS	16
A. EM Surveys	16
B. Geology of the Site	18
3. RESULTS AND DISCUSSION	19
A. EM Instrument Coils Parallel to Fissure Distance Versus Conductivity Plots	20
B. EM-38 and EM-31 Instruments with Coils Perpendicular to the Fissure, Distance Versus Conductivity Plots	21
C. SAS Split Window Boundary Program with the EM-38 and EM-31 Instruments Parallel to the Fissure	21
D. Results of Split Window Program with EM Instrument Coils Perpendicular to the Fissure	22
4. CONCLUSIONS	22

V. CASE STUDY 3: THE USE OF THE EM METHOD IN EVALUATING MINE	
SPOILS	26
1. INTRODUCTION	26
2. SITE DESCRIPTION AND EM SURVEYS	27
A. EM Surveys	27
B. Geology of the Site	28
C. Soil Sampling and Analysis	29
3. RESULTS AND DISCUSSION	30
A. Results and Discussion of Regression Models	31
4. CONCLUSIONS	32
Summary and Recommendations	33
REFERENCES	34
APPENDICES	
APPENDIX A: TABLES	
APPENDIX B: FIGURES	

ABSTRACT

Three case studies were performed on environmental problems in New Mexico. The studies consisted of using the Electromagnetic (EM) Induction method to detect brine contamination and a fissure. It was also used in the reclamation process to determine the salinity of mine spoils .

In the first case study, three electromagnetic surveys were performed and soil samples were analyzed at different depths for salinity. The EM Induction Method conclusively determined the brine depths of penetration and lateral spread.

In the second case study, seven surveys were performed across the San Marcial fissure with the EM-38, EM-31, and EM-34 at different modes and heights above the ground (inverse method). By using the EM method and a statistical analysis program, the subsurface fissure was detected by the distinct increases and decreases in conductivity.

The last case study was performed at the Navajo Mine where spoil was sampled every 330 feet to determine whether it could support natural vegetation. EM measurements were taken at the same locations as samples and subsequently correlated using a statistical program, SAS. These results correlated so well that the mine can potentially save thousands of dollars in sampling costs.

I. INTRODUCTION

It is important to detect location and movement of subsurface waste material to properly manage environmental problems. Few techniques exist to quickly and inexpensively delineate subsurface plumes. The Electromagnetic (EM) Induction Method provides fast and low-cost detection of many subsurface waste materials which change the electrical conductivity where they are deposited. These types of waste materials have been documented in the literature since 1979.

The EM method has been used to map contaminant plumes migrating from landfills under different hydrological conditions: sandy aquifers in New York, U.S.A., and Ontario, Canada (McNeil et al., 1990); porous sandstone in Yorkshire, U.K. (Barker, 1990 a,b); sands over irregular crystalline bedrock in Ontario (Greenhouse et al., 1987); clayey till in Indiana, U.S.A. (Roberts et al., 1989); sand and gravel in New Hampshire, U.S.A. (Fitzgerald et al., 1987); stratified drift in Connecticut, U.S.A. (Grady and Haeni, 1984); and limestone, shales, and fractured clay in Ontario (Slaine and Greenhouse, 1982).

The method has also been used for subsurface detection and mapping of a variety of industrial waste materials: metal hydroxide sludge in New England, U.S.A. (Hankins et al., 1991);

low-level radioactive waste in Tennessee, U.S.A. (Nyquist and Blair, 1991); caustic soda used to process bituminous sands in Alberta, Canada (King and Pesowski, 1991); ash and other wastes from local industries (Jordan et al., 1991); low-level radioactive materials (Sherwin and Witten, 1991); organics and metals at the Ciba-Geigy superfund site in New Jersey, U.S.A. (Barton and Ivanhenko, 1991); undocumented wastes reported to be oils, sulfides, waxes, and non-chlorinated hydrocarbons in Louisiana, U.S.A., (Primeaux, 1985); liquid radioactive wastes (Barlow and Ryan, 1984; Ketelle and Pin, 1984); and drilling fluids in an arid environment (Medlin and Knuth, 1986). When a landfill in Novo Horizonte in Brazil, contaminated a small farmhouse well, the EM-34 was used to detect a weather zone in the geology and the contaminants leading to the farmhouse (Greenhouse et al., 1987). Acid sludge was deposited from the reclamation process in unlined lagoons in glacial overburden at a plant in Breslau, Ontario (Greenhouse et al., 1987). In addition, 12,000 liters of contaminated water containing 918 mg/L of chloride, 323 mg/L of bromide, and a variety of organic and heavy metal tracers were injected into a sandy unconfined aquifer on Canadian Forces Base at Camp Borden, Ontario. EM instruments detected the migration of the plumes (Greenhouse et al., 1987).

In agriculture, the EM induction method is widely used for mapping soil salinity to prevent crop degradation under dryland and irrigated conditions in Canada (De Jong et al., 1979), Pakistan (Hendrickx et al., 1990), Senegal (Boivin et al., 1988), Syria (Job et al., 1987), and the U.S.A. (Rhoades and Corwin, 1981). At mine sites, EM induction is used to locate seepages of acidified groundwater containing sulfides and chlorides (King and Sartorelli, 1991; Ladwig 1982; Slaine and Greenhouse 1982). In New Mexico, Young (1994) found a strong correlation between groundwater sulfate concentration and the apparent electrical conductivity measured with the Geonics EM-34 ground conductivity meter. Young concluded that EM induction can be used to characterize sulfate-bearing groundwater plumes caused by mining activities. In petroleum producing areas, liquid organic contaminants can be detected under favorable conditions using meticulous survey procedures. Accumulations of jet fuel were mapped in North Carolina, U.S.A. (Saunders and Cox, 1987) and New York (Germeroth and Schmerl, 1987; Saunders and Germeroth, 1985); tetrachloroethylene contaminating a sand and gravel delta in Maine, U.S.A. (Fitzgerald et al., 1987); and hydrocarbons resulting from gasoline spills (Valentine and Kwader, 1985; Saunders et al., 1983). Hydrocarbon thickness (free floating product) on the water table was estimated in California,

U.S.A. (Saunders et al., 1983), and organic plumes were detected in sandy to clayey marine terraces (Valentine et al., 1985). In southwest Texas, the EM-34 and Protem 47 were used to map an area affected by leakage from three brine evaporation ponds (Lahti and Hoekstra , 1991). Public water supply wells in northern Kentucky were found to be contaminated with brine, which was rising into the aquifer through improperly plugged oil and gas wells. Subsequently, the EM-34 identified zones of increased chlorides (Sartorelli et al., 1990). In northeastern Ohio, a well became contaminated following the completion of a nearby gas well. The EM-34 located a buried pit which was used for drilling fluids that became the contamination source (Lyverse, 1989).

The EM method has also been used to determine geological features in the subsurface by detecting weathered zones and fractures in the bedrock (Payne, date unknown). The EM method was also employed to detect faults and fractures in the bedrock in the Republic of Volta, Africa (Placky et al., 1981); to map voids in limestone in Texas, U.S.A. (Poteet, 1989); to locate high-yield wells in fractured dolomite in Chicago, Illinois, U.S.A.; and to locate potential well sites over sandstone and granite in northern Wisconsin (Jansen and Taylor, 1989). In Vendee, France, the EM-16 and EM-31 mapped a water-bearing fault in granite (Bresson, 1979).

II. ELECTROMAGNETIC INDUCTION METHOD

In an electromagnetic survey one measures the effect of a conducting soil profile on a time-varying electromagnetic field , and uses this measure to obtain an estimate of the distribution of the electrical conductivity with depth. The source of this time-varying electromagnetic field is an alternating current in a transmitter coil, Tx (Figure 1). This primary magnetic field induces small currents in the conductive soil, which in turn generates a secondary magnetic field that is sensed by a receiver coil, Rx. This secondary field will have an amplitude and phase different from the primary field. These differences arise not only from the soil properties (such as water content and ionic content of the water), but also from the spacing of the coils and their orientation with, and distance from, the soil surface at the time of measurement. McNeil (1980b) showed that for conductivity values of less than 130 milliSiemens per meter (mS/m), the apparent conductivity of the soil measured by the instrument is given by

$$EC_a = \frac{4}{2\pi f \mu_o s^2} \left(\frac{H_s}{H_p} \right) \quad (1)$$

where EC_a is the apparent conductivity of the soil $(S/m)^1$; H_p and H_s are, respectively, the intensities of the secondary and primary

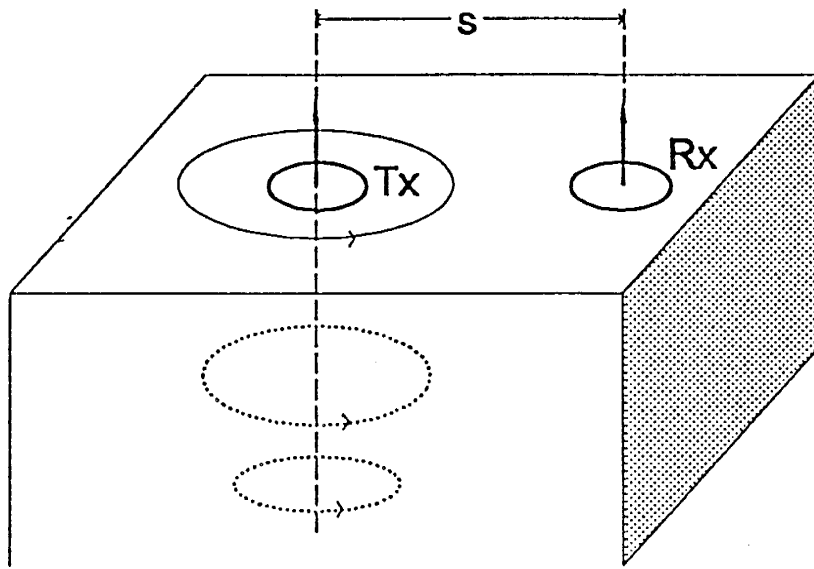


Figure 1. Transmitter coil Tx, receiver coil Rx, and induced current flow (intermittent lines) for the electromagnetic induction method.

magnetic fields at the receiver coil amp per meter (amp/m); f is the frequency of the current; μ_0 is the magnetic permeability of air (Henrys/m); and s is the intercoil spacing. The physics of the EM Induction Method are well understood and allow the calculation of the contribution to the secondary magnetic field which arises from a soil layer at depth z with a given electrical conductivity (McNeil, 1980b; Wait, 1982). Figure 2 illustrates that, with the coils in the horizontal position the soil layer at a depth of approximately $0.4 s$ provides a maximum contribution to the secondary magnetic field. However, the soil layer at a depth of $1.5 s$ still makes a significant contribution. With the coils in the vertical position, the top layer makes the largest contribution. Therefore, we can determine directly whether the electrical conductivity of the soil is increasing or decreasing with depth. Hendrickx and others (1992) used this feature to classify of saline soils.

In these studies, electromagnetic surveys were conducted with three different ground conductivity meters: the Geonics EM-38, EM-31, and EM-34 (Geonics Limited, Ontario, Canada) (McNeil, 1980a,b). Photos 1 and 2 illustrate the EM-38 and EM-31 devices which non-invasively measure the EC_a , the bulk soil electrical conductivity in mS/m. Readings take less than five seconds per location and are

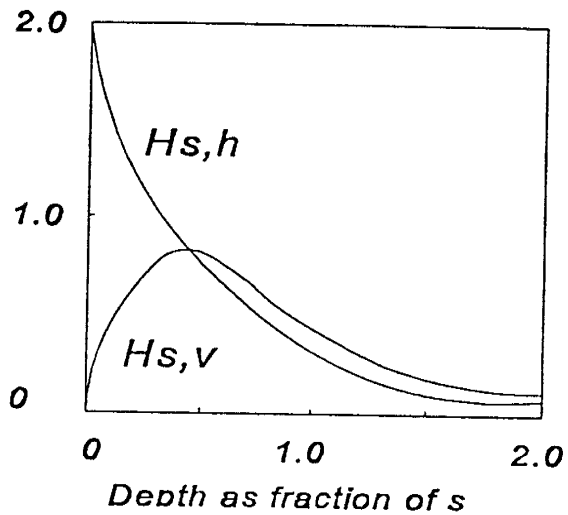


Figure 2. Relative contribution to the secondary magnetic field for vertical ($H_{s,v}$) and horizontal ($H_{s,h}$) coils as a function of depth. The depth is expressed as a fraction of the distance between the coils (from McNeill 1980b).

Photo 1. Use of the EM-38 in the vertical mode



Photo 2. Use of the EM-31 in the horizontal mode (Photo below)



either recorded by a data-logger connected to the instrument or written in a field notebook.

III. CASE STUDY 1: DETECTION OF SALINE BRINES FROM EVAPORATION PITS

1. INTRODUCTION

Geophysical methods are used by engineers, geologists, and hydrologists to locate certain environmental problem areas and assess the extent of environmental contamination within these areas. Typically, in an attempt to determine the degree of contamination at a site, numerous borings and monitoring wells are drilled. Not only are these drillings are not only expensive, but it is also difficult to determine exactly where they should be placed to produce an accurate site characterization.

The presence of saline plumes indicates brine water contamination that could eventually render an aquifer useless. Therefore, it is important to accurately detect both the existence and extent of such plumes and how they migrate. These plumes in soil can destroy the natural vegetation and promote growth of plants which can tolerate saline environments. Some vegetation, such as the salt cedar, are a problem in New Mexico because they consume large amounts of water and thus deplete the aquifers

storage and lower the water table. Studying how the brine contamination migrates can facilitate subsequent intrusive phases of an investigation, such as placement of monitoring wells (Hoekstra et al., 1992) or determination of the aerial and vertical extent requiring remediation.

One of the most useful geophysical methods to detect saline plumes is the EM Induction Method. EM methods measure physical properties related to exploration objectives. EM methods define the lateral and vertical conductivity stratification (sections) of the subsurface. Such sections may infer important parameters for environmental and groundwater investigations (Hoekstra et al., 1992). This is true because conductivity depends on physical properties of the soil and rocks influencing permeability and groundwater quality, such as dissolved solids in the groundwater and soil, and fractures and shear zones (Hoekstra et al., 1992). Greenhouse and Slaine (1983) implemented the EM method on acid sludge waste from an oil reclamation process and deposited it in lagoons. The groundwater conductivity increased as a result of the chlorides and sulfates in the acid sludge. Results of the EM-31 and EM-34 strongly suggest the EM method mapped the contaminant migrations and provided important results for future well

installations (Greenhouse and Slaine, 1983). Because salt ions produce an electrical charge, it is easy to detect a plume: the higher the saline concentration, the higher the electrical conductivity. Certain EM instruments are used downhole, thereby measuring deep levels of penetration (to m), but only over a limited area. This downhole type also involves time-consuming procedures and significant expense. In addition, portable EM instruments (which penetrate to depths of 60 m) permit measurements to be taken over a wide area, and they are also faster and easier to use than the downhole type.

Geonics Limited produces various portable EM instruments, but only three were used in this study: the EM-38, capable of being used by one person at depths of .75 m and 1.5 m; the EM-31, also for use by one person, but at depths of 3.0 m and 6.0 m; and the EM-34, which requires two persons to operate but reaches depths ranging from 7.5 m to 60 m.

2. SITE DESCRIPTIONS AND EM SURVEYS

The field area is located 22 miles east of Hagerman, New Mexico, in the Roswell Artesian Basin at an abandoned pit on the New Mexico Tech/Howe Sulimar Queen Field Laboratory site. The oil pit was constructed in 1969 as an evaporation pit for brine water. Not only was this brine water encountered during drilling

operations, but it also settled to the bottom of nearby production tanks. The pit was also used for emergency diversion of fluids. In 1992, the pit was abandoned when water flooding operations began in the field. This particular evaporation pit is approximately 9 m (30 ft) square. Inside the pit, the gradient (slope of surface from higher to lower) is southwest to northeast. The local topographic gradient is southeast to northwest.

A. EM Surveys

Three geophysical surveys were performed at the site using the EM-38, EM-31, and EM-34. The surveys were performed using the EM-38 and EM-31 where 22 lines were surveyed in all directions from the center of the pit. The survey lines emanated 100 m from the center of the pit, with reading sites staked at 10 m intervals. To the northwest, west, and southwest, the survey lines were less than 100 m due to the presence of metal objects, such as pipelines and tanks, which would interfere with the electrical conductivity readings. Although the EM-34 was utilized on a grid similar to the EM-38 and EM-31 fewer readings were taken. The intercoil spacings used for the EM-34 were 10 m, 20 m and 40 m. This allowed depths of penetration of 7.5 m, 15 m, 30 m and 60 m.

For all three surveys, when metal objects interfered with readings, the results were ignored and only valid readings were

used to construct conductivity contour maps. The computer program used to contour the conductivity readings was Surfer by Golden Software. To observe how far the saline plumes traveled, the readings taken at the pit were compared to the background readings (100 m from the center of the pit).

B. Geology of the Site

The site geology consists of 50 m of alluvium sand and gravels underlain by the Seven Rivers Formation. The Seven Rivers Formation consists of anhydrite, dolomite, and limestone interbedded with sandstone and red shale. The hydrogeologic properties of the Seven Rivers Formation are very similar to the alluvium (Havenor, 1968). The top meter of the soil consists of fine sand with some clay. In the next 2 m, the clay content increases in the fine sand. From 3 m to 4 m, a caliche layer is found with indurated nodules up to 2 cm in diameter.

3. RESULTS AND DISCUSSION

Four maps were created at depths ranging from 0.75 m to 30 m (Figure 3). Results indicate that the brine moved in a west to northwest direction and was spreading from the pit vertically as well as horizontally. At a depth of .75 m (100 m from the center of the pit), the measurements indicate background conductivity values ranging from 0.9 mS/m to 15 mS/m. At a depth of 3.0 m, the

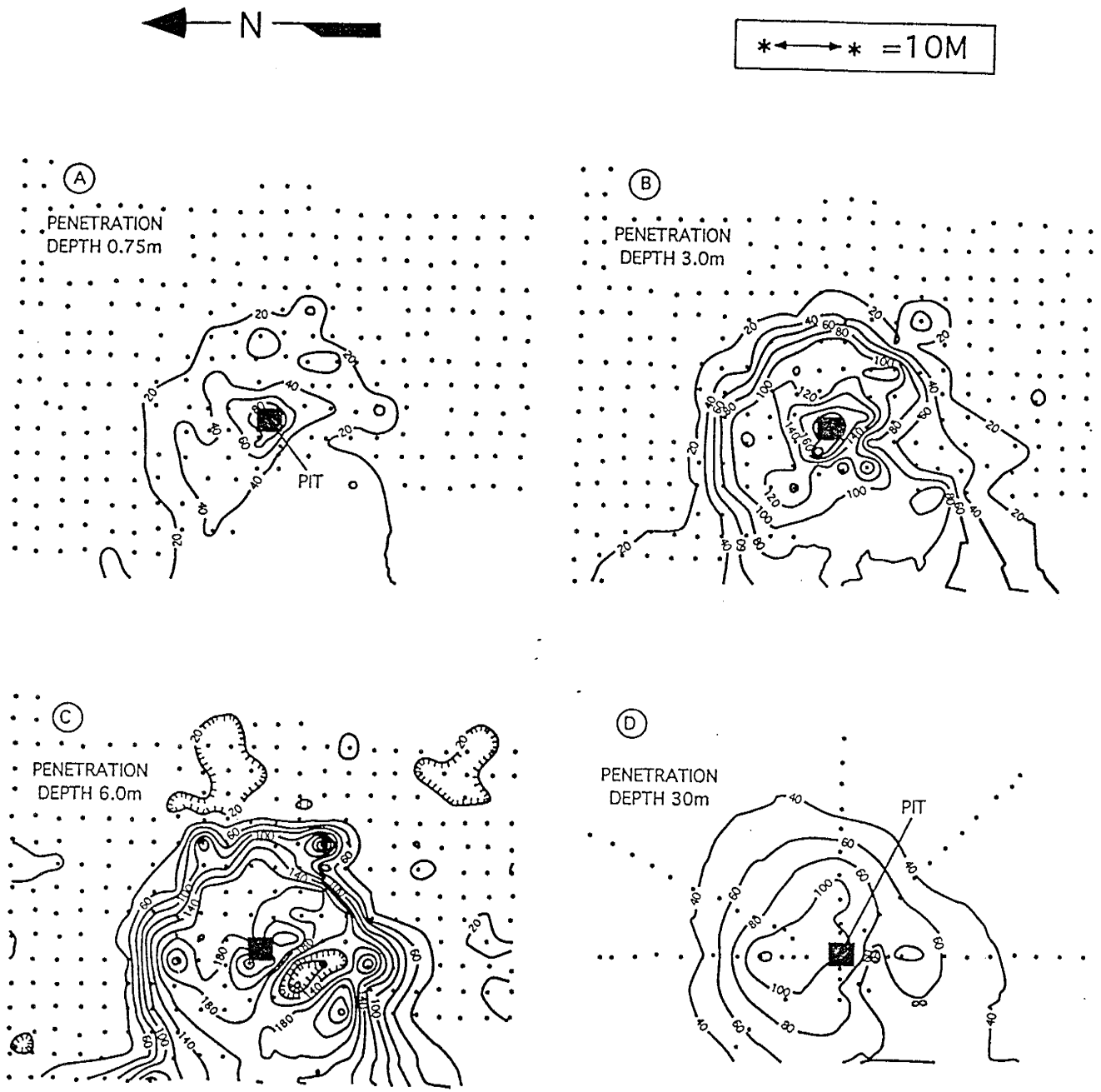


Figure 3. Salinity contour maps for penetration depths 0.75, 3.0, 6.0, and 30.0 meter.

background conductivity values ranged from 9 mS/m to 24 mS/m; at a depth of 6.0 m, the background conductivities range from 17 mS/m to 30 mS/m. Last, at depth of 30 m, the background conductivities ranged from 35 mS/m to 70 mS/m. These slight increases in conductivity with depth are attributable to increases in soil moisture content with depth. Water contains ions in solution and soil moisture increases with depth; thus, the greater the soil moisture content, the higher the electrical conductivity. The highest contoured conductivity values occurred at a depth of 6 m, indicating the salinity in the soil was increasing and spreading in a west-northwest direction from the center of the pit. This effect was observed when comparing the contoured maps from 0.75 m to 6 m. Conductivity values at a depth of 0.75 m in the center of the pit were 140 mS/m; at a depth of 6 m, the conductivity was 220 mS/m. Conductivity values at the center of the pit were 160 mS/m at a depth of 0.75 m. At 6 m, conductivity values were 200 mS/m, demonstrating that salinity increases with depth. Soil samples taken from the top meter of the soil inside the pit contained 3,000 parts per million (ppm) of potassium chloride (KCL). At a depth of 3 m to 4 m, sample salinities were 24,000 ppm KCL. Therefore, the maximum salinity occurred just above and inside the less permeable caliche layer. Below the 4 m depth the

salinities remained relatively high, indicating seepage occurred through the caliche layer. In all of the surveys performed from depths of 0.75 m to 30 m, the brine spread horizontally 50 m to 60 m from the pit in all directions, with the major portion migrating in a west to northwest direction. Figure 4 illustrates that, at the center of the pit, the brine traveled vertically to a depth of at least 30 m. Comparing background values of conductivity east of the pit to the center of the pit demonstrates that there is an increase of 65 mS/m at the 30 m depth. At the same depth, an increase of 67.3 mS/m was also observed when comparing background conductivity values north of the pit to the center of the pit. Both of these increases are attributed to the penetration of brine water to this depth.

4. CONCLUSIONS

- The EM instruments used in this study proved that the brine had traveled to a depth of at least 30 m. The results of the EM measurements indicate that the brine also traveled laterally 50 m to 60 m from the center of the pit to a depth of 30 m in a west to northwest direction (down gradient). Figure 4 compares measurements taken at the center of the pit to background readings north and east of the pit at a 60 m depth; these measured increases were 6.1 mS/m and 25.1 mS/m,

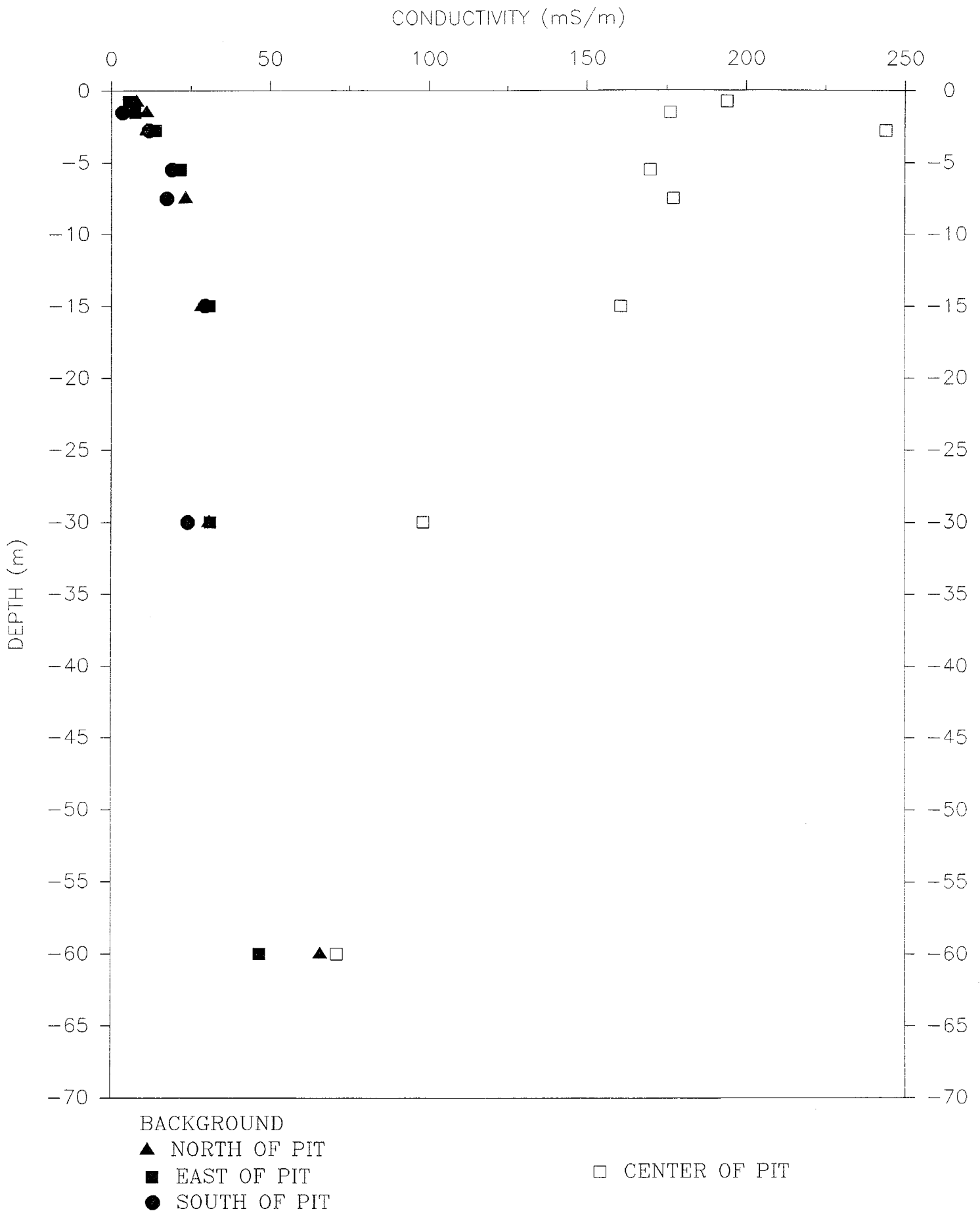


Figure 4. Comparison of background conductivity values (100 meters from the center of the pit) to conductivity measurements from the center of the pit.

respectively. With such slight increases, it could not be determined whether the brine has penetrated to this depth. EM instrument (EM-34) used in this study could only acquire measurements at the specified depths of 7.5 m, 15 m, 30 m and 60 m; therefore, it was not possible to determine whether the brine may have traveled between the depths of 30 m and 60 m.

- This study conclusively exhibited that the EM Method pinpointed the lateral spread and vertical percolation of brine water dumped in an oil evaporation pit.

IV. CASE STUDY 2: THE USE OF THE EM METHOD IN DETECTING THE SAN MARCIAL FISSURE

1. INTRODUCTION

Fissures and cracks in the earth are important to study because they provide a quick path for contaminants to travel. These underground subsurface piping systems are usually difficult to locate without drilling numerous borings. These voids created in the subsurface can not be seen from the ground until the fissure subsides and collapses onto itself, thereby leaving depressions or holes in the ground (Photographs 3 and 4). Locating fissures is especially important when choosing sites where hazardous waste or radioactive material will be deposited. If fissures are present,



Photo 3. Collapse of the San Marcial Fissure West of I-25



Photo 4. Fissure location at Transect C
Note: Depressions and collapses of fissure

contaminants from these sites could travel into the groundwater faster , thereby contaminating the aquifer and soil.

The EM Induction Method is one method to accurately locate fissures. Fissures are voids in the subsurface that create underground piping systems. Due to these voids, as one crosses the fissure the electrical conductivity measured by the EM instruments is normally lower than the surrounding soil. However, if the fissure is filled with water or the soil moisture content is high, then the electrical conductivity will increase dramatically.

Fissures typically measure only several meters deep (Baumgardner and Scanlon, 1992). Therefore, portable and shallower penetrating EM instruments, rather than downhole EM instruments, are used. In this study three EM instruments were employed using an inverse method (the instruments are raised above the ground surface at different heights) EM-38 and EM-31 made by Geonics Limited. The EM-34 was used at 10 m, 20 m, and 40 m intercoil spacings (the distance between the transmitting coil and receiving coil) The EM-38 and EM-31 were also used in this study. All of these instrument's are manufactured by Geonics Limited.

2. SITE DESCRIPTIONS AND EM SURVEYS

The field area is located in Socorro County, 18 miles south-southwest of San Antonio, New Mexico. The San Marcial fissure was discovered by the New Mexico Highway Department when a crack appeared across the southbound lane of the newly constructed Interstate 25 (I-25). During the night of August 4, 1981 the fissure developed. The length of the crack was 1,374.95 m (4,511.00 feet(ft)) long. Half of the length extended on both sides of I-25 and former US 85 (Budding, Payne, Sanford, and Schlue, 1982). The only evidence related to this ground failure was the water runoff from the arroyos into the fissure. Reportedly, on this same date .5-inch of rain fell at the Bosque Del Apache headquarters, located 21 kilometers (km) (13.04 miles) northeast of the site. Fifteen km (9.32 miles) northwest of the site, trace amounts of precipitation had fallen (Budding, Payne, Sanford, and Schlue, 1982).

A. EM Surveys

The EM-38, EM-31, and EM-34 were used to detect the San Marcial Fissure. Measurements were taken at the surface, knee, and hip with the EM-38 and EM-31 in a vertical and horizontal mode (Table 1, Appendix A). The EM-34 was used to take measurements at the surface in the vertical and horizontal modes. The coils of the

EM-38 and EM-31 instruments were placed perpendicular and parallel to the fissure in order to observe any differences in detecting the fissure. The EM-34 was only used at transect A, parallel to the fissure. The intercoil spacings used were 10 m, 20 m, and 40 m with the coils parallel to the fissure. These separations produced depths of penetration of 7.5 m, 15 m, 30 m, and 60 m respectively. Seven transects (A through G) were placed across the crack. Transects A through E are to the west of I-25, and transects F and G are east of I-25 and Old US 1 (US 85) (Figure 1, Appendix B). At transects A, D, E, and G, the fissure could not be seen from the surface. At transects B, C, and F, the fissure was visible from the surface (Table 2, Appendix A). EM measurements were taken at intervals ranging from 1 m to 5 m apart along each transect. EM intervals at each transect are noted below:

Transect A - 5 m apart

Transect B - 2 m apart

Transect C - 2 m apart

Transect D - 1 m apart

Transect E - 1 m apart

Transect F - 1 m apart

Transect G - 1 m apart

The length of the transects varied from 40 m to 100 m. The spacing

from one transect to the other ranged from 40 m to 200 m apart (Figure 1, Appendix B).

The EM instruments' conductivity measurements were analyzed by two different methods. The first approach plotted conductivity versus distance to observe any anomalies as the EM instruments passed over the fissure. The second approach utilized a split window program within a statistical program, SAS, to determine boundary conditions of the fissure. The split window program measured differences between each window width to produce F values to show boundaries (in this case, fissure locations).

B. Geology of the Site

The San Marcial fissure lies in the Santa Fe Group, which consists of the Sierra Ladrones and Popotosa Formations. In general, the site consists of alluvial deposits which are seen from the ground surface. The only existing site-specific geology documentation was written by Budding and others (1982). Seismic refraction profiles were shot along I-25, with one geophone southwest and four northeast of the fissure. Results of the seismic survey indicate the following:

0 m to 47 m (0 to 154 ft)
Unsaturated, moderately indurated alluvial deposits

47 m to 81 m (154 to 265 ft)
Saturated, moderately indurated alluvial deposits
or
Unsaturated substantially indurated alluvial deposits

81 m to unknown depth
Mid-Tertiary volcanic rocks or weathered Precambrian rock

3. RESULTS AND DISCUSSION

Results of the surveys across the San Marcial fissure indicated that the EM instruments detected the fissure location and possibly other fissures. Figures 2 through 32 (Appendix B) illustrate the plots of conductivity versus distance as the EM instruments traversed across the fissure. Tables 5 through 18 (Appendix A) indicate the results of the SAS split window program and its correlation with the distance versus conductivity plots of Sigma Plot, where a fissure may be located.

Results of the EM surveys across the San Marcial fissure show two types of signals. One signal acquired is a sharp increase followed by a sharp decrease; the other is a sharp increase. Transect A (Figures 2 and 3, Appendix B) illustrates the sharp increase in conductivity followed by a sharp decrease with the coils parallel to the fissure. Transect D, Figure 25 (Appendix B) illustrates the sharp increase in conductivity with the coils of

the instrument perpendicular to the fissure. Whether the instrument coils were parallel or perpendicular to the fissure, the same type of signals were acquired in both positions. Supporting data relevant to the type of signals acquired are provided in Appendix B.

A. EM Instrument Coils Parallel to Fissure Distance Versus Conductivity Plots

A summary table (Table 1) illustrates the modes and heights of EM measurements taken, and number of increases and decreases in conductivity, the number of times it was difficult to determine whether increases or decreases existed. Results indicate a majority of the readings taken with the EM-38 and EM-31 increased in conductivity, except in two modes and heights: EM-38HS and EM-31HK. The fissure on average was detected by an increase or decrease in conductivity by 5 out of 7 transects in each mode and height. Only at 2 transects was it difficult to determine whether the fissure was detected. The EM-34 results were inconclusive in determining whether the fissure was detected at this depth as a result of the EM-34 being implemented at one transect. However, of the six modes and heights used, three detected increases, two detected decreases, and one transect was difficult to decipher. Supporting data are provided in Appendix B, Figures 2 through 18.

Description of measurements	Number of Transects	Number of Transects which had increases in conductivity at fissure	Number of Transects which had decreases in conductivity at fissure	Number of Transects which were hard to decipher
EM-38VS	7	4	1	2
EM-38VK	7	4	2	1
EM-38VH	7	3	2	2
EM-38HS	7	2	3	2
EM-38HK	7	2	4	1
EM-38HH	7	2	1	4
EM-31VS	7	4	1	2
EM-31VK	7	4	1	2
EM-31VH	7	3	1	3
EM-31HS	7	3	2	2
EM-31HK	7	4	1	2
EM-31HH	7	2	1	4
EM-34-10 VS	1	1	0	0
EM-34-10 HS	1	0	0	1
EM-34-20 VS	1	0	1	0
EM-34-20 HS	1	1	0	0
EM-34-40 VS	1	0	1	0
EM-34-40 HS	1	1	0	0

Table 1. Summary of Distance vs Conductivity Plots with EM Instrument Coils Parallel to Fissure.

B. EM-38 and EM-31 Instruments with Coils Perpendicular to the Fissure, Distance Versus Conductivity Plots

Results of the EM surveys with the coils perpendicular to the fissure (Figures 19 through 32, Appendix B) indicate similar types of signals received as compared to the coils parallel to the fissure. Table 2 summarizes data from the EM instrument coils perpendicular to the fissure. As the instrument crossed over the fissure, an increase or decrease in conductivity averaged 5 out of 7 transects with modes and heights of the instruments in each mode and height. Only at 1 transect was it difficult to determine whether there was an increase, decrease, or if the fissure did not exist.

C. SAS Split Window Boundary Program with the EM-38 and EM-31 Instruments Parallel to the Fissure

Tables 5 through 11 (Appendix A) show the results where the split window program detected possible fissures along each transect. Bolded values indicate agreement with the distance versus conductivity plots. Because the SAS split window method was used to determine where the fissure (s) are located, window widths varying from 2 to 8 were used to detect the fissure. The SAS program showed agreement with the distance versus conductivity plot locations with 4 transects. On 3 transects, the fissure was undetectable or difficult to decipher (Table 3, Appendix A).

Description of measurements	Number of Transects	Number of Transects which had increases in conductivity at fissure	Number of Transects which had decreases in conductivity at fissure	Number of Transects which were hard to decipher
EM-38VS	7	2	3	2
EM-38VK	7	3	3	1
EM-38VH	7	3	3	1
EM-38HS	7	4	2	1
EM-38HK	7	4	2	1
EM-38HH	7	3	3	1
EM-31VS	7	2	4	1
EM-31VK	7	4	2	1
EM-31VH	7	4	2	1
EM-31HS	7	3	3	1
EM-31HK	7	3	3	1
EM-31HH	7	3	3	1

Table 2. Summary of Distance vs Conductivity Plots with EM Instrument Coils Perpendicular to Fissure.

Results show almost an equal probability in detecting the fissure with the coils parallel in conjunction with the SAS program.

D. Results of Split Window Program with EM Instrument Coils Perpendicular to the Fissure

Tables 12 through 18 (Appendix A) show the results of the split window program for different window widths. Again, bolded values indicate agreement with the distance versus conductivity plots of fissure locations. Table 4 (Appendix A) lists the number of transects which agreed with conductivity versus distance plots and the SAS program to detect the fissure. All instrument modes and heights detected the fissure at all transects except one. At 6 transects, the fissure was detected and only 1 transect was the fissure not detected.

4. CONCLUSIONS

- From the distance versus conductivity plots when the EM instruments traveled over the fissure, three signals were acquired as follows: a sharp increase in conductivity followed by a sharp decrease in conductivity, and a sharp decrease in conductivity. A third signal was received when an arroyo or collapsed fissure was passed over by the EM instruments, thereby creating a gradual increase in conductivity. The increase in conductivity may be attributable to the high soil moisture content. The increase may also be a result of clay

material present in the fissure. Clay material is typically more conductive than other soils as a result of its ability to hold more water and carry an electrical charge.

- A method to locate fissures below the ground was discovered by using the SAS split window program and the distance versus conductivity plots in conjunction with field observations. In this study, EM instruments were used such that coils of the instrument were both perpendicular and parallel to the fissure. There was very little difference on the signal acquired from the distance versus conductivity plots as to which one (coils parallel or perpendicular to the fissure) better detects the fissure. Statistically, when the coils are perpendicular to the fissure 5 out of 7 transects detect an increase or decrease in conductivity as compared to 5 transects with the coils parallel to the fissure. Both positions detected fissures at the same locations along each transect in most modes and heights.
- Based on the distance versus conductivity plots when all modes and heights of the conductivity readings exhibited the three aforementioned signals, the EM instruments detected a fissure. In some cases these plots may have discovered collapsed fissures which look like an arroyo, but provide a typical

conductivity signal on the distance versus conductivity plots. Thus, the split window program was implemented to confirm the fissure locations.

- The SAS split window program was used at different widths to determine fissure(s) along each transect. Window widths were run at 2, 3, 4, 5, and 8 to determine the fissure location. It appeared that the window widths of 3, 5, and 8 most successfully found the fissure. In addition, although it is not known why this occurred, the results successfully identified the fissure location. Some modes and heights could not detect the fissure by the split window program and distance versus conductivity plots. In some cases, the fissure was located at deeper depths and was not detected in the HS, HK, and HH modes and heights. Instead, the fissure was detected in the VS, VK, and VH modes and heights for the EM instruments.
- The EM instruments detected the fissure at all locations along the transects except at Transect E. At this transect, the fissure was not detected because the fissure did not extend far enough west of I-25 (Figure 1, Appendix B).
- A comparison was made of the number of transects the SAS program showed agreement with the distance versus conductivity

plots to detect the fissure. In one case the coils were parallel, and in the other the coils were perpendicular. The results indicated that when the coils were perpendicular to the fissure, 98 percent of the transects surveyed were able to detect the fissure location while only 52 percent of the transects surveyed were able to detect the fissure with the coils parallel to the fissure. Therefore, the results were better when the coils were perpendicular to the fissure.

- Soil borings were not taken at the transects to determine if the fissure actually exists. However, based on the results presented in this study, the EM instruments provide a method to detect surface and subsurface fissures. By acquiring significant increases and decreases in conductivity, or gradual increases in conductivity with the conductivity versus distance plots, it is possible to locate fissures in the earth by using these data with SAS split window program.

V. CASE STUDY 3: THE USE OF THE EM METHOD IN EVALUATING MINE SPOILS

1. INTRODUCTION

Historically, mining industry activities have destroyed land and wildlife. Over the last 20 years, strict environmental laws have been instituted to prevent environmental problems. Salinity surveys of mine spoils require numerous soil samples and large amounts of money for laboratory analyses. Such surveys determine whether the spoil (that is, the top layer removed to access the coal and fly ash) can support plant life and restore the land to its natural surrounding. These surveys also satisfy the mining permit requirements while improving reclamation success. Use of the Electromagnetic (EM) Induction Method can reduce soil sampling costs. The current method collects approximately 15 to 20 spoil samples in one day. In contrast, the EM Induction Method collects hundreds of EM readings in one day, thereby reducing labor and sample analysis costs. Because salt ions in the spoil emit an electrical charge, it is quite easy to detect salinity at sampled locations: the higher the saline concentration, the higher the electrical conductivity.

Other researchers have used the EM-38 to perform salinity surveys and show relationships between the EM readings and salinity

surveys. Hendrickx and others (1990) used the EM-38 to measure soil electrical conductivity for detailed salinity surveys in Faisalabad (Pakistan) at more than 3,400 sampling locations. Statistical analyses revealed a linear relationship between the data standard deviation and means (Hendrickx et al. 1990). The EM-38 survey corresponded well with the results of an agronomic survey, but the EM-38 yielded results which were more sensitive to salinity changes.

2. SITE DESCRIPTION AND EM SURVEYS

The study area is located outside of Farmington, New Mexico, in the San Juan Basin at the Navajo Mine. There are numerous sites at the Navajo Mine; the South Barber site is where this study was conducted. The South Barber area encompasses approximately 220 acres planned for reclamation. Land reclamation is accomplished by regrading the spoil and seeding it with native plant species. Spoil and top dressing samples are analyzed for salinity, pH, and other parameters to evaluate the spoils ability to support plant species.

A. EM Surveys

The EM Induction Method was used to perform a salinity survey of a spoil. Thirty-five site locations were sampled for salinity at depths of 0.3, 0.6, 0.9, and 1.2 m (1, 2, 3, and 4 feet). At

the same locations EM measurements were taken with the EM-38 in the horizontal and vertical modes.

B. Geology of the Site

Coal is present throughout the San Juan Basin in the creaceous deposits. The major deposits are found in the Crevasse Canyon, as well as the Menefee and the Fruitland Formations. The Navajo Mine strips coal from the Fruitland Formation by removing as much as 76 m (250 ft) of overburden material (Stone et al. 1983). Approximately 200 billion tons of coal are present in the Fruitland Formation to depths of 1,371.60 m (4500 ft). Thus, there are large areas to be reclaimed.

Mining operations place a tremendous strain on the local water resources in the area. Strip mining uses water to irrigate reclaimed lands. More than 2,000 acre-ft/yr of water are currently used at the Navajo Mine (Beaumont et al., 1976). Water is also used to wash coal and control dust on mine roads. Because water is not usually encountered at the Navajo Mine during the strip mining process, the San Juan River acts as the water resource supply.

The mining activities also impact the quantity and quality of water resources. The quantity is affected by the amount of water used for reclamation. The quality of water is impacted by mining raising aquifers closer to the surface, thereby increasing the risk

of pollution. Evaporation of stored water increases salinity; leakage of impounded saline water could contaminate local surface and groundwaters (Stone et al., 1983). In addition, fly ash (which is highly saline) is added to the soil as part of the reclamation process. Fly ash is a source of salinity and trace metals.

The spoil consists of coarse fragments mixed with fines. The size of the fragments vary in size from 4x2x2 m to 2x1x1 m. Fragments with a diameter between 5 to 20 cm are in the spoil that contain, on the average, 60 to 80 percent coarse fragments with a range from 20 to 95 percent.

C. Soil Sampling and Analysis

Spoil samples were taken with a backhoe at depths of 0.3, 0.6, 0.9, and 1.2 m to acquire a representative sample. The coarse fragments were separated from the fines and laboratory analyzed for electrical conductivity, EC_e , to determine the salinity. At each location, the mean of the four sampling depths produced a mean salinity profile (EC_{mean}). A correlation was made between the EM-38's electrical conductivity readings and the EC_{mean} to derive correlation coefficients. A regression analysis was then performed between the EC_{mean} and the EM-38's electrical conductivity (EC_{ver}) readings in the vertical mode. This analysis assessed how the EM-38 can be used to reduce the number of EC samples. The

relationship between the EC_{ver} and EC_{mean} created two models, a "full model" and a "reduced model." An experiment was then performed by using the EM-38 survey to choose seven spoil sampling locations. These locations were selected at the 5, 10, 25, 50, 75, and 90 percentiles of 35 measured EM_{ver} values. This resulted in a regression model with the maximum sensitivity. The "reduced model" was acquired by using the EC_{mean} and EC_{ver} data from the seven locations. The full model was then compared to the reduced model by observing the residuals between the EC_{means} and the predicted EC values.

3. RESULTS AND DISCUSSION

The results for each location yielded a mean for the four EC_{mean} depth samples ranging from 4.4 to 16.2 deciSiemens/meter (dS/m), a difference of 12.50 dS/m. This indicates there is good dispersion among the data and close correlations will result at sites with large differences. The majority of the EM-38 data ranged between 6.25 to 13.75 dS/m. The linear correlation coefficient between the EC_{mean} and EM-38 measurements in the horizontal mode was 0.50. The linear correlation coefficient between the EC_{mean} and the vertical mode of the EM-38 measurements was 0.57. Both coefficients are significant at a level of 0.01, proving that a correlation does exist.

A. Results and Discussion of Regression Models

Results of the regression analysis between the EC_{mean} and the vertical mode of the EM-38 (EM_{ver}) produced a significant model, the "full model" :

$$EC_{mean} = 7.3 + 0.085 EM_{ver} \quad (R^2=0.32, n=35, F=15.7) \quad (2)$$

The F value received was at a significant level of 0.01. As part of the experiment, the reduced model was created from the EC_{mean} and EM_{ver} of seven locations which yielded a "reduced model":

$$EC_{mean} = 6.2 + 0.114 EM_{ver} \quad (R^2=0.70, n=7, F=11.9) \quad (3)$$

The F value for the "reduced model" is significant at the 0.05 level. Figure 5 represents the original EC_{mean} and EM_{ver} data points together with the linear regression lines representing the "full model" and "reduced model."

Therefore, the reduced model performed as well as the full model. The results indicate that a relatively small number of samples can properly calibrate the EM-38 measurements without affecting the accuracy of the salinity.

Both models are identical, as is shown in the sums of the squares of the differences between predicted and measured EC_{mean} values that were, respectively, 247 and 262 for the "full" and "reduced model." Evidently, high EM_{ver} value always coincided with high salinity. A low EM_{ver} value generally coincide with a low

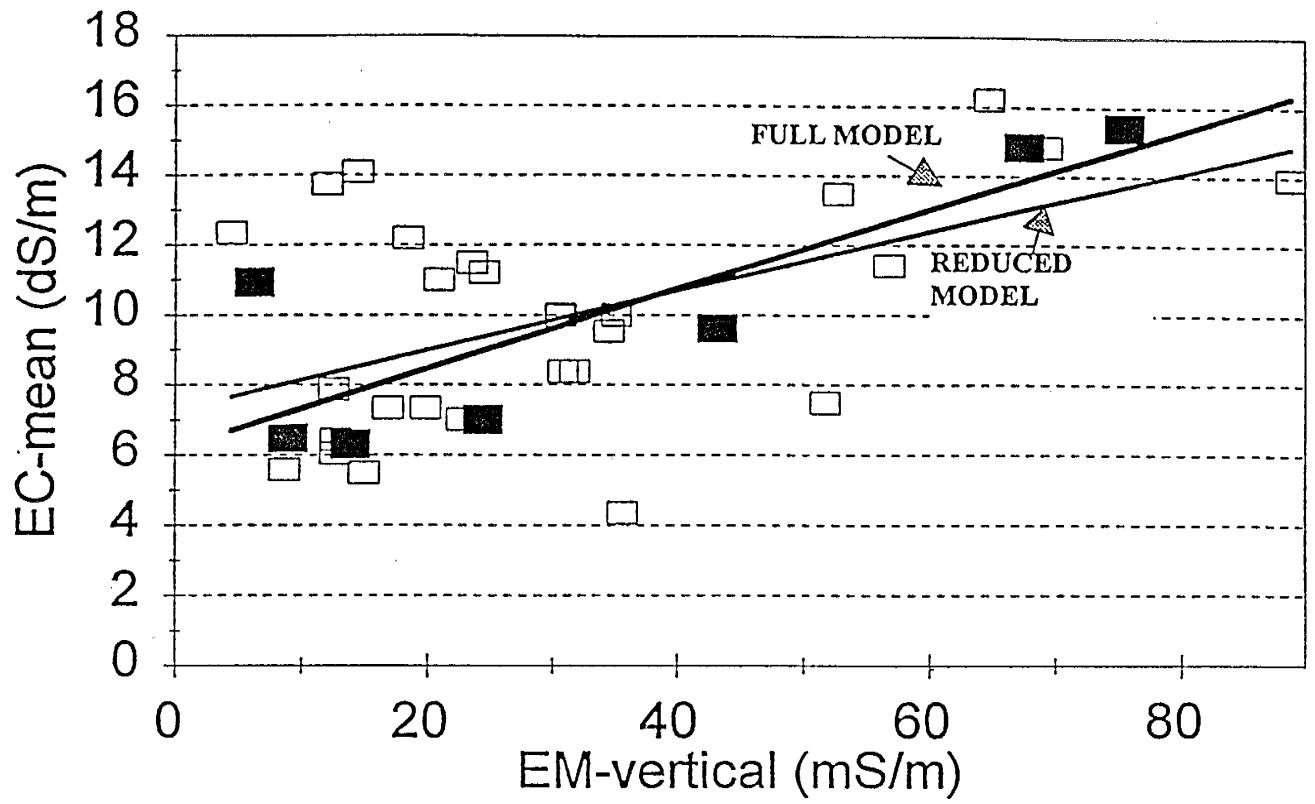


Figure 5 . The original EC_{mean} and EM_{ver} data points with the linear regression lines representing the "full model" and the "reduced model". The filled data points were used for the derivation of the "reduced model."

EC_{mean} value, but there are a few exceptions where EM_{ver} values below 20 mS/m coincided with EC_{mean} values above 12 dS/m. Because the coarse fragments often have salinities 1 to 2 dS/m higher than the fines, this bias can not be caused by the coarse fragments. The most likely explanation for this anomaly is found in the occurrence of large cavities in the mine spoil. Cavities with a diameter of 30 cm or more are quite common and larger ones have been encountered. Because the electrical conductivity of an air-filled cavity is almost zero, a decrease in the apparent EC of the profile is measured by the EM instrument. In this study, approximately 15 percent of all data points were affected by the "cavity effect."

4. CONCLUSIONS

This study proved a definite relationship between salinity of the mine spoils' EC_{mean} and the EM_{ver} with the EM-38. Using the EM Induction Method with salinity samples at a few locations resulted in an 80 percent reduction of soil samples. The Navajo Mine can reduce the amount of salinity samples by using the EM Induction Method presented in this study. This method can not only be used on the Navajo Mine, but also at other mines where salinity surveys are needed as part of the reclamation process.

Summary and Recommendations

In this independent study, three case studies from New Mexico were presented where EM surveys were performed on environmental problems: delineation of brine migration, detection of a fissure, and reclamation of mine spoils. In each study, the EM Induction Method provided a quick and cost effective method by reducing the number of soil or spoil samples required for confirmation. EM surveys provide a reliable method to detect environmental problems in the oil, coal, and hazardous waste industries. The EM surveys should be used in conjunction with soil sampling to verify geological features and contaminant migration.

REFERENCES

- Baumgardner, R. W. and Scanlon, B. R., 1992. Surface Fissures in the Hueco Bolson and Adjacent Basins West Texas. Bureau of Economic Geology, Geological Circular No. 92-2.
- Barker, R.D., 1990a. Investigation of Groundwater Salinity by Geophysical methods, in Geotechnical and Environmental Geophysics-Volume II (S.H. Ward, ed), Society of Exploration Geophysicists. pp. 201-211.
- Barker, R.D., 1990b. Improving the Quality of Resistivity Sounding Data in Landfill Studies, in Alistair Brown, series ed., Investigations in Geophysics No. 5: Geotechnical and Environmental Geophysics, Stanley H. Ward, ed (3 vols., Tulsa: Society of Exploration Geophysics, 1990), II, pp. 245-251.
- Barlow, P.M. and Ryan, B.J., 1984. An Electromagnetic Method For Delineating Groundwater Contamination, Wood River Junction, Rhode Island, in Selected Papers in the Hydrologic Sciences: USGS Water-Supply Paper 2270, Seymour Subitzky, ed. (Reston, Virginia: U.S. Geological Survey, 1984), pp. 35-49.
- Barton, G.J. and Ivanhnenko, T., 1991. Electromagnetic-Terrain-Conductivity and Ground-Penetrating-Radar investigation at and near the Ciba-Geigy Superfund Site, Ocean County, New Jersey: Quality Control and Quality Assurance Plan and Results, in Proceedings of the Symposium on the Application of Geophysics to Engineering and Environmental Problem, March 11-14, 1991.
- Beaumont, E.C., Shomaker, J.W. and Stone, W.J., eds., 1976. Guidebook to Coal Geology of Northwest New Mexico: New Mexico Bureau of Mines and Mineral Resources, Circular 154, 58 pp.
- Boivin, P., Brunet, D., and Job, J.O., 1988. Conductivimetric Electromagnetique et Cartographie Automatique des Sols Sales; Une Methode Rapide et Fiable. Cah. ORSTOM, ser. Pedol., Vol XXIV, No. 1:39-148. (in French)
- Brandvold, D., Bretz, R., Cayias, J., Docher, A., Grande, C., Haas, S., Haneberg, W., Hendrickx, J., Kieft, T., Stephens, C. and Tyner, L., 1993 January PERF PROJECT REPORT 92-07 IN-PLACE SLURRY-PHASE PRODUCTION PIT BIOREMEDIATION.

Bresson, G., 1979. Application de Certaines Methods Geophysics a la Prospection des Eaux Souterraines. 34 pp.

De Jong, E., Ballantyne, A.K., Cameron, D.R. and Read, D.W.L. 1979. Measurement of Apparent Electrical Conductivity of Soils by an Electromagnetic Induction Probe to Aid Salinity Surveys. Soil Sci. Soc. Am. J. 43:810-812.

Fitzgerald, L.J., Angers, A.K, and Radvill, M.E., 1987. The Application of VLF Geophysical Equipment to Hazardous Waste Site Investigations in New England, paper (14 pp., 7 figures) received from NUS Corporation.

Germeroth, R. M. and Schmerl, H., 1987. Jet Fuel From the Ground Up, Civil Engineering, LVIL, February 2, pp. 64-66.

Grady, S.J. and Haeni, F.P., 1984. Application of Electromagnetic Techniques in Determining Distribution and Extent of Groundwater Contamination at a Sanitary Landfill, Farmington, Connecticut, in Proceedings of the NWWA/EPA Surface and Borehole Geophysical Methods in Ground Water Investigations, February 7-9, 1984. San Antonio, Texas (Dublin, Ohio: Water Well Journal Publishing Co.) pp. 338-367.

Greenhouse, J.P., and Slaine, D.D., 1983. The Use of Reconnaissance Electromagnetic Methods To Map Contaminant Migration. Groundwater Monitoring Review. pp. 47-59.

Greenhouse, J.P., Monier Williams M.E., Ellert, N. and Saline, D.D., 1987. Geophysical Methods in Groundwater Contamination Studies in Applications of Geophysics and Geochemistry.

Hankins, J.B., Danielson, R.M. and Gregson, P.A., 1991. Delineation of Metal Hydroxide Sludge Disposal Areas Using Electromagnetics and Ground-Penetrating Radar, in Proceedings of the 1991 FOCUS Conference on Eastern Regional Ground Water Issues, October 29-31, 1991, Portland Marriott at Sable Oaks, Portland, Maine (Dublin, Ohio: National Water Well Publishing Co.) pp. 675-691

Havenor, K.C., 1968. Structure, Stratigraphy and Hydrogeology of the Northern Roswell Artesian Basin Chaves County New Mexico, N. Mex. Inst. Min. and Tech., State Bur. Mines and Mineral Res., Circular 93.

Hendrickx, J.M., Baerends, B., Raza, Z.I., Sadiq, M., and Chaudry, M.A., 1990. Monitoring Soil Salinity with An Electromagnetic Induction Method. Submitted for publication in the Soil Science Society of American Journal.

Hoekstra, P. Lahti, R., Hild, J., Bates, C.R., and Phillips D., Fall 1992. Case Histories of Shallow Time Domain Electromagnetics in Environmental Site Assessment: Case History-Mapping Migration of Oil Field Brines from Evaporation Pits and Ponds. In Groundwater Monitoring Review, pp. 110-117.

Jansen, J. and Taylor R., 1989. Geophysical Methods of Groundwater Exploration on Groundwater Contamination Studies in Fracture Controlled Aquifers in the Proceedings of the Third National Outdoor Action Conference on Aquifer Restoration Groundwater Monitoring and Geophysical Methods, May 22-25, 1989, Orange County Convention Center Orlando Florida, pp. 855-869.

Job, J.O., Loyer, J.Y. and Ailoul, M., 1987. Utilisation de la Conductivite Electromagnetique Pour la Mesure Directe de la Salinite des Sols. Cah ORSTOM, ser. Pedol., Vol XXIII, No. 2:123-131 (in French).

Jordan, T.E., Leask, D.G., Saline, D.D., MacLeod, I.N. and Dobush, T.M., 1991. The Use of High Resolution Electromagnetic Methods for Reconnaissance Mapping of Buried Wastes, in Proceedings of the Fifth National Outdoor Action Conference on Aquifer Restoration, Ground Water Monitoring and Geophysical Methods, May 13-16, 1991, Las Vegas, Nevada (Dublin, Ohio: Water Well Journal Publishing Co., 1991), pp. 849-861.

King, A. and Pesowski, M., 1991. Environmental applications of surface geophysics, Paper No. 156 presented at the Canadian Institute of Mining and Metallurgy 93rd Annual General Meeting, April 28-May 2, 1991, Vancouver, B.C.

King, A. and Sartorelli, A.N., 1991. Mapping Acidified Groundwater Using Surface Geophysical Methods, Poster Session Presentation P1.7, Second International Conference on the Abatement of Acid Drainage. Centre Sheraton, September 16-18, 1991, Montreal, Quebec.

Ladwig, K.J., 1982. Electromagnetic Induction Methods for Monitoring Acid Mine Drainage, Ground Water Monitoring Review, III, 1 (Winter 1982,) pp. 46-52.

Lahti, R.M. and Hoekstra, P., 1991. Geophysical Surveys for Mapping Migration of Brines from Evaporation Pits and Ponds, in Proceedings of the Symposium on the Application of Geophysics to Engineering and Environmental Problems, March 11-14, 1991. University of Tennessee, Knoxville, Tennessee (Golden, Colorado: Society of Engineering & Mineral Exploration Geophysicists, 1991), pp. 65-79.

Lyverse, M.A., 1989. Surface Geophysical Techniques and Test Drilling Used to Assess Groundwater Contamination by Chlorides in an Alluvial Aquifer in Proceedings of the Third National Outdoor Action Conference on Aquifer Restoration Groundwater Monitoring and Geophysical Methods, May 22-25, 1989. Orange County Convention Center, Orlando, Florida pp. 993-1006.

Medlin, E. and Knuth, M., 1986. Monitoring the Effects of a Ground Water Recovery System with EM, in Proceedings of the Surface and Borehole Geophysical Methods and Ground Water Instrumentation Conference and Exposition, October 15-17, 1986, Denver, Colorado, (Dublin, Ohio: Water Well Journal Publishing Co., 1986), pp. 368-378.

McNeil, J.D., 1980a. Electrical Conductivity of Soil and Rocks. Tech. Note TN-5. Geonics Ltd., Ontario, Canada. 22 pp.

McNeil, J.D., 1980b. Electromagnetic Terrain Conductivity Measurements at Low Induction Numbers. Tech. Note TN-6. Geonics Ltd., Ontario, Canada. 15 pp.

McNeil, J.D., Bosnar, M., and Snelgrove, F.B., 1990. Resolution of an Electromagnetic Borehole Conductivity Logger for Geotechnical and Ground Water Applications, Tech Note TN-25 (Geonics Ltd). 28 pp., 16 figures.

Nyquist, J.E. and Blair, M.S., 1991. A Geophysical Tracking and Data Logging System: Description and Case History, Geophysics, LVI(7). pp. 1114-1121.

Palacky, G.J., Ritsema, I.L. and DeJong, S.J., 1981. Electromagnetic Prospecting For Groundwater in Precambrian Terrains In the Republic of Upper Volta in Geophysical Prospecting. pp 932-955.

Payne, M.I., date unknown. The Electromagnetic Traversing Method of Groundwater Exploration in Crystalline Rock Terrain.

Poteet, D.R., 1989. Using Terrain Conductivity to detect Subsurface Voids and Caves in a Limestone Formation in the Proceedings of the Multidisciplinary Conference on Sinkholes, St. Petersburg Beach, Florida. October 2-4, 1989. pp 271-279

Primeaux, A.D., 1985. Geophysical Survey to Investigate Contaminant Migration from a Waste Site, in Proceedings of the Second Canadian/American Conference on Hydrogeology, Banff. June 25-29, 1985 (Dublin, Ohio: National Water Well Publishing Co., 1985), pp. 151-155.

Rhoades, J. D., Corwin, D. L., 1981. Determining Soil Electrical Conductivity-Depth Relations Using an Inductive Electromagnetic Soil Conductivity Meter. Soil Sci. Soc. Am. J. 45: pp. 255-260.

Roberts, R.L., Hinze, W.J., and Leap, D.I., 1989. A Multi-technique Geophysical Approach to Landfill Investigations, in Proceedings of the Third National Outdoor Action Conference on Aquifer Restoration. Groundwater Monitoring and Geophysical Methods, May 22-25, 1989. Orange County Convention Center, Orlando, Florida (Dublin, Ohio: National Water Well Publishing Co). pp. 797-811

Saline, D.D. and Greenhouse, J.P., 1982. Case Studies of Geophysical Contaminant Mapping at Several Waste Disposal Site, in Proceedings of the Second National Symposium on Aquifer Restoration and Ground Water Monitoring. May 26-28, 1982. The Fawcett Center, Columbus, Ohio. (Dublin, Ohio: National Water Well Publishing Co.) pp. 299-315.

Sanford, Schlue, Budding and Payne., 1982. Report On The San Marcial Crack. Geophysics Open File Report 41, Geoscience Department and Geophysics Research Center, New Mexico Institute of Mining and Technology.

Saunders, W.R., Castle, R.W. and Foget, C.R., 1983. Delineation of Subsurface Petroleum Spills Using Terrain Conductivity Measurements. Oil Spill Conference 1983. San Antonio, Texas. pp. 415-417.

Saunders, W.R., Germeroth, R.M., 1985. Electromagnetic Measurements for Subsurface Hydrocarbon Investigations, in Proceedings of the NWWA/APIC Conference on Petroleum Hydrocarbons and Organic Chemicals in Ground Water - Prevention, Detection and Restoration, November 13-15, 1985, The Westin Galleria, Houston Texas (Dublin, Ohio: Water Well Journal Publishing Co.), 1985), pp. 310-321.

Sherwin, J. and Witten, A., 1991. Geophysical Methods Used to Investigate a Radioactive Waste Burial Site, in Proceedings of the Symposium on the Application of Geophysics to Engineering and Environmental Problems, March 11-14, 1991. University of Tennessee, Knoxville, Tennessee (Golden, Colorado: Society of Engineering and Mineral Exploration Geophysicists, 1991) 343 pp.

Stone, W.J., Lyford, F.P., Frenzel, P.F., Mizell, N.H. and Padgett, E.T., 1983. Hydrogeology and the Water Resources of the San Juan Basin, New Mexico: New Mexico Bureau of Mines and Mineral Resources, Hydrologic Report 6. pp. 48-57.

Valentine, R.M. and Kwader, T., 1985. Terrain Conductivity as a Tool for Delineating Hydrocarbon Plumes in A Shallow Aquifer- A Case Study in NWWA, pp. 52-63.

Wait, J.R., 1982. Geo-Electromagnetism Academic Press, New York.

Complimentary Uses of EM-31 and Dipole-Dipole resistivity to Locate the Source of Oil Brine Contamination: A Case Study; Proceedings of the Second National Outdoor Action Conference on Aquifer Restoration, Groundwater Monitoring, and Geophysical Methods: May 23-26, 1988, Las Vegas Hilton, Las Vegas, Nevada. pp 583-595.

APPENDICES

APPENDIX A:
TABLES

<u>MODE OF INSTRUMENT</u>	<u>EM-38 DEPTH OF PENETRATION (m)</u>	<u>EM-31 DEPTH OF PENETRATION (m)</u>
VERTICAL SURFACE	1.50	5.49
VERTICAL KNEE	0.97	4.94
VERTICAL HIP	0.55	4.59
HORIZONTAL SURFACE	0.75	2.75
HORIZONTAL KNEE	0.20	2.20
HORIZONTAL HIP	0.05	1.85

	<u>EM-34 DEPTH OF PENETRATION (m) at INTERCOIL SPACING OF:</u>		
	<u>10.00 m</u>	<u>20.00 m</u>	<u>40.00 m</u>
VERTICAL SURFACE	15.00	30.00	60.00
HORIZONTAL SURFACE	7.50	15.00	30.00

Table 1. Depth of penetration of EM instruments at different heights above the ground.

TRANSECTS IN WHICH THE FISSURE
IS VISIBLE FROM THE SURFACE

TRANSECTS IN WHICH THE FISSURE
IS NOT VISIBLE FROM THE SURFACE

B

C

F

A

D

E

G

Table 2. Transects in which fissure is visible from the surface and transects in which fissures are not visible.

Description of measurements	Number of Transects	Number of Transects fissure was detected	Number of Transects fissure was not detected	Number of Transects which were hard to decipher
EM-38VS	7	6	1	0
EM-38VK	7	4	3	0
EM-38VH	7	3	4	0
EM-38HS	7	4	3	0
EM-38HK	7	3	4	0
EM-38HH	7	3	4	0
EM-31VS	7	4	2	1
EM-31VK	7	3	3	1
EM-31VH	7	3	3	1
EM-31HS	7	3	3	1
EM-31HK	7	4	2	1
EM-31HH	7	4	3	0

Table 3. Summary of SAS Statistical Program showing agreement with Distance VS Conductivity Plots with Coils of EM Instrument Parallel to Fissure.

Description of measurements	Number of Transects	Number of Transects fissure was detected	Number of Transects fissure was not detected	Number of Transects which were hard to decipher
EM-38VS	7	7	0	0
EM-38VK	7	7	0	0
EM-38VH	7	7	0	0
EM-38HS	7	7	0	0
EM-38HK	7	7	0	0
EM-38HH	7	7	0	0
EM-31VS	7	7	0	0
EM-31VK	7	7	0	0
EM-31VH	7	7	0	0
EM-31HS	7	7	0	0
EM-31HK	7	7	0	0
EM-31HH	7	6	1	0

Table 4. Summary of SAS Statistical Program showing agreement with Distance VS Conductivity Plots with Coils of EM Instrument Perpendicular to Fissure.

	EM38VS	EM38VK	EM38VH	EM38HS	EM38HK	EM38HH
WIDTH	2	2	2	2	2	3
STATION	11	13	8 10 13 16	15	7 10 15	4 16
METERS	47.5	51	35 45 51 60	55	30 45 55	15 60
WIDTH	5,8	5	5	3,5	3	5
STATION	11,11	11,16	10,16	5 12 15,12 15	5 10 16	11 16
METERS	47.5,47.5	47.5,60	45,60	20 50 55,50 55	20 45 55	47.5 60
	EM31VS	EM31VK	EM31VH	EM31HS	EM31HK	EM31HH
WIDTH	3	3	3	3	3	3
STATION	6 11 16	6 11 16	7 11 16	5 11 15	5 12 15 16	7 11
METERS	25 47.5 60	25 47.5 60	30 47.5 60	20 47.5 55	20 50 55 60	30 47.5
WIDTH	5	---	---	5	5	---
STATION	11 16	---	---	16	12 16	---
METERS	47.5 60	---	---	60	50 60	---

Table 5. Transect A1-A2 EM Instrument Coils Parallel to the Fissure

Note: **Bolded numbers indicate fissure location agreement between distance versus conductivity plots and SAS program. Regular font values show distances where fissures may have been detected. The window widths are defined by the SAS program.**

	EM38VS	EM38VK	EM38VH	EM38HS	EM38HK	EM38HH
WIDTH	3	3	3	3	3	3
STATION	9 25	7 8 9 10 24 25	7 8 24	9 28	8 9 19	8 9 20
METERS	15 34	12 14 15 16 32 34	12 14 32	15 40	14 15 25	14 15 26
WIDTH	5	5	5	5	3	3
STATION	9 10 24	7 8 9 10	6 7 8	8 9 10 28	20 24 30	21 24 30
METERS	15 16 32	12 14 15 16	10 12 14	14 15 16 40	26 32 44	27 32 44
WIDTH	5	5	5	---	5	5
STATION	25 26	17 24 25	9 17 24	---	7 8 9 10	7 8 9 10
METERS	34 36	23 32 34	15 23 32	---	12 14 15 16	12 14 15 16
WIDTH	8	8	8	---	5	5
STATION	9 10 23 24 25	7 8 24	8 9 10 11 23 24	---	19 20 21 22	19 20 21 22
METERS	15 16 30 32 34	12 14 32	14 15 16 17 30 32	---	25 26 27 28	25 26 27 28

Table 6. (page 1 of 3) Transect B1-B2 EM Instrument Coils Parallel to the Fissure

	EM31VS	EM31VK	EM31VH	EM31HS	EM31HK	EM31HH
WIDTH	2	3	3	3	3	3
STATION	6 9 11	5 6 17	17 30	4 9 20 24,	4 8 9 14 30,	7 8 22 30
METERS	10 15 17	8 10 23	23 44	6 15 26 32,	6 14 15 20 44,12 14 28 44	
WIDTH	3	3	---	---	---	---
STATION	6 11 16 17 22 23, 18 22 23		---	---	---	---
METERS	10 17 22 23 28 30, 24 28 30		---	---	---	---
WIDTH	5	5	5	5	5	5
STATION	5 6 7 8 16 17	5 6 7 16 17	5 6 7 16 17,	7 8 9 10,	7 8 9	7 8 9
METERS	8 10 12 14 22 23	8 10 12 22 23,8 10 12 22 23,12 14 15 16,	12 14 15 16,	12 14 15	12 14 15	12 14 15
WIDTH	5	5	5	5	5	5
STATION	18 21 22 23	18 22 23 24	18 23 24	18 19 20 21,	19 20 21 22,	19 20 21 22
METERS	24 27 28 30	24 28 30 32	24 30 32	24 25 26 27,	25 26 27 28,	25 26 27 28

Table 6. (page 2 of 3) Transect B1-B2 EM Instrument Coils Parallel to the Fissure

	EM31VS	EM31VK	EM31VH	EM31HS	EM31HK	EM31H
WIDTH	8	8	---	---	---	---
STATION	8 9 10 16 17 18, 8 9 10 16-21		---	---	---	---
METERS	14 15 16 22 23 24, 14 15 16 22-27		---	---	---	---

Table 6. (page 3 of 3) Transect B1-B2 EM Instrument Coils Parallel to the Fissure

Note: Bolded numbers indicate fissure location agreement between distance versus conductivity plots and SAS program. Regular font values show distances where fissures may have been detected. The window widths are defined by the SAS program.

	EM38VS	EM38VK	EM38VH	EM38HS	EM38HK	EM38HH
WIDTH	2	2	---	---	---	---
STATION	13 16 23 31 35,8 16 20 31 35,	---	---	---	---	---
METERS	20 23 32 48 56,14 23 27 48 56,	---	---	---	---	---
WIDTH	3	3	3	3	3	3
STATION	7 8 13 16 20 28 35,8 16 22 35,	3 8 12 16 31	8 16 20 35,	7 8 16 25 35,	3 8 16 25 31	
METERS	12 14 20 23 27 42 56,14 23 30 56,	4 14 19 23 48	14 23 27 56,	12 14 23 36 56,	4 14 23 36 48	
WIDTH	5	5	5	5	5	5
STATION	7 8 9 16 27 36,	7 8 9	7 8 9 16	7 8 9 21 27,	7 8 9 16,	7 8 9 16 17
METERS	12 14 16 23 40 58	12 14 16	12 14 16 23	12 14 16 28 40,12 14 16 23,12 14 16 23 24		
WIDTH	---	5	---	---	5	5
STATION	---	16 17	---	---	17 18 25 26	24 25 26 36
METERS	---	23 24	---	---	24 25 36 38	34 36 38 58
WIDTH	8	---	---	---	---	---
STATION	8 9 10 16-20	---	---	---	---	---
METERS	14 16 17 23-27	---	---	---	---	---

Table 7. (page 1 of 2) Transect C1-C2 EM Instrument Coils Parallel to the Fissure

	EM31VS	EM31VK	EM31VH	EM31HS	EM31HK	EM31HH
WIDTH	3	---	---	---	3	---
STATION	8 9 20 21	---	---	---	8 18 24 27 28	---
METERS	14 16 27 28	---	---	---	14 25 34 40 42	---
WIDTH	3	---	---	---	---	---
STATION	34 38 39	---	---	---	---	---
METERS	54 62 64	---	---	---	---	---
WIDTH	5	5	5	5	5	5
STATION	8 9 20 21	6 7 8 9	7 8 9 19,	7 8 9 17 18,	7 8 9	8 9'10 16
METERS	14 16 27 28	10 12 14 16	12 14 16 26,12	14 16 24 25,12	14 16	14 16 17 23
WIDTH	5	5	5	5	5	---
STATION	27 28	20 21 27 28	20 21 27 28,	19 24 25 26,	18 19 25 26	---
METERS	40 42	27 28 40 42	27 28 40 42,	26 34 36 38,	25 26 36 38	---

Table 7. (page 2 of 2) Transect C1-C2 EM Instrument Coils Parallel to the Fissure

Note: Bolded numbers indicate fissure location agreement between distance versus conductivity plots and SAS program. Regular font values show distances where fissures may have been detected. The window widths are defined by the SAS program.

	EM38VS	EM38VK	EM38VH	EM38HS	EM38HK	EM38HH
WIDTH	2	---	---	---	---	---
STATION	13	---	---	---	---	---
METERS	12	---	---	---	---	---
WIDTH	3	3	---	---	---	---
STATION	10 13 17 22 72	4 58	---	---	---	---
METERS	9 12 16 21 71	3 57	---	---	---	---
WIDTH	5	5	5	5	5	5
STATION	10 11 17	11 12 16 17,16 17 22 39 46, 44-47 52 53 67,16 17 22 37 38,16 17 22 46 47				
METERS	9 10 16	10 11 15 16,15 16 21 38 45, 43-46 51 52 66,15 16 21 36 37,15 16 21 45 46				
WIDTH	5	5	5	---	5	5
STATION	44-47 53 54	45-47 67-69,47 52 53 68 69	---	---	45 46 51 52 67 68,52 53 62 67-69	
METERS	43-46 52 53	44-46 66-68,46 51 52 67 68	---	---	44 45 50 51 66 67,51 52 61 66-68	
WIDTH	8	8	8	8	8	8
STATION	8-11 44-47 54	43-47 66-68,22 45-47 66-68, 44-47 53 66 67,44-47 53-55 67 68,45-47 67 68				
METERS	7-10 43-46 53	42-46 65-67,21 44-46 65-67, 43-46 52 65 66 43-46 52-54 66 67,44-46 66 67				

Table 8. (page 1 of 3) **Transect D1-D2 EM Instrument Coils Parallel to the Fissure**

	EM31VS	EM31VK	EM31VH	EM31HS	EM31HK	EM31HH
WIDTH	3	3	---	---	---	---
STATION	40 69	6 45 69	---	---	---	---
METERS	39 68	5 44 68	---	---	---	---
WIDTH	5	5	5	5	5	5
STATION	7 8 14-16 22 23, 6-15 39 40,	10-13 44	11-13 37,	24 25 33 34,	10 43-45 51	
METERS	6 7 13-15 21 22, 5-14 38 39	9-12 43	10-12 36,	23 24 32 33	9 42-44 50	
WIDTH	5	5	5	5	5	5
STATION	40 41 54 67-69, 45 46 54 67-69,	53 67 68	45-48 65-68,	54 55 66-68	52 65-67	
METERS	39 40 53 66-68, 44 45 53 66-68,	52 66 67	44-47 64-67,	53 54 65-67	51 64-66	
WIDTH	8	8	8	8	8	8
STATION	8-16 32 33 40 41,	8-15 32 53 54, 8-16 32 44,	9-12 43-48,	12 13 24 25,	9-11 42-46	
METERS	7-15 31 32 39 40,	7-14 31 52 53, 7-15 31 43,	8-11 42-47,	11 12 23 24,	8-10 41-45	

Table 8. (page 2 of 3) Transect D1-D2 EM Instrument Coils Parallel to the Fissure

	EM31VS	EM31VK	EM31VH	EM31HS	EM31HK	EM31HH
WIDTH	8	8	8	---	8	8
STATION	53 54 66-68	66-68, 45 52 53 65-68	---	---	32-34 54 55 65-68, 52-54 64-67	
METERS	52 53 65-67	65-67, 44 51 52 64-67	---	---	31-33 53 54 64-67, 51-53 63-66	

Table 8. (page 3 of 3) **Transect D1-D2 EM Instrument Coils Parallel to the Fissure**

Note: *Bolded numbers indicate fissure location agreement between distance versus conductivity plots and SAS program. Regular font values show distances where fissures may have been detected. The window widths are defined by the SAS program.*

	EM38VS	EM38VK	EM38VH	EM38HS	EM38HK	EM38HH
WIDTH	2	---	---	3	3	3
STATION	4 22 24 27 29 49	---	--- 4 7 11 16 39 40 55 56 65,3 7 10 13,			4 7 40 58
METERS	3 21 23 26 28 48	---	--- 3 6 10 15 38 39 54 55 64,			3 6 39 57
WIDTH	3	---	5	5	3	
STATION	4 29 40 65	---	12-19 38-41 48,	11 16 39 40 55	66 71	
METERS	3 28 39 64	---	11-18 37-40 47,	10 15 38 39 54	65 70	
WIDTH	5	5	5	5	5	
STATION	17 19 40 69,	38-41 48 58,	57 65-71	56 65 66-71	7 32 40 41 58 69	
METERS	16 18 39 68,	37-40 47 57,	56 64-70	55 64 65-70	6 31 39 40 57 68	
WIDTH	8	5	8	8	8	
STATION	15-19 40 41 64-67,	65 66 71,	15-18 37-41,	11 19 38-40 39,	39 40 56-59 66-68	
METERS	14-18 39 40 63-66,	64 65 70,	14-17 36-40	10 18 37-39,	38 39 55-58 65-67	
WIDTH	---	8	8	8	---	
STATION	---	15-19 38-41 65-68,	66-68	63-68	---	
METERS	---	14-18 37-40 64-67,	65-67	62-67	---	

Table 9. (page 1 of 3) Transect E1-E2 EM Instrument Coils Parallel to the Fissure

	EM31VS	EM31VK	EM31VH	EM31HS	EM31HK	EM31HH
WIDTH	3	3	3	3	3	3
STATION	6 19 22 26 27	19 22 26 53	19 67	20 33 36	8 20 53 68	3 7 40 56 57 66
METERS	5 18 21 25 26	18 21 25 52	18 66	19 32 35	7 19 52 67	2 6 39 54 56 65
WIDTH	3	3	5	5	5	5
STATION	53 56 60 63	57 60 68	6-9 18-21 25,	20 36-38,	7 8 20 37	7 15 16 21-23
METERS	52 55 59 62	56 59 67	5-8 17-20 24,	19 35-37	6 7 19 36	6 14 15 20-22
WIDTH	5	5	5	5	5	5
STATION	6 19 24-27 53,	6 7 17-20 25-27,	26 61-64,	64 67 68	38 68	37 38 56 57 65 66
METERS	5 18 23-26 52	5 6 16-20 24-26,	25 60-63,	63 66 67	37 67	36 37 55 56 64 65
WIDTH	8	5	8	8	8	8
STATION	18-27 52-56 60-65,	34 53 63 68,	8-10 17-26,	8 20-24	8 9 20 22-24,	8 9 20-23
METERS	17-26 51-55 59-64,	33 52 62 67,	7-9 16-25,	7 19-23	7 8 19 21-23	7 8 19-23

Table 9. (page 2 of 3) Transect E1-E2 EM Instrument Coils Parallel to the Fissure

	EM38VS	EM38VK	EM38VH	EM38HS	EM38HK	EM38HH
WIDTH	2	---	---	---	---	---
STATION	6 10 16 31 35	---	---	---	---	---
METERS	10 18 28 43 48	---	---	---	---	---
WIDTH	2	---	---	---	---	---
STATION	38 40 45 47	---	---	---	---	---
METERS	54 58 68 72	---	---	---	---	---
WIDTH	3	3	---	3	---	---
STATION	6 7 10 19 31 34,6 9 10 13 25 31,	---	---	10 13 30 39 40 43	---	---
METERS	10 12 18 31 43 46,10 16 18 24 37 43	---	---	18 22 42 54 58 64	---	---
WIDTH	3	3	---	---	---	---
STATION	35 38-40 45 46, 32 35 38 39 44	---	---	---	---	---
METERS	48 54-58 68 70, 44 48 54 56 66	---	---	---	---	---
WIDTH	4	---	---	---	---	---
STATION	6 23 28 35-41 45	---	---	---	---	---
METERS	10 35 40 48-60 68	---	---	---	---	---

Table 10. (page 1 of 4) Transect F1-F2 EM Instrument Coils Parallel to the Fissure

	EM38VS	EM38VK	EM38VH	EM38HS	EM38HK	EM38HH
WIDTH	5	5	5	5	5	5
STATION	5 6 21 25 26 28 35-41,	14 19 25 26, 24-26 35-38	10 15 21 35-40, 9 14 32-37	10 15 21 35-40, 9 14 32-37	10 15 21 35-40, 9 14 32-37	10 11 29
METERS	8 10 33 37 38 40 48-60,	26 31 37 38, 36-38 48 54	18 27 33 48-58,16 26 44-52	18 27 33 48-58,16 26 44-52	18 27 33 48-58,16 26 44-52	18 20 41
WIDTH	6	5	---	---	---	5
STATION	6 7 19-21 24-26 38-41,	38 39	---	---	---	34-36 41
METERS	10 12 31-33 36-38 54-60	54-56	---	---	---	46-50 60
WIDTH	7	---	---	---	---	---
STATION	7 23-26 28 25-41	---	---	---	---	---
METERS	12 35-38 40 57-60	---	---	---	---	---
WIDTH	8	8	8	8	8	8
STATION	8 9 25 28 35-41 17 18 24-26 35-40, 16-18 24-26, 9 10 18 19 37-40,9 14 32-37, 10 11 32-38	17 18 24-26 35-40, 16-18 24-26, 9 10 18 19 37-40,9 14 32-37, 10 11 32-38	17 18 24-26 35-40, 16-18 24-26, 9 10 18 19 37-40,9 14 32-37, 10 11 32-38	17 18 24-26 35-40, 16-18 24-26, 9 10 18 19 37-40,9 14 32-37, 10 11 32-38	17 18 24-26 35-40, 16-18 24-26, 9 10 18 19 37-40,9 14 32-37, 10 11 32-38	17 18 24-26 35-40, 16-18 24-26, 9 10 18 19 37-40,9 14 32-37, 10 11 32-38
METERS	14 16 37 40 48-60 29 30 36-38 48-58 28-30 36-38,16 18 30 31 52-58,16 26 44-52, 18 20 44-54	29 30 36-38 48-58 28-30 36-38,16 18 30 31 52-58,16 26 44-52, 18 20 44-54	29 30 36-38 48-58 28-30 36-38,16 18 30 31 52-58,16 26 44-52, 18 20 44-54	29 30 36-38 48-58 28-30 36-38,16 18 30 31 52-58,16 26 44-52, 18 20 44-54	29 30 36-38 48-58 28-30 36-38,16 18 30 31 52-58,16 26 44-52, 18 20 44-54	29 30 36-38 48-58 28-30 36-38,16 18 30 31 52-58,16 26 44-52, 18 20 44-54
WIDTH	---	---	8	---	---	---
STATION	---	---	35-40	---	---	---
METERS	---	---	34-39	---	---	---

Table 10. (page 2 of 4) Transect F1-F2 EM Instrument Coils Parallel to the Fissure

	EM31VS	EM31VK	EM31VH	EM31HS	EM31HK	EM31HH
WIDTH	2	3	3	3	3	3
STATION	11 15 16 30 35 37,	9 10 16 36,	5 10 18	7 10 23	10 11 23	10 11 23 33
METERS	20 27 28 42 48 52,16 18 28 50,	8 18 30	12 18 35	18 20 35	18 20 35 45	
WIDTH	3	3	3	3	3	3
STATION	5 10 11 15 27,	39 42	34 40 44	32 35 40	34 43	34 40 44
METERS	8 18 20 27 39,	56 62	46 58 66	44 48 58	46 64	46 56 66
WIDTH	3	5	5	5	5	5
STATION	30 25-39 41,	9-12 17 38 39,	10 18 35 40	11 22-24,10 23 33-36 43	11 23 33 34 40	
METERS	42 37-56 60,16-22 29 54 56,	18 30 48 58	20 34-36,18 35 45-50 64	20 35 45 46 58		
WIDTH	5	8	8	5	8	8
STATION	9-12 17 18 36 37 41,9-13 18-23,	8-12 18-21	32-35 40,	10 11 24	10 11 23 31-41	
METERS	16-22 29 30 50 52 60,16-24 30-34,14-22 30-33 44-48 58	18 20 36	18 20 35 43-60			

Table 10. (page 3 of 4) Transect F1-F2 EM Instrument Coils Parallel to the Fissure

	EM31VS	EM31VK	EM31VH	EM31HS	EM31HK	EM31HH
WIDTH	8	8	8	8	8	---
STATION	9-12 20 21 33-41,	36 38 39	34-41,10 11 22 23 31-41	32 34	---	---
METERS	16-22 32 33 45-60,	50 54 56	46-60,18 20 34 35 43-60	44 46	---	---

Table 10. (page 4 of 4) Transect F1-F2 EM Instrument Coils Parallel to the Fissure

Note: Bolded numbers indicate fissure location agreement between distance versus conductivity plots and SAS program. Regular font values show distances where fissures may have been detected. The window widths are defined by the SAS program.

	EM38VS	EM38VK	EM38VH	EM38HS	EM38HK	EM38HH
WIDTH	3	3	---	3	3	3
STATION	3 9 16 23	3 10 11 14 21	---	19 23 28 39,	3 21 25	11 12 21 23 30
METERS	2 8 15 22	2 9 10 13 20	---	18 22 27 38	2 20 24	10 11 20 22 29
WIDTH	3	3	---	---	3	5
STATION	28 35 38	24 25 33	---	---	30 36 39, 11 12 19-21 30	
METERS	27 34 37	23 24 32	---	---	29 35 38, 10 11 18-20 29	
WIDTH	5	5	5	5	5	---
STATION	10 21 28	5 14 15 20-25 36, 5 11 20-25 35,	19 23 28	20 21 30	---	---
METERS	9 20 27	4 13 14 19-24 35, 4 10 19-24 34,	18 22 27	19 20 29	---	---
WIDTH	8	8	8	8	8	8
STATION	10 11 23 24 28	21	11 21	16 28 31 19-21 29-34,	19-21 29-34	
METERS	9 10 22 23 27	20	10 20	15 27 30 18-20 28-33,	18-20 28-33	
WIDTH	---	---	---	---	---	---
STATION	---	---	---	---	---	---
METERS	---	---	---	---	---	---

Table 11. (page 1 of 3) Transect G1-G2 EM Instrument Coils Parallel to the Fissure

	EM31VS	EM31VK	EM31VH	EM31HS	EM31HK	EM31HH
WIDTH	3	3	3	3	3	3
STATION	5 16 19 23	3 19 22-25	6 23 33 36	19 23 25 30	9 29 35	4 9 12 20
METERS	4 15 18 22	2 18 21-24	5 22 32 35	18 22 23 29	8 28 34	3 8 11 19
WIDTH	3	3	---	---	---	3
STATION	37 38	29 37	---	---	---	25 29 33 34
METERS	36 37	28 36	---	---	---	24 28 32 33
WIDTH	5	5	5	5	5	5
STATION	5 10 16 22-25 36	22-26 36,	6 15 17	11 24 25 30,	17 22-24	11 14 22 23
METERS	4 9 15 21-24 35	21-25 35,	5 14 16	10 23 24 29,	16 21-23	10 13 21 22
WIDTH	8	8	5	8	5	5
STATION	8 9 21-27	21-27	21-26 36	11 22 23 30	29 35	30 32-35
METERS	7 8 20-26	20-26	20-25 35	10 21 22 29	28 34	29 31-34
WIDTH	---	---	8	---	8	8
STATION	---	---	8 15 16 23 24	---	14 15 23 29-33	11 12 20 33
METERS	---	---	7 14 15 22 23	---	13 14 22 28-32	10 11 19 32

Table 11. (page 2 of 3) Transect G1-G2 EM Instrument Coils Parallel to the Fissure

	EM31VS	EM31VK	EM31VH	EM31HS	EM31HK	EM31HH
WIDTH	---	---	8	---	8	8
STATION	---	8 15 16 23 24	8 15 16 23 24	---	14 15 23 29-33	11 12 20 33
METERS	---	7 14 15 22 23	7 14 15 22 23	---	13 14 22 28-32	10 11 19 32

Table 11. (page 3 of 3) Transect G1-G2 EM Instrument Coils Parallel to the Fissure

Note: *Bolded numbers indicate fissure location agreement between distance versus conductivity plots and SAS program. Regular font values show distances where fissures may have been detected. The window widths are defined by the SAS program.*

	EM38VS	EM38VK	EM38VH	EM38HS	EM38HK	EM38HH
WIDTH	5	5	5	3, 5	5	5
STATION	10	10 15	10 15	5 10 14, 10 15	10 15	10 15
METERS	45	45 55	45 55	20 45 52, 45 55	45 55	45 55
WIDTH	---	---	---	7	---	---
STATION	---	---	---	12	---	---
METERS	---	---	---	50	---	---
	EM31VS	EM31VK	EM31VH	EM31HS	EM31HK	EM31HH
WIDTH	3	2,3	2,3	3	---	3
STATION	6 10 15	7 12 14, 7 10 16	9 12 16, 6 10 16	5 10 15	---	5 10 16
METERS	25 45 55	30 50 52, 30 45 60	40 50 60, 25 45 60	20 45 55	---	20 45 60
WIDTH	5	5	5	5	5	5
STATION	7 15 16	7 16	11 16	10 15	10 15	10 15
METERS	30 55 60	30 60	47.5 60	45 60	45 60	45 55

Table 12. Transect A1-A2 EM Instrument Coils Perpendicular To the Fissure

Note: Bolded numbers indicate fissure location agreement between distance versus conductivity plots and SAS program. Regular font values show distances where fissures may have been detected. The window widths are defined by the SAS program.

	EM38VS	EM38VK	EM38VH	EM38HS	EM38HK	EM38HH
WIDTH	5	5	5	5	5	5
STATION	9	7	14	7 14 17	7 15 21	6 15
METERS	16	14	21	14 21 24	14 22 28	12 22

	EM31VS	EM31VK	EM31VH	EM31HS	EM31HK	EM31HH
WIDTH	5	5	5	5	5	5
STATION	6	7 17 23	6 17 23	7 19 24	7 19 24	7 20
METERS	12	14 24 32	12 24 32	14 26 34	14 26 34	14 27

Table 13. Transect B1-B2 EM Instrument Coils Perpendicular to the Fissure

Note: *Bolded numbers indicate fissure location agreement between distance versus conductivity plots and SAS program. Regular font values show distances where fissures may have been detected. The window widths are defined by the SAS program.*

	EM38VS	EM38VK	EM38VH	EM38HS	EM38HK	EM38HH
WIDTH	3	3	3	3	3	3
STATION	9 18 21	21 25 35	7 21 25	7 17 25 35	7 16	25 35
METERS	16 25 28	28 36 56	12 28 36	12 24 36 56	12 22	36 56
WIDTH	5	5	5	5	5	5
STATION	9 10 25	8 16 25	7 16 25	8 25 36	7 16 25	7 24
METERS	16 17 36	14 23 36	12 23 36	14 36 58	12 22 36	12 34
WIDTH	8	8	8	8	8	8
STATION	9 10 24	9 29	8 29	8 25 29	8 17 25	8 25
METERS	16 17 34	16 44	14 44	14 36 44	14 24 36	14 36

Table 14. (page 1 of 2) **Transect C1-C2 EM Instrument Coils Perpendicular to the Fissure**

	EM31VS	EM31VK	EM31VH	EM31HS	EM31HK	EM31HH
WIDTH	3	3	---	---	---	---
STATION	9 21 28	9 21 28	---	---	---	---
METERS	16 28 42	16 28 42	---	---	---	---
WIDTH	5	5	5	5	---	5
STATION	9 21 28	10 21 27 28	8 22 27	8 16 28	---	8 20
METERS	16 28 42	18 28 40 42	14 30 40	14 23 42	---	14 27
WIDTH	8	8	8	8	8	---
STATION	9 20 28	8 20 28	8 20 28	8 17 28	8 19 27	---
METERS	16 26 42	14 26 42	14 26 42	14 24 42	14 26 40	---

Table 14. (page 2 of 2) Transect C1-C2 EM Instrument Coils Perpendicular to the Fissure

Note: *Bolded numbers indicate fissure location agreement between distance versus conductivity plots and SAS program. Regular font values show distances where fissures may have been detected. The window widths are defined by the SAS program.*

	EM38VS	EM38VK	EM38VH	EM38HS	EM38HK	EM38HH
WIDTH	2	2	2	---	2	2
STATION	11 63	6 7 8 27 49	27 50 61	----	4	9 50 56
METERS	10 62	5 6 7 26 48	26 49 60	---	3	8 49 55
WIDTH	3, 8	---	3	3	3	3
STATION	12 41, 10 52	---	11 17 40 51	11 18 38	12 17 38 51 68	10 16 28 38 40 44 51 68
METERS	11 40, 9 51	---	10 16 39 50	10 17 37	11 16 37 50 67	9 15 27 37 39 43 50 67
WIDTH	5	5	5	5	5	5
STATION	10 46 58 68	12 40 52 68	18 40 52 68	12 18 38 52 68	16 17 38 52 68	10 38 51 68
METERS	9 45 57 67	11 39 54 67	17 39 51 67	11 17 37 51 67	15 16 37 51 67	9 37 50 67

Table 15. (page 1 of 2) **Transect D1-D2 EM Instrument Coils Perpendicular to the Fissure**

	EM31VS	EM31VK	EM31VH	EM31HS	EM31HK	EM31HH
WIDTH	2	2	---	2	2	2
STATION	18 39 46 56	6 12 24 65	---	18 20	7 28 34 60	49
METERS	17 38 45 55	5 11 23 64	---	17 19	6 27 33 59	48
WIDTH	3	3	3	3	3	3
STATION,	13 22 34 39 64 70 , 8 14 22 40 48 68	15 40 7 19 20 40 52 54 68	4 18 34 68	3 17 33 67	18 39 40 44 57 65 72	17 38 39 43 57 64 71
METERS	12 21 33 38 63 69 , 7 13 21 39 47 67	14 39 6 18 19 39 51 53 67	3 17 33 67	3 17 33 67	17 38 39 43 57 64 71	17 38 39 43 57 64 71
WIDTH	5	5	5	5	5	5
STATION	8 14 34 40 54 70	14 22 34 40 68	13 14 40 68	20 34 40 52 68	5 19 20 34 39 40 65-68	18 41 57 65-68
METERS	7 13 33 39 53 69	13 21 33 39 67	12 13 39 67	19 33 39 51 67	4 18 19 33 38 39 64-67	17 40 56 64-67

Table 15. (page 2 of 2) Transect D1-D2 EM Instrument Coils Perpendicular to the Fissure

Note: *Bolded numbers indicate fissure location agreement between distance versus conductivity plots and SAS program. Regular font values show distances where fissures may have been detected. The window widths are defined by the SAS program.*

	EM38VS	EM38VH	EM38VH	EM38VH	EM38HS	EM38HK	EM38HH
WIDTH	2	2	2	2	2	2	2
STATION	72 74	27 29 46 57 59 62 73	20 45 47 57 70	16 18 49 68	8 20 67	26 32 44 51	25 31 43 50
METERS	71 73	26 28 45 56 58 61 72	19 44 46 56 69	15 17 48 67	7 19 66		
WIDTH	3	3	3	---	---	---	8
STATION	4 19 20 30 34 64	59 62	20 24 42 67	---	---	20 34 42 67	
METERS	3 18 19 29 33 63	58 61	19 23 41 66	---	---	19 33 41 66	
WIDTH	5	5	5	5	5	5	5
STATION	18 19 20 30 65	20 42 67	6 20 35 42 67	5 20 30 50 65	6 20 42 53 67	20 34 42 48 67	
METERS	17 18 19 29 64	19 41 66	5 19 34 41 66	4 19 29 49 64	5 19 41 52 66	19 33 41 47 66	

Table 16. (page 1 of 2) Transect E1-E2 EM Instrument Coils Perpendicular to the Fissure

	EM38VS	EM38VK	EM38VH	EM38HS	EM38HK	EM38HH
WIDTH	2	---	---	---	---	---
STATION	21 24 31	---	---	---	---	---
METERS	33 36 43	---	---	---	---	---
WIDTH	3	3	3	3	3	3
STATION	11 21 24 31 42	7 11 21 24 28 32 42	18 21 25 28 31 38	4 21 25 35 43	4 21 24 38	4 10 21 44
METERS	20 33 36 43 62	12 20 33 36 40 44 62	30 33 37 40 43 54	6 33 37 48 64	6 33 36 54	6 18 33 66
WIDTH	5	5	5	---	---	---
STATION	9 21 24 32 34	9 21 26 30 38 43	9 21 30 38 43	---	---	---
METERS	16 33 36 44 64	16 33 38 42 54 64	16 33 42 54 64	---	---	---
WIDTH	8	---	---	---	---	---
STATION	9 21 26 34 41	---	---	---	---	---
METERS	16 33 38 46 60	---	---	---	---	---

Table 17. (page 1 of 2) Transect F1-F2 EM Instrument Coils Perpendicular to the Fissure

	EM31VS	EM31VK	EM31VH	EM31HS	EM31HK	EM31HH
WIDTH	3	3	3	3	3	3
STATION	12 18 28 34 38 43	7 10 13 22 25 32 42	3 9 14 23 26 33 38	10 17 24 28 33 38 41	10 13 22 30 33 38	9 23 34 38 42 45
METERS	22 30 40 46 54 64	12 18 24 34 37 43 62	4 16 26 35 38 45 54	18 29 36 40 45 54 60	18 24 34 42 45 54	16 35 46 54 62 68
WIDTH	5	5	5	5	5	5
STATION	7 12 33 38 43	7 12 21 32 37 39	9 19 26 34 40	10 19 28 33 41	10 21 33 39	8 33 38
METERS	12 22 45 54 64	12 22 33 44 52 56	16 31 38 46 58	18 31 40 45 60	18 33 45 56	14 45 54
WIDTH	8	---	---	---	---	8
STATION	31 41	---	---	---	---	9 30 38
METERS	14 43 60	---	---	---	---	16 42 54

Table 17. (page 2 of 2) **Transect F1-F2 EM Instrument Coils Perpendicular to the Fissure**

Note: *Bolded numbers indicate fissure location agreement between distance versus conductivity plots and SAS program. Regular font values show distances where fissures may have been detected. The window widths are defined by the SAS program.*

	EM38VS	EM38VK	EM38VH	EM38HS	EM38HK	EM38HH
WIDTH	3	---	---	---	---	---
STATION	3 11 15 25 35	---	---	---	---	---
METERS	2 10 14 24 34	---	---	---	---	---
WIDTH	4	---	---	---	---	---
STATION	4 11 15 35	---	---	---	---	---
METERS	3 10 14 34	---	---	---	---	---
WIDTH	5	---	---	---	---	---
STATION	11 25 30 35	---	---	---	---	---
METERS	10 24 29 34	---	---	---	---	---
WIDTH	8	8	8	8	8	8
STATION	11 21 24 25	8 13 20-25	8 13 20-25	19-22 29 33	19-24 33	19-24
METERS	10 20 23 24	7 12 19-24	7 12 19-24	18-21 28 32	18-23 32	18-23
WIDTH	8	8	8	8	8	8
STATION	19-25	19-25	18-26	20-26	21-26	20-25
METERS	18-24	18-24	17-25	19-25	20-25	19-24

Table 18. Transect G1-G2 EM Instrument Coils Perpendicular to the Fissure

Note: *Bolded numbers indicate fissure location agreement between distance versus conductivity plots and SAS program. Regular font values show distances where fissures may have been detected. The window widths are defined by the SAS program.*

APPENDIX B:
FIGURES

EM38
 DISTANCE VS CONDUCTIVITY OVER SAN MARCIAL FISSURE
 TRANSECT A1-A2
 COILS PARALLEL TO FISSURE

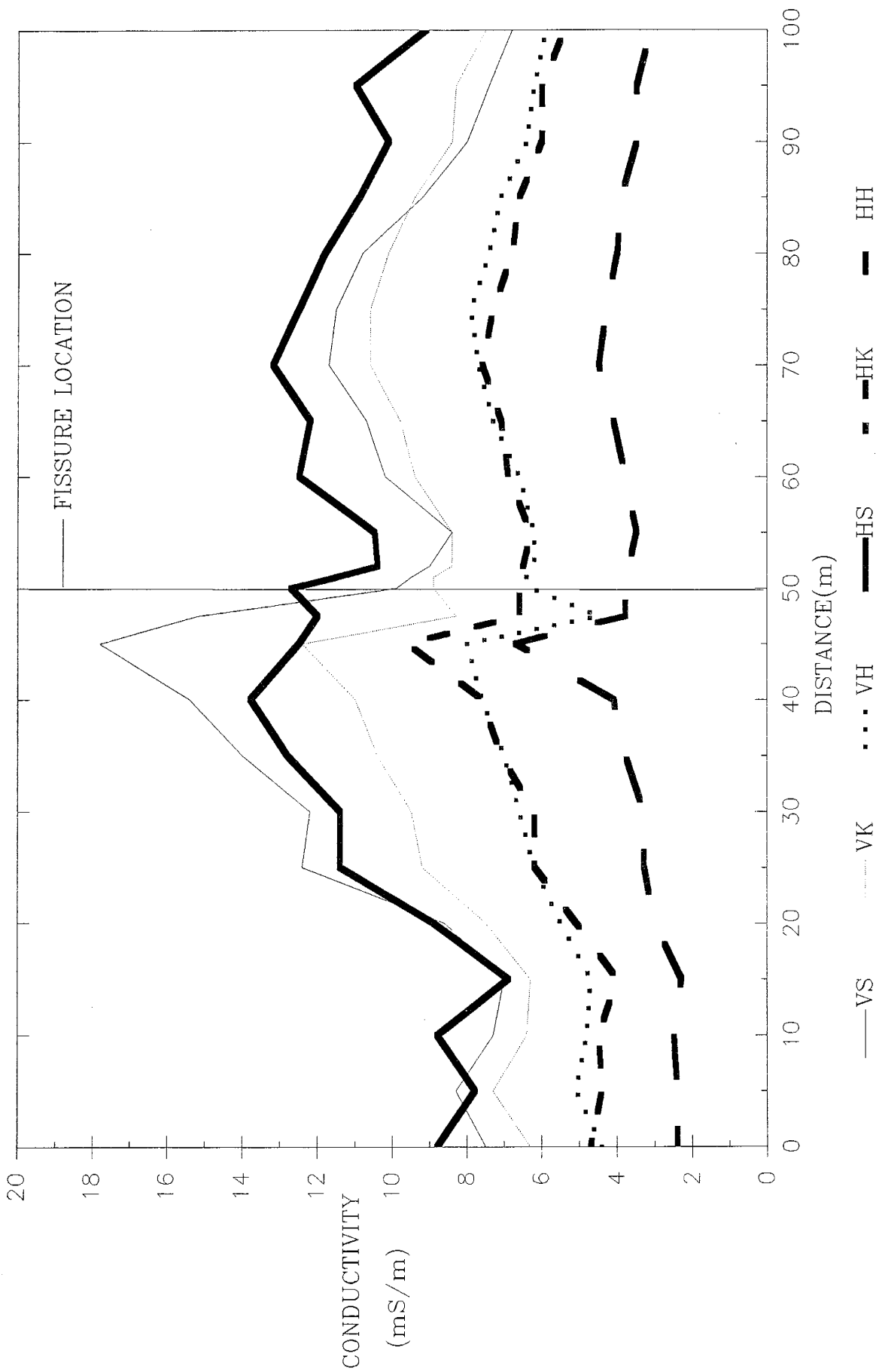


Figure 2. Conductivity vs distance measured with the EM-38 at three heights (surface, knee and hip) at two configurations (vertical and horizontal modes)

EM31
 DISTANCE VS CONDUCTIVITY OVER SAN MARCIAL FISSURE
 TRANSECT A1-A2
 PARALLEL TO FISSURE

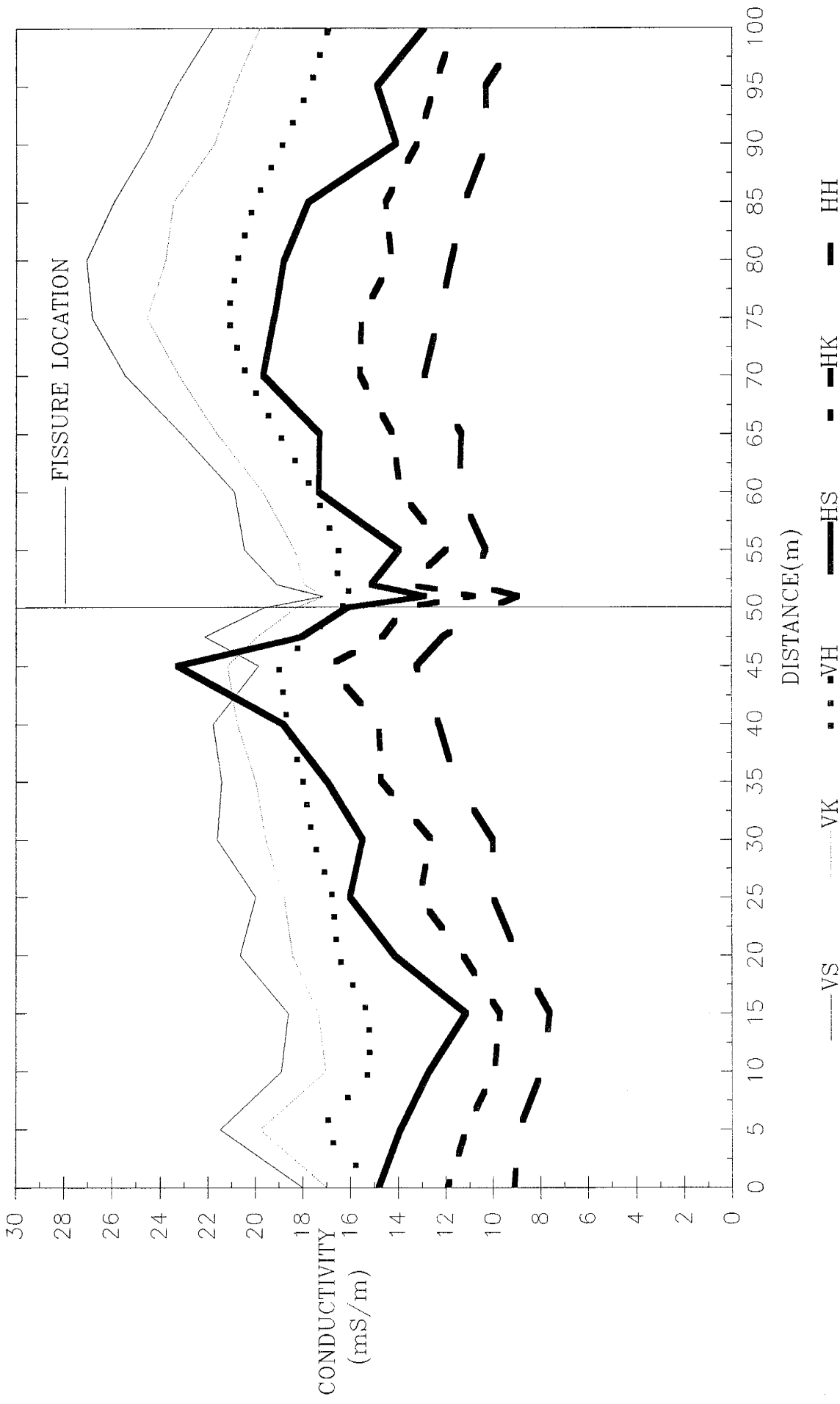


Figure 3. Conductivity vs distance measured with the EM-31 at three heights (surface, knee, and hip) at two configurations (vertical and horizontal modes)

EM34-10
 DISTANCE VS CONDUCTIVITY OVER SAN MARCIAL FISSURE
 TRANSECT A1-A2
 COILS PARALLEL TO FISSURE

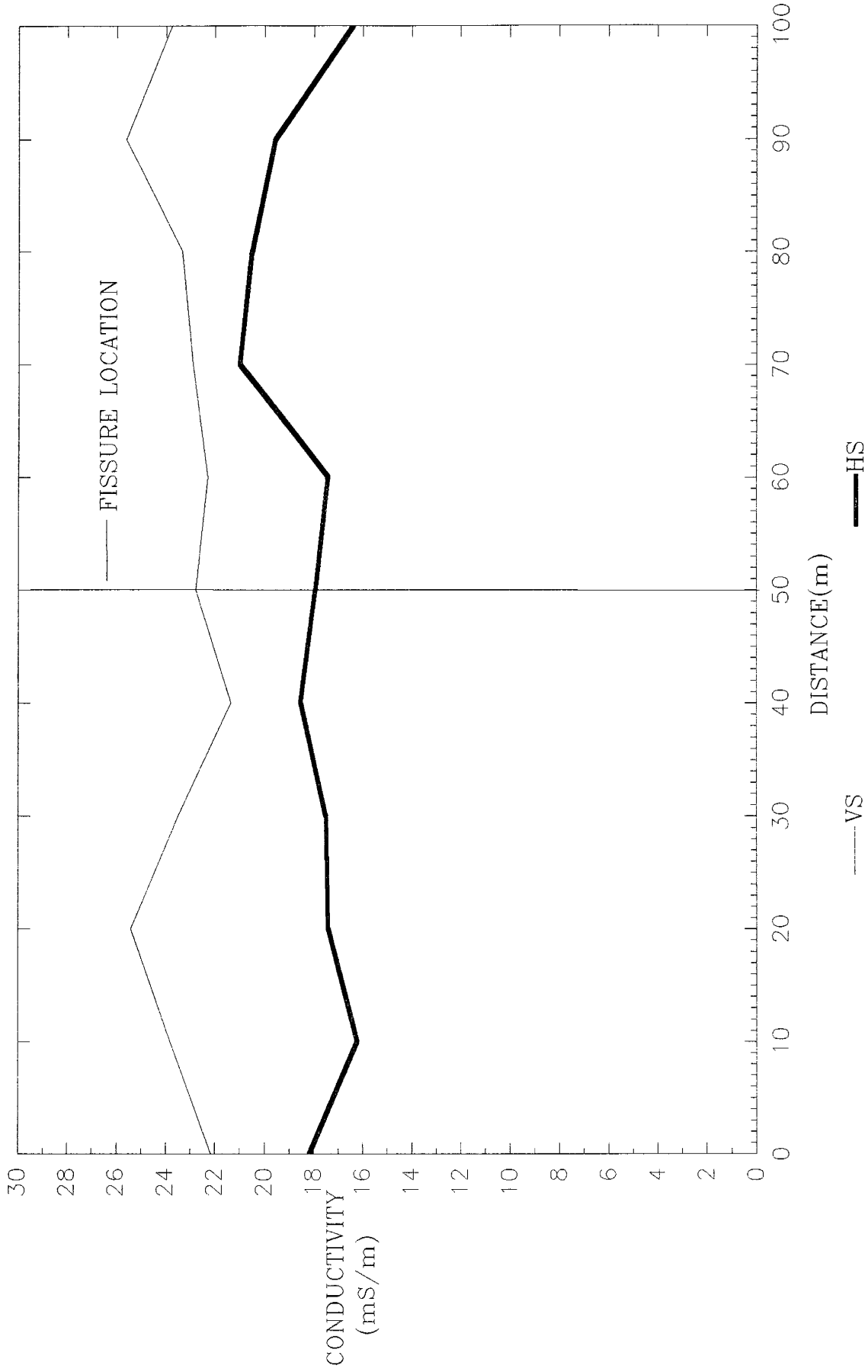


Figure 4. Conductivity vs distance measured with the EM-34 at the 10 meter intercoil spacing at two configurations (vertical and horizontal modes)

EM34-20
 DISTANCE VS CONDUCTIVITY OVER SAN MARCIAL FISSURE
 TRANSECT A1-A2
 COILS PARALLEL TO FISSURE

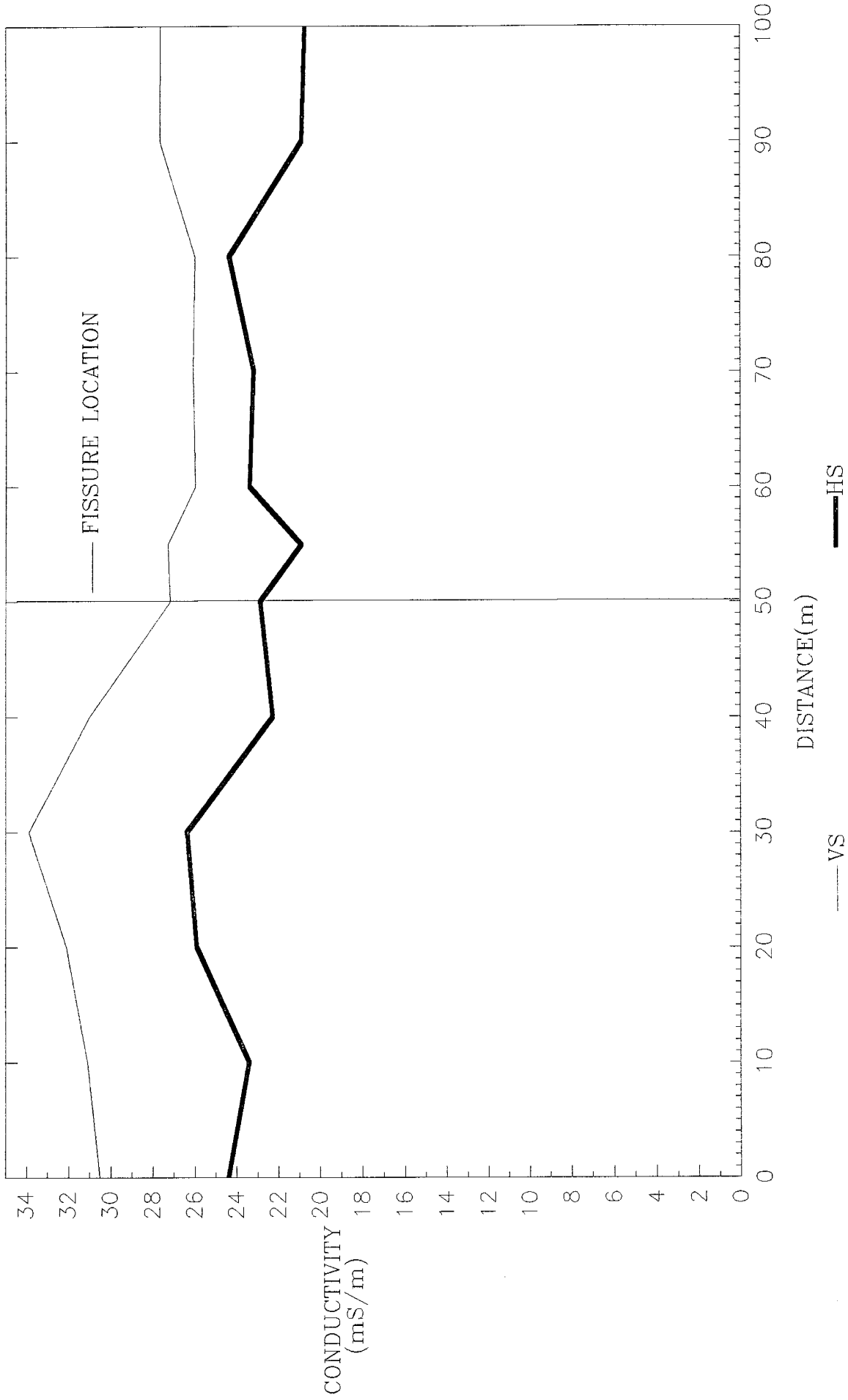


Figure 5. Conductivity vs distance measured with the EM-34 at the 20 meter intercoil spacing at two configurations (vertical and horizontal modes)

EM34--40
 DISTANCE VS CONDUCTIVITY OVER SAN MARCIAL FISSURE
 TRANSECT A1-A2
 PARALLEL TO FISSURE

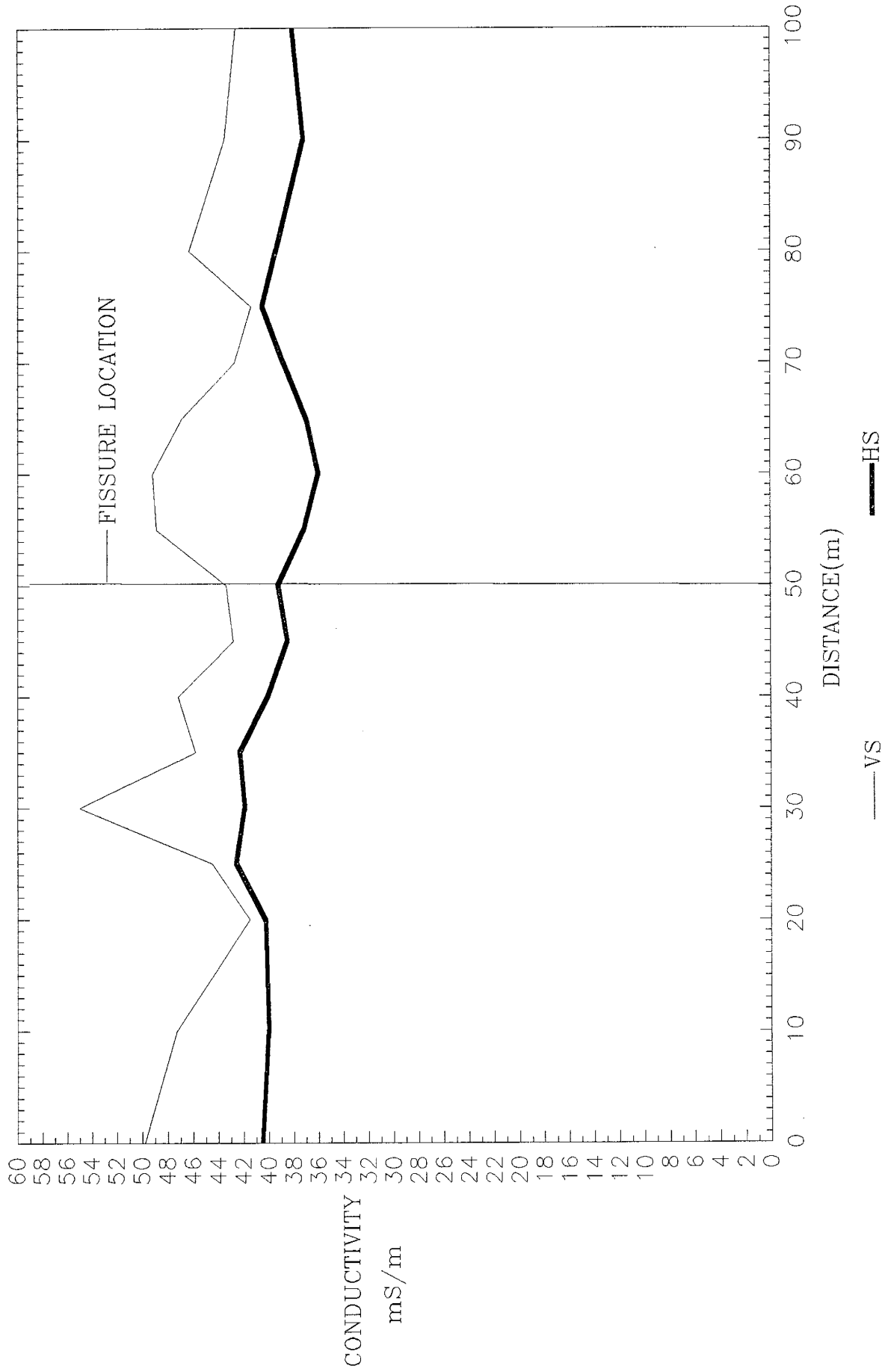


Figure 6. Conductivity vs distance measured with the EM-34 at the 40 meter intercoil spacing at two configurations (vertical and horizontal modes)

EM38
 DISTANCE VS CONDUCTIVITY OVER THE SAN MARCIAL FISSURE
 TRANSECT B1-B2
 COILS PARALLEL TO FISSURE

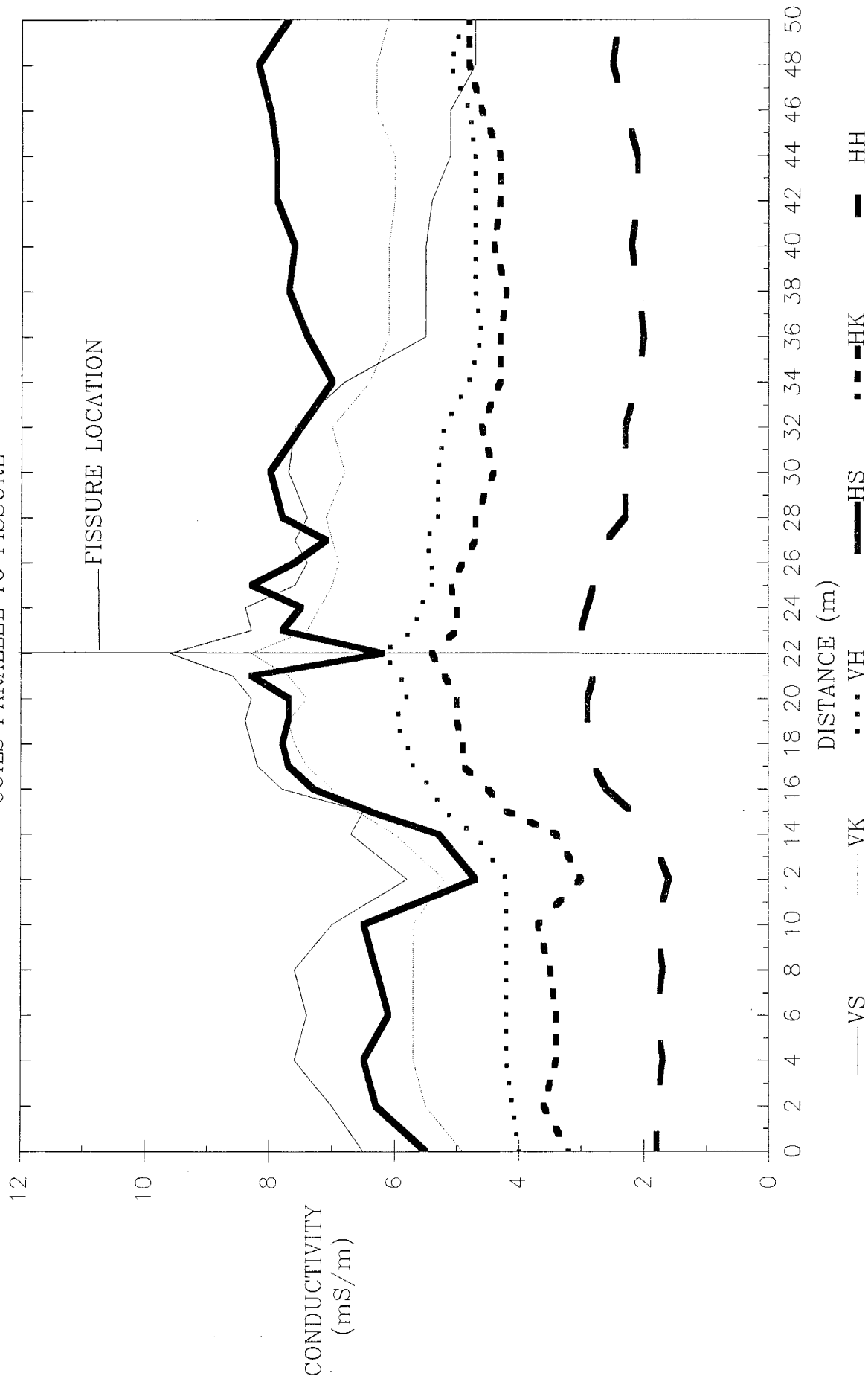


Figure 7. Conductivity vs distance measured with the EM-38 at three heights (surface, knee, and hip) at two configurations (vertical and horizontal modes)

EM31
 DISTANCE VS CONDUCTIVITY OVER THE SAN MARCIAL FISSURE
 TRANSECT B1-B2
 COILS PARALLEL TO FISSURE

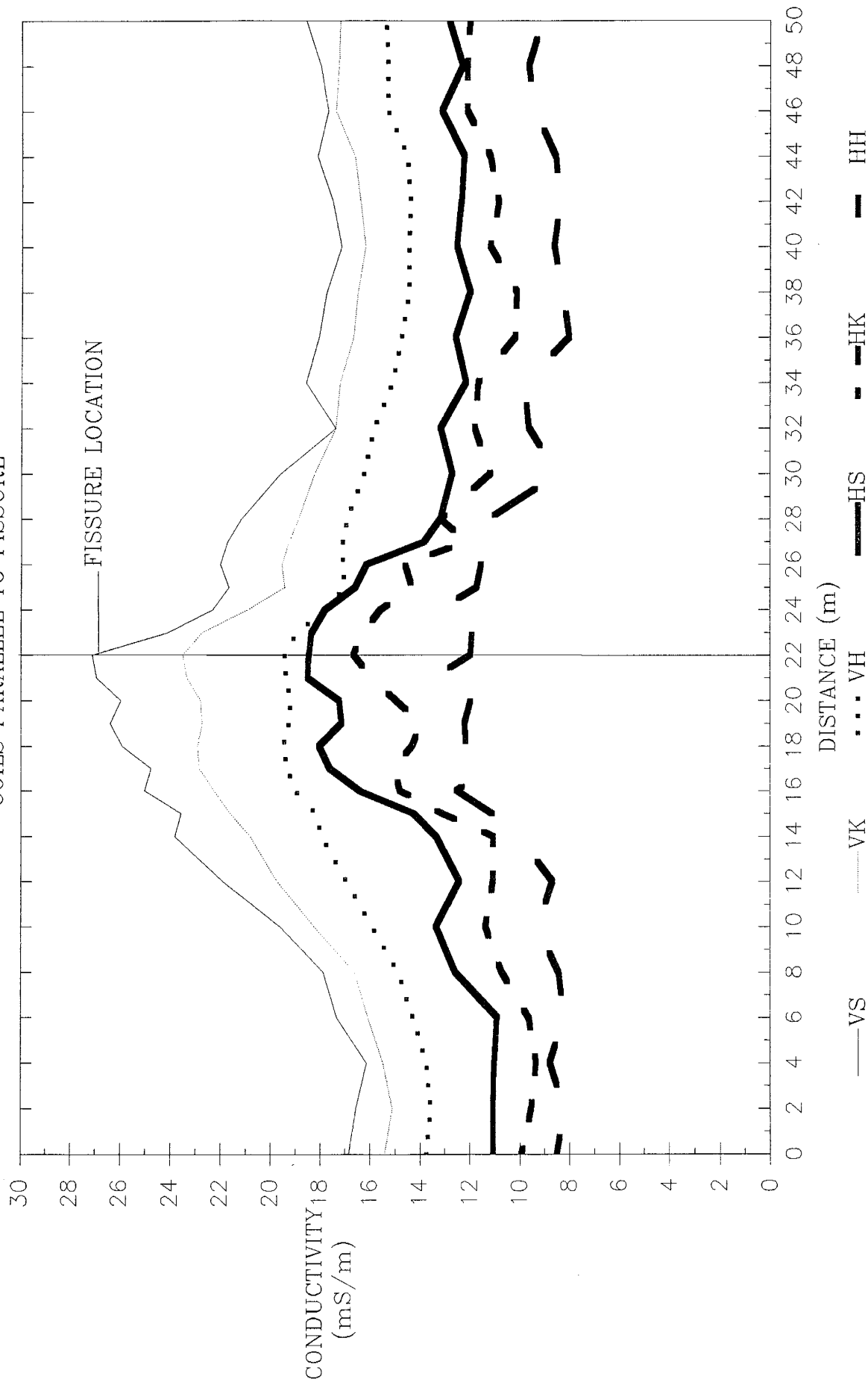


Figure 8. Conductivity vs distance measured with the EM-31 at three heights (surface, knee, and hip) at two configurations (vertical and horizontal modes)

EM38

DISTANCE VS CONDUCTIVITY OVER THE SAN MARCIAL FISSURE
TRANSECT C1-C2
COILS PARALLEL TO FISSURE

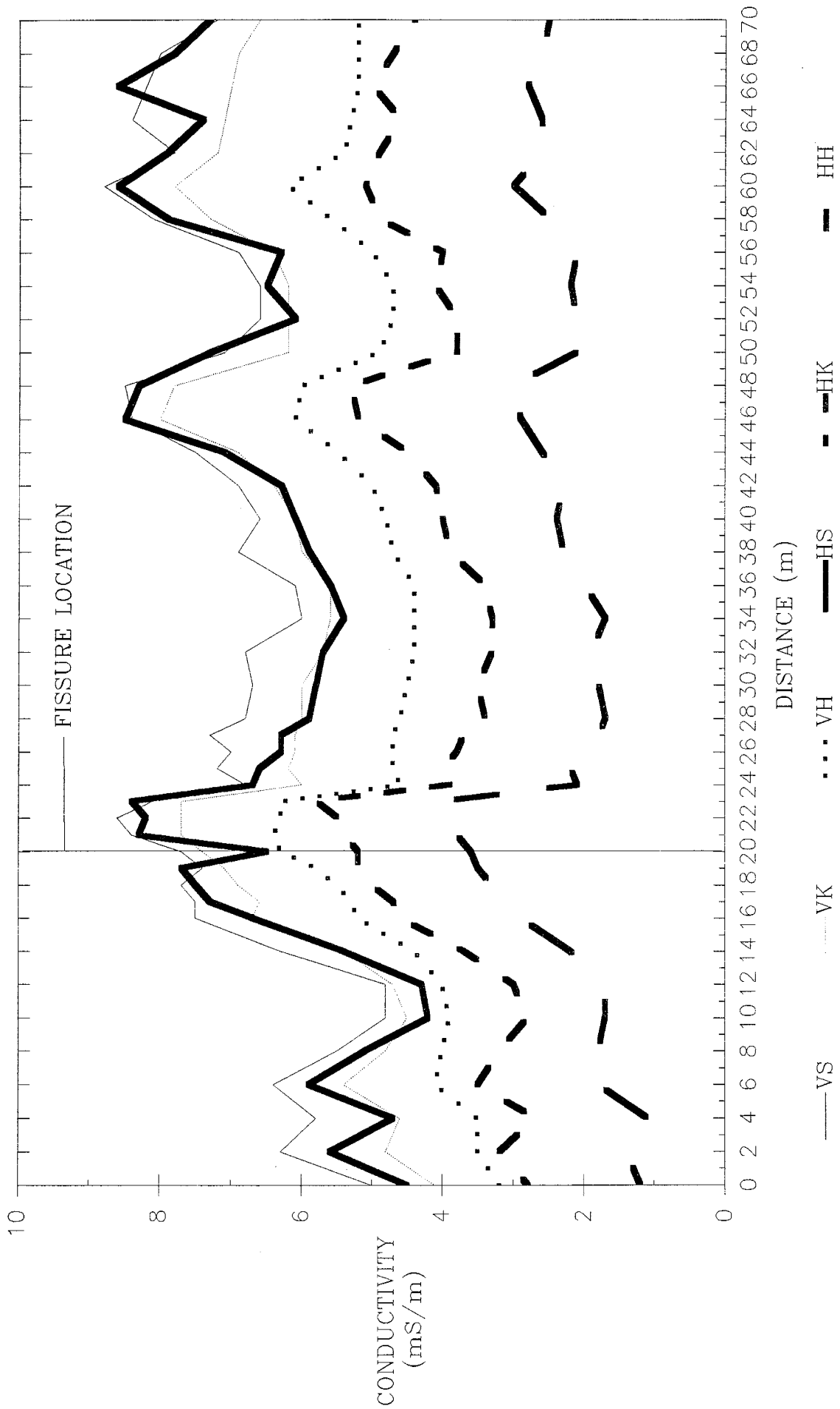


Figure 9. Conductivity vs distance measured with the EM-38 at three heights (surface, knee, and hip) at two configurations (vertical and horizontal modes)

EM31
 DISTANCE VS CONDUCTIVITY OVER THE SAN MARCIAL FISSURE
 TRANSECT C1-C2
 COILS PARALLEL TO FISSURE

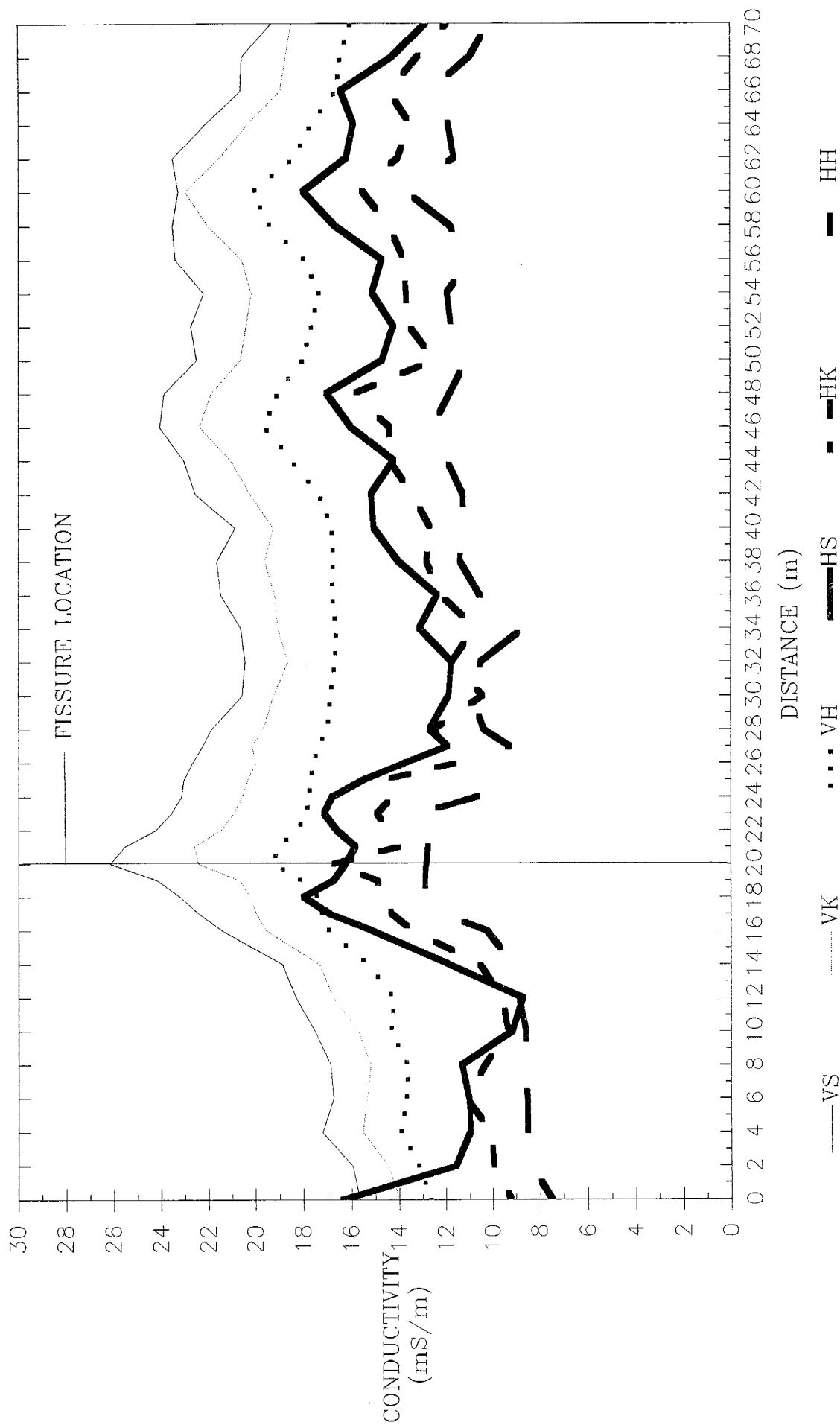


Figure 10. Conductivity vs distance measured with the EM-31 at three heights (surface, knee, and hip) at two configurations (vertical and horizontal modes)

EM38
 DISTANCE VS CONDUCTIVITY OVER THE SAN MARCIAL FISSURE
 TRANSECT D1-D2
 COILS PARALLEL TO FISSURE

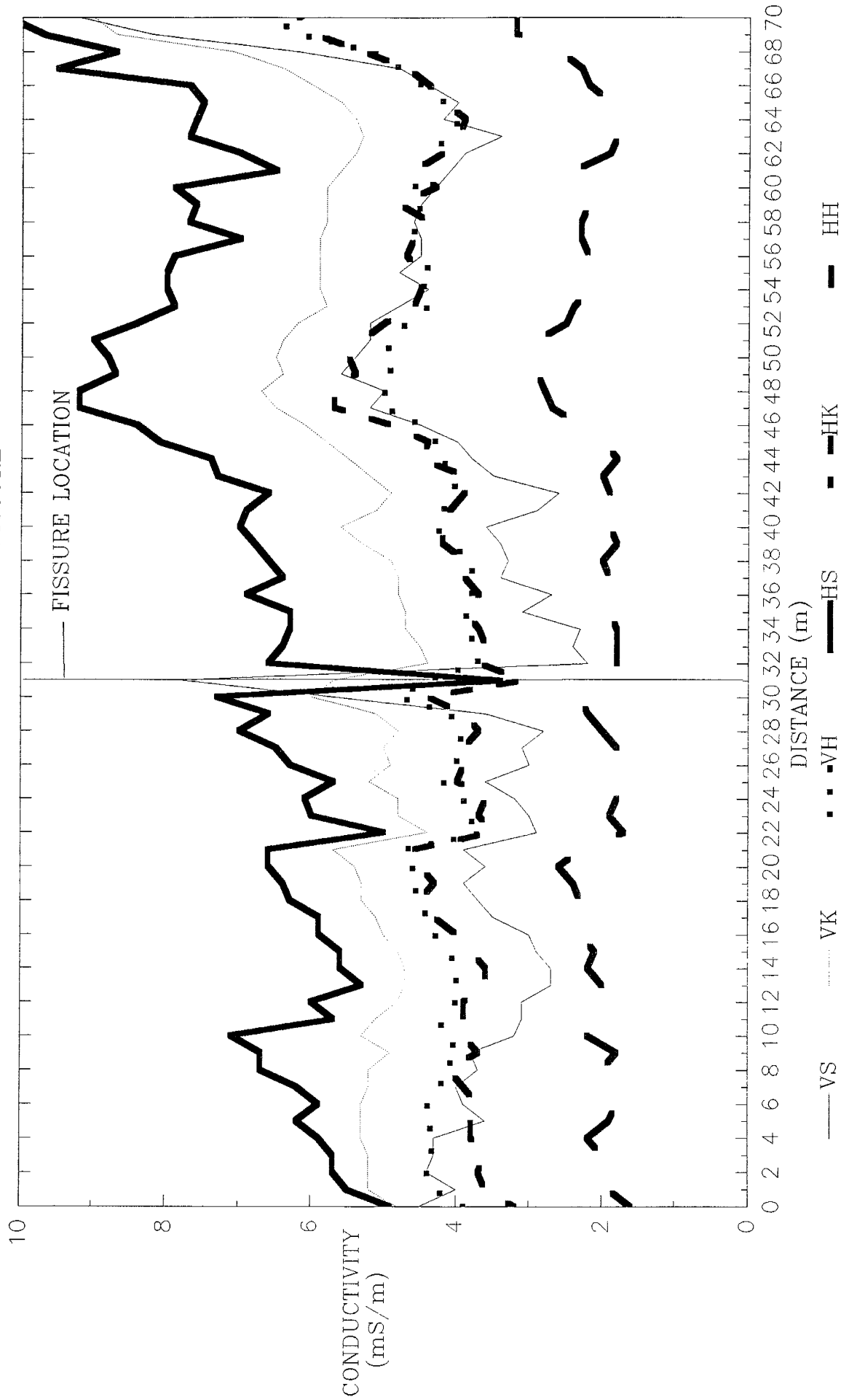


Figure 11. Conductivity vs distance measured with the EM-38 at three heights (surface, knee, and hip) at two configurations (vertical and horizontal modes)

EM31
 DISTANCE VS CONDUCTIVITY OVER THE SAN MARCIAL FISSURE
 TRANSECT D1-D2
 COILS PARALLEL TO FISSURE

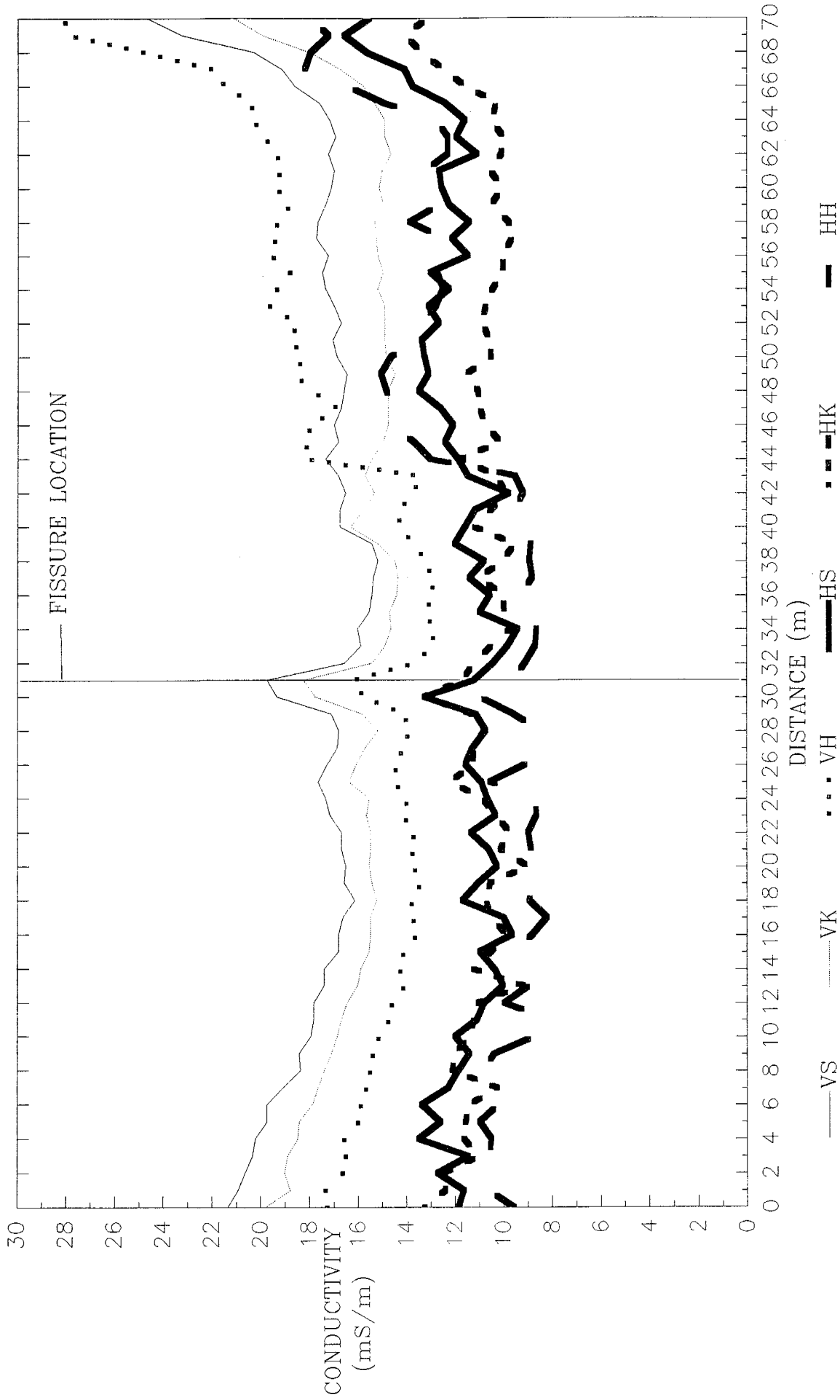


Figure 12. Conductivity vs distance measured with the EM-31 at three heights (surface, knee, and hip) at two configurations (vertical and horizontal modes)

EM38
 DISTANCE VS CONDUCTIVITY OVER THE SAN MARCIAL FISSURE
 TRANSECT E1-E2
 COILS PARALLEL TO FISSURE

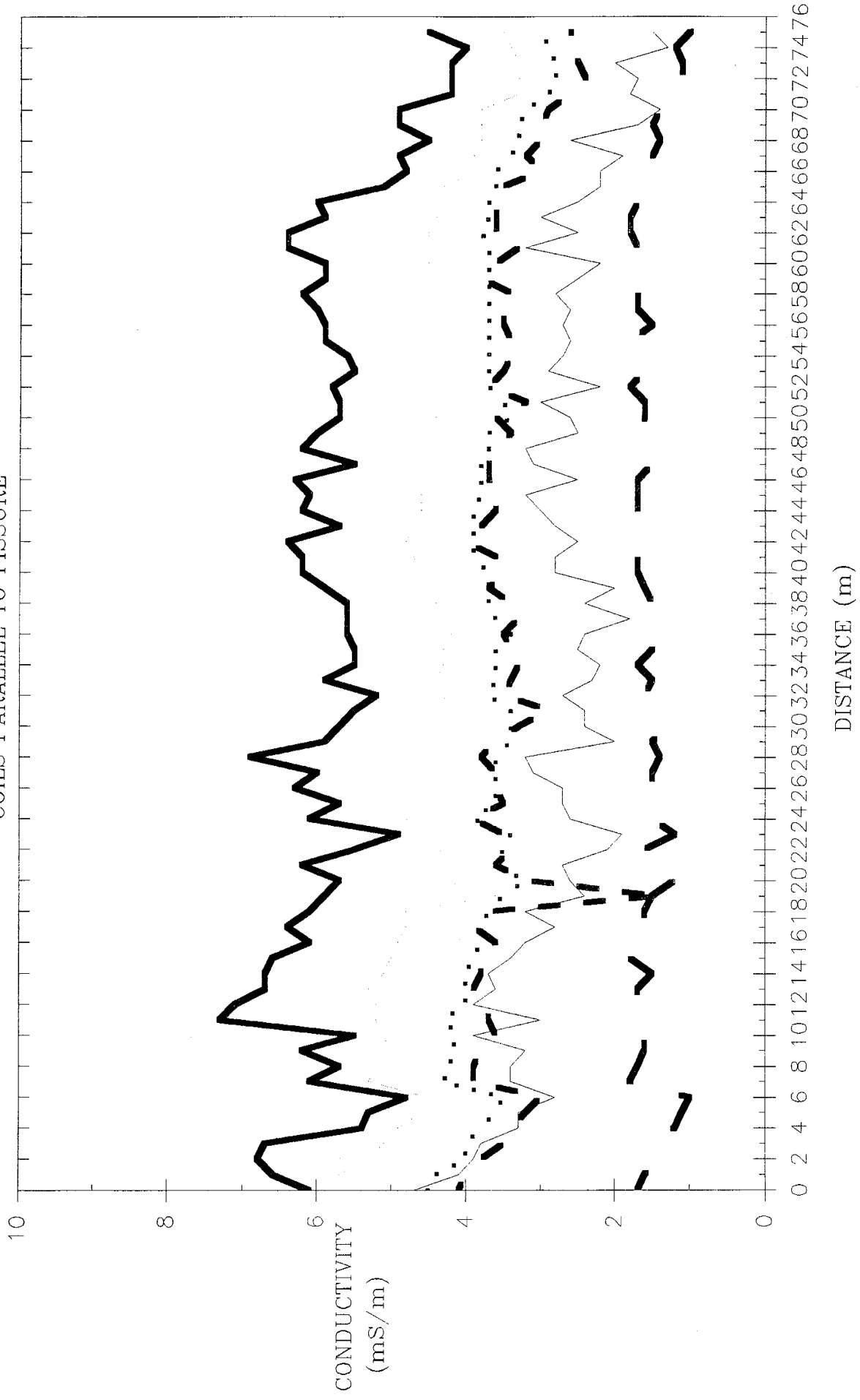


Figure 13. Conductivity vs distance measured with the EM-38 at three heights (surface, knee, and hip) at two configurations (vertical and horizontal modes)

EM31
 DISTANCE VS CONDUCTIVITY OVER THE SAN MARCIAL FISSURE
 TRANSECT E1-E2
 COILS PARALLEL TO FISSURE

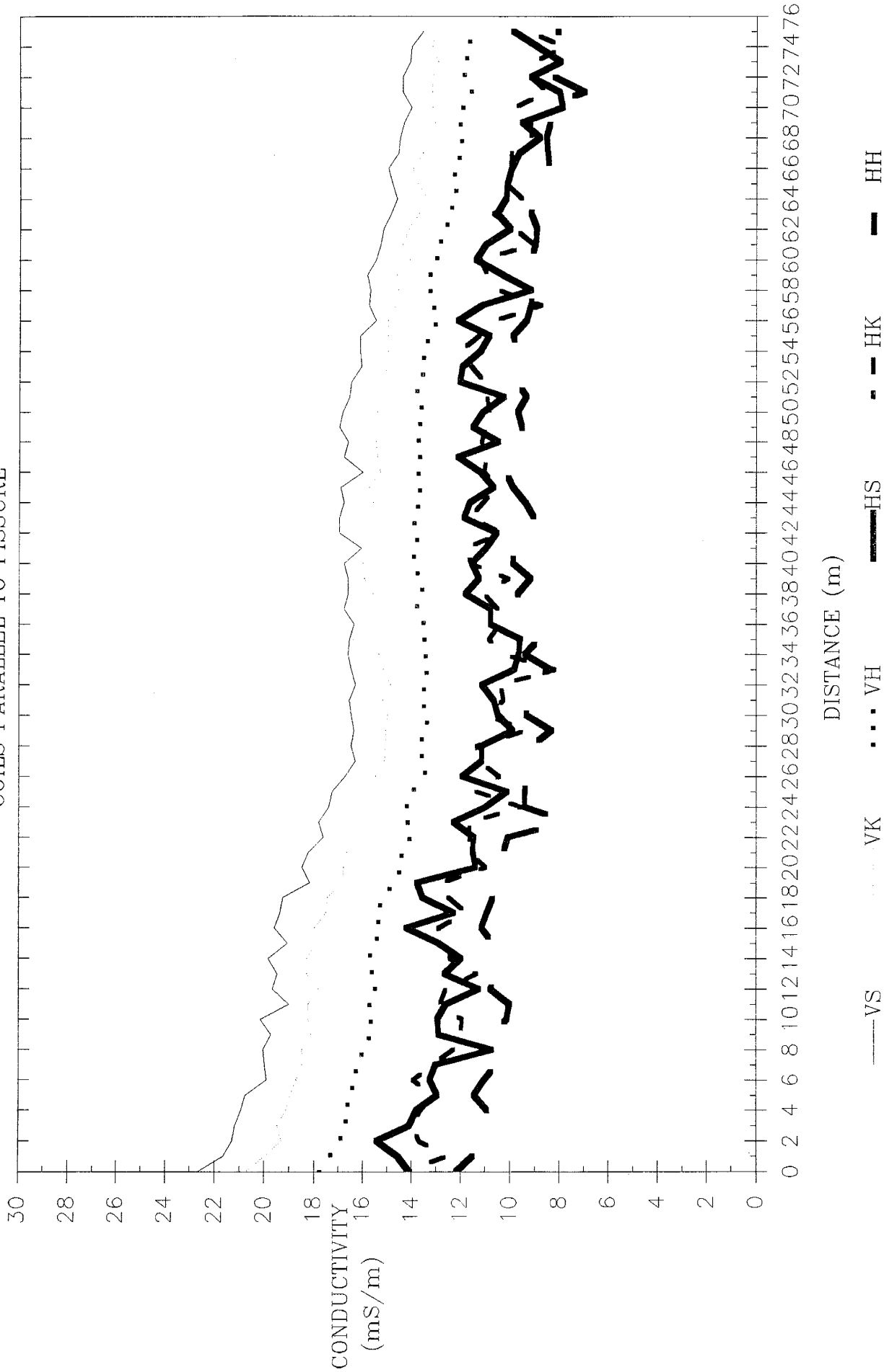


Figure 14. Conductivity vs distance measured with the EM-31 at three heights (surface, knee, and hip) at two configurations (vertical and horizontal modes)

EM38

DISTANCE VS CONDUCTIVITY OVER THE SAN MARCIAL FISSURE

TRANSECT F1-F2

COILS PARALLEL TO FISSURE

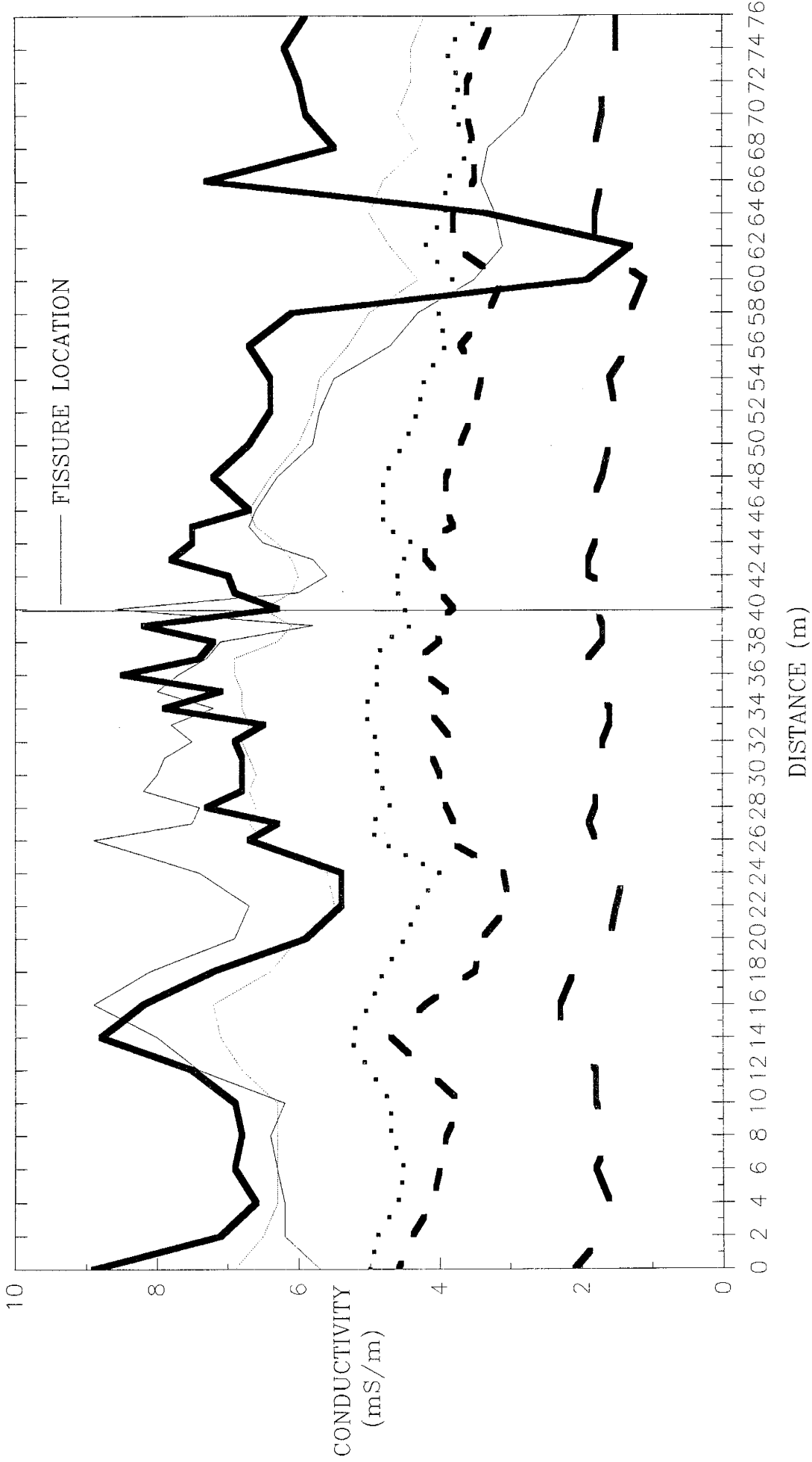


Figure 15. Conductivity vs distance measured with the EM-38 at three heights (surface, knee, and hip) at two configurations (vertical and horizontal modes)

EM31

DISTANCE VS CONDUCTIVITY OVER THE SAN MARCIAL FISSURE

TRANSECT F1-F2

COILS PARALLEL TO FISSURE

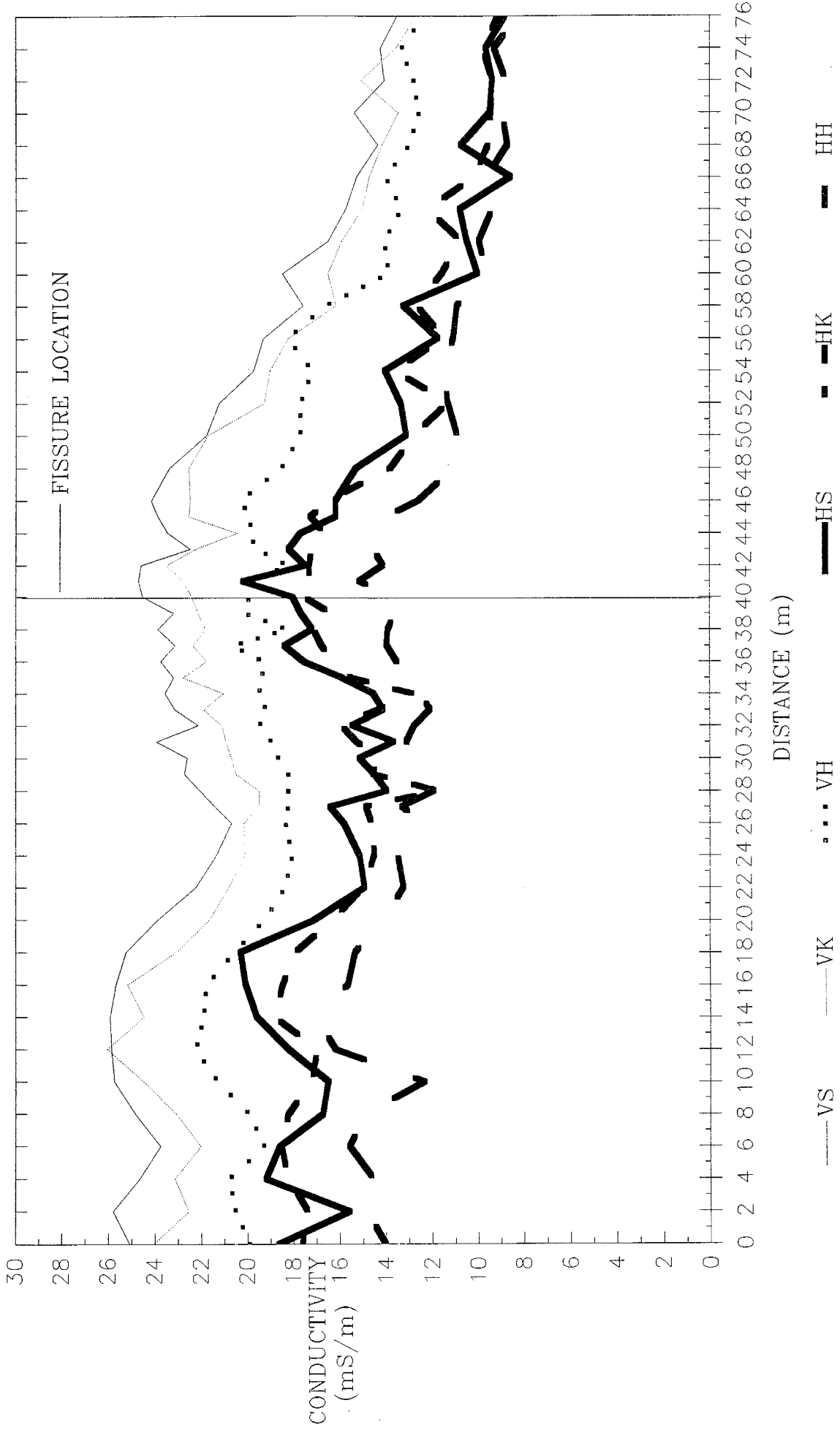


Figure 16. Conductivity vs distance measured with the EM-31 at three heights (surface, knee, and hip) at two configurations (vertical and horizontal modes)

EM38
 DISTANCE VS CONDUCTIVITY OVER THE SAN MARCIAL FISSURE
 TRANSECT G1-G2
 COILS PARALLEL TO FISSURE

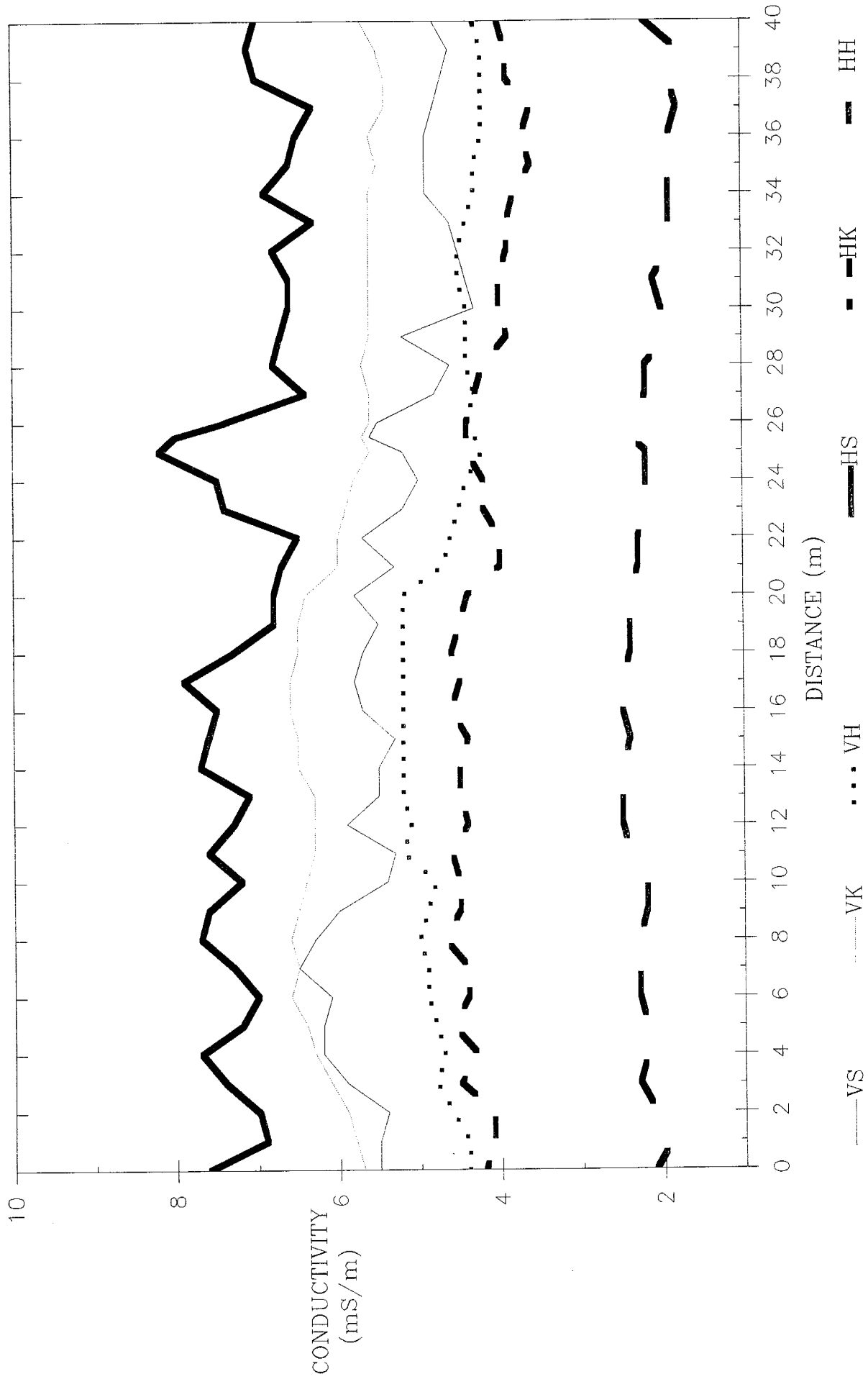


Figure 17. Conductivity vs distance measured with the EM-38 at three heights (surface, knee, and hip) at two configurations (vertical and horizontal modes)

EM31
 DISTANCE VS CONDUCTIVITY OVER THE SAN MARCIAL FISSURE
 TRANSECT G1-G2
 COILS PARALLEL TO FISSURE

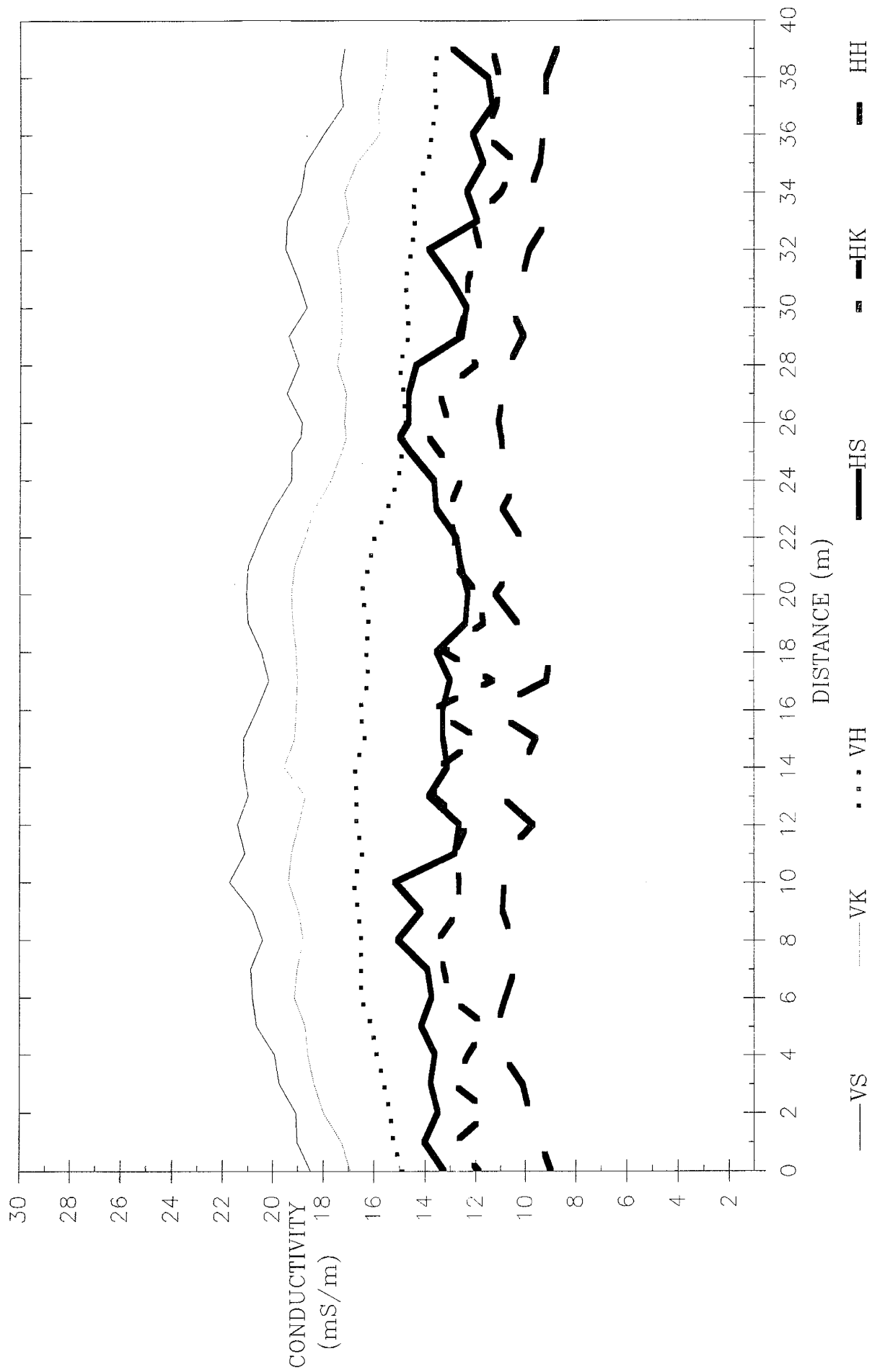


Figure 18. Conductivity vs distance measured with the EM-31 at three heights (surface, knee, and hip) at two configurations (vertical and horizontal modes)

EM38
 DISTANCE VS CONDUCTIVITY OVER SAN MARCIAL FISSURE
 TRANSECT A1-A2
 COILS PERPENDICULAR TO FISSURE

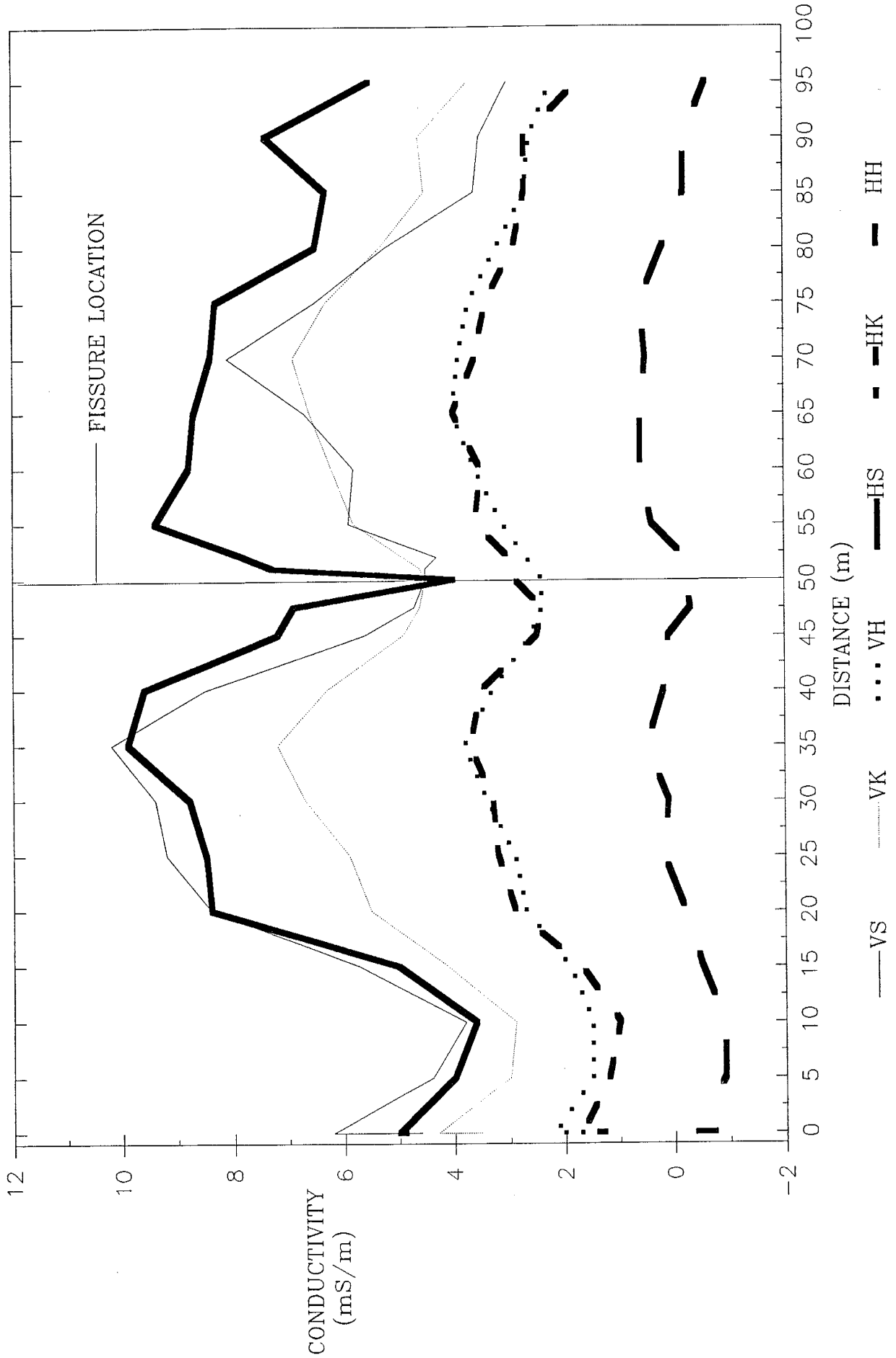


Figure 19. Conductivity vs distance measured with the EM-38 at three heights (surface, knee, and hip) at two configurations (vertical and horizontal modes)

EM31
 DISTANCE VS CONDUCTIVITY OVER SAN MARCIAL FISSURE
 TRANSECT A1-A2
 COILS PERPENDICULAR TO FISSURE

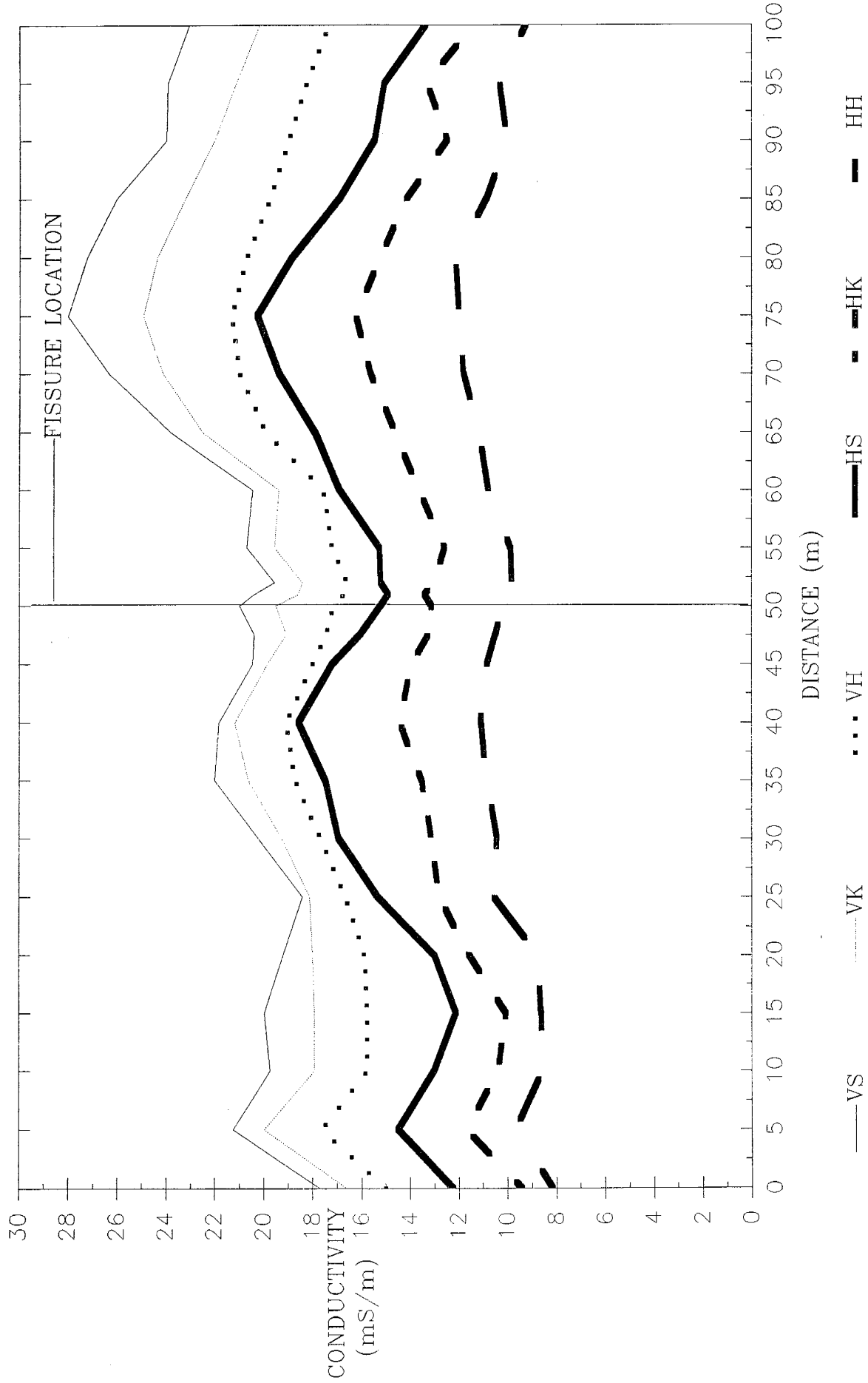


Figure 20. Conductivity vs distance measured with the EM-31 at three heights (surface, knee, and hip) at two configurations (horizontal and vertical modes)

EM38
 DISTANCE VS CONDUCTIVITY OVER THE SAN MARCIAL FISSURE
 TRANSECT B1-B2
 COILS PERPENDICULAR TO FISSURE

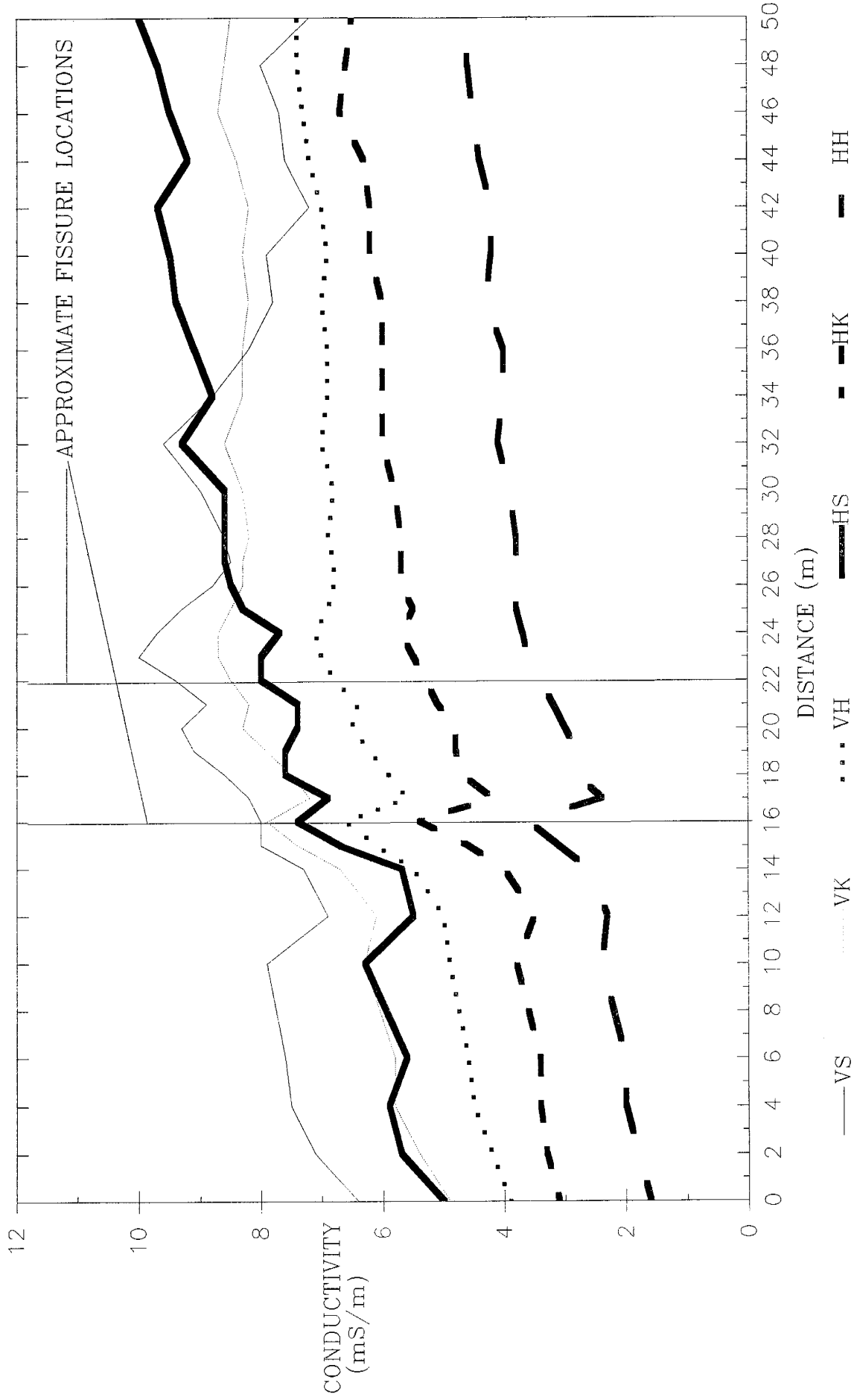


Figure 21. Conductivity vs distance measured with the EM-38 at three heights (surface, knee, and hip) at two configurations (vertical and horizontal modes)

EM31
 DISTANCE VS CONDUCTIVITY OVER THE SAN MARCIAL FISSURE
 TRANSECT B1-B2
 COILS PERPENDICULAR TO FISSURE

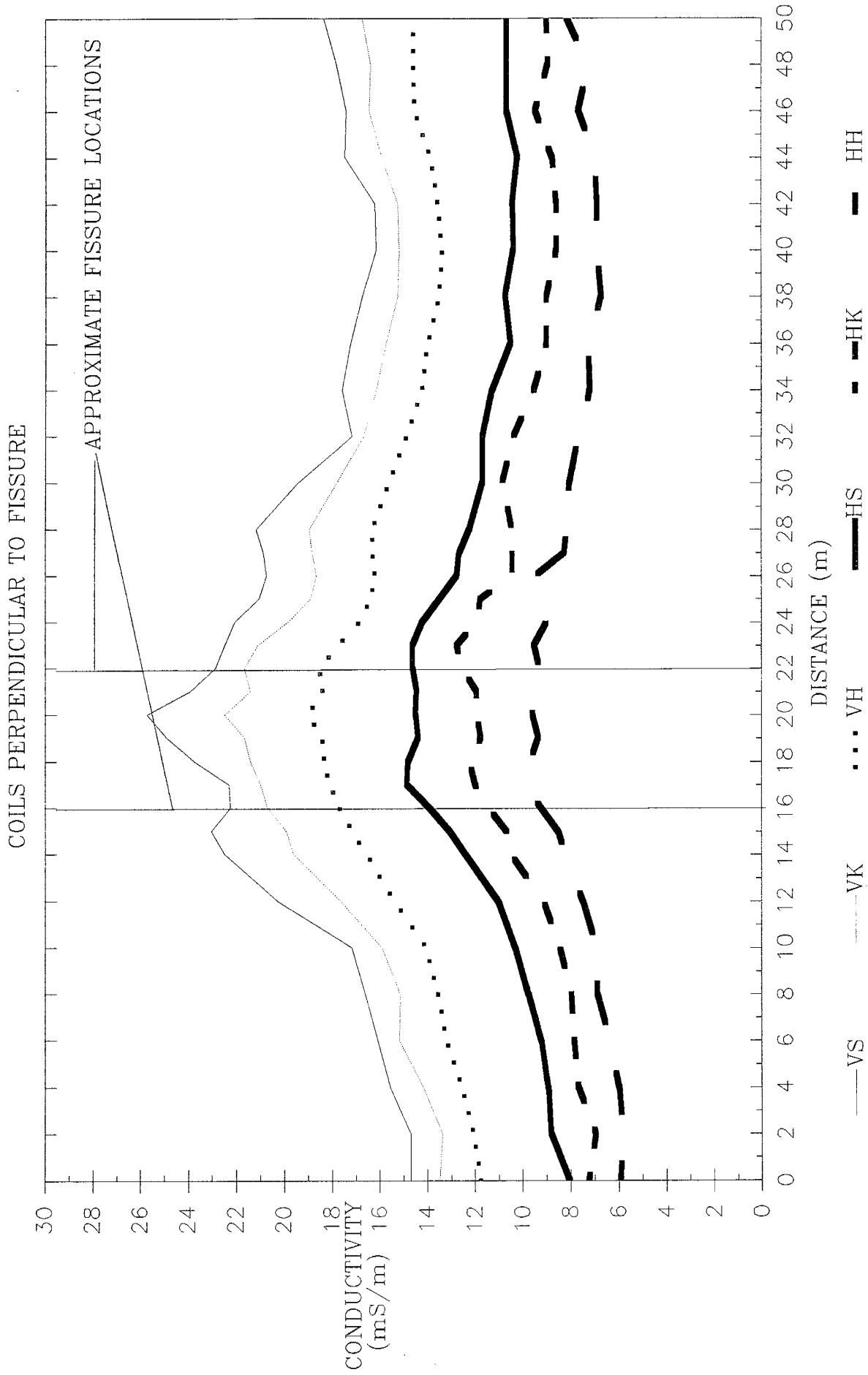


Figure 22. Conductivity vs distance measured with the EM-31 at three heights (surface, knee, and hip) at two configurations (vertical and horizontal modes)

EM38

DISTANCE VS CONDUCTIVITY OVER THE SAN MARCIAL FISSURE
TRANSECT C1-C2

COILS PERPENDICULAR TO FISSURE

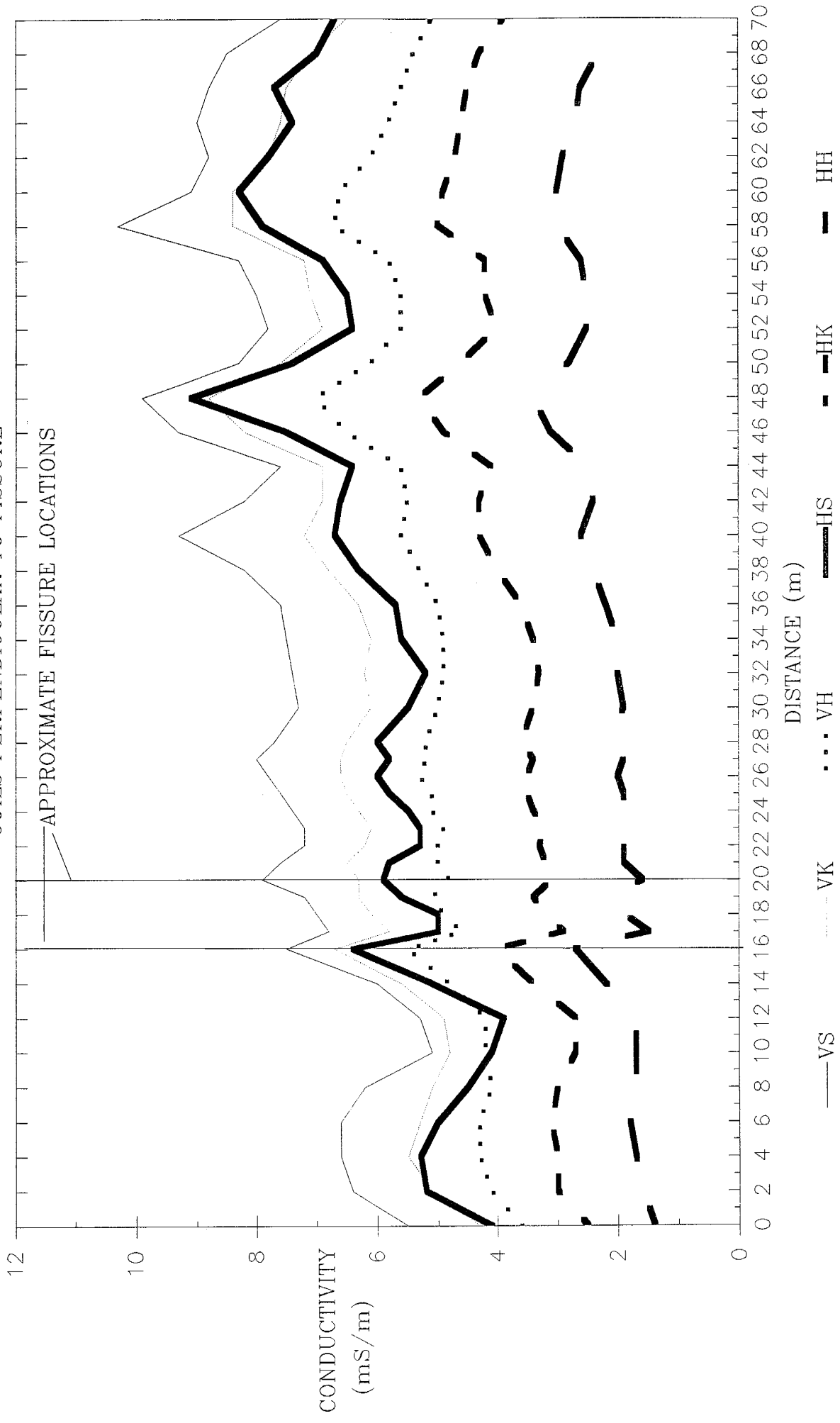


Figure 23. Conductivity vs distance measured with the EM-38 at three heights (surface, knee, and hip) at two configurations (vertical and horizontal modes)

EM31

DISTANCE VS CONDUCTIVITY OVER THE SAN MARCIAL FISSURE
TRANSECT C1--C2

COILS PERPENDICULAR TO FISSURE

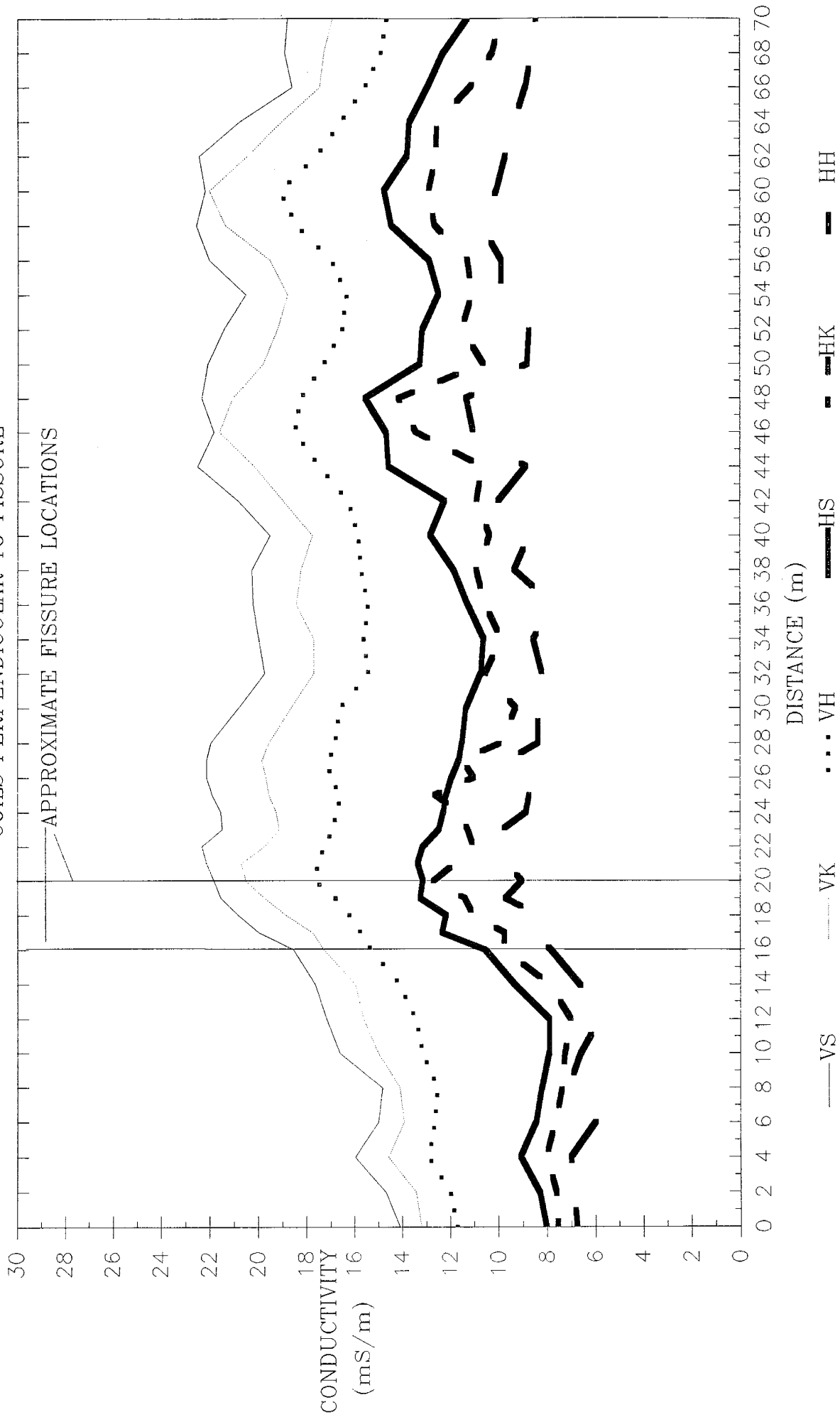


Figure 24. Conductivity vs distance measured with the EM-31 at three heights (surface, knee, and hip) at two configurations (vertical and horizontal modes)

EM38
 DISTANCE VS CONDUCTIVITY OVER THE SAN MARCIAL FISSURE
 TRANSECT D1-D2
 COILS PERPENDICULAR TO FISSURE

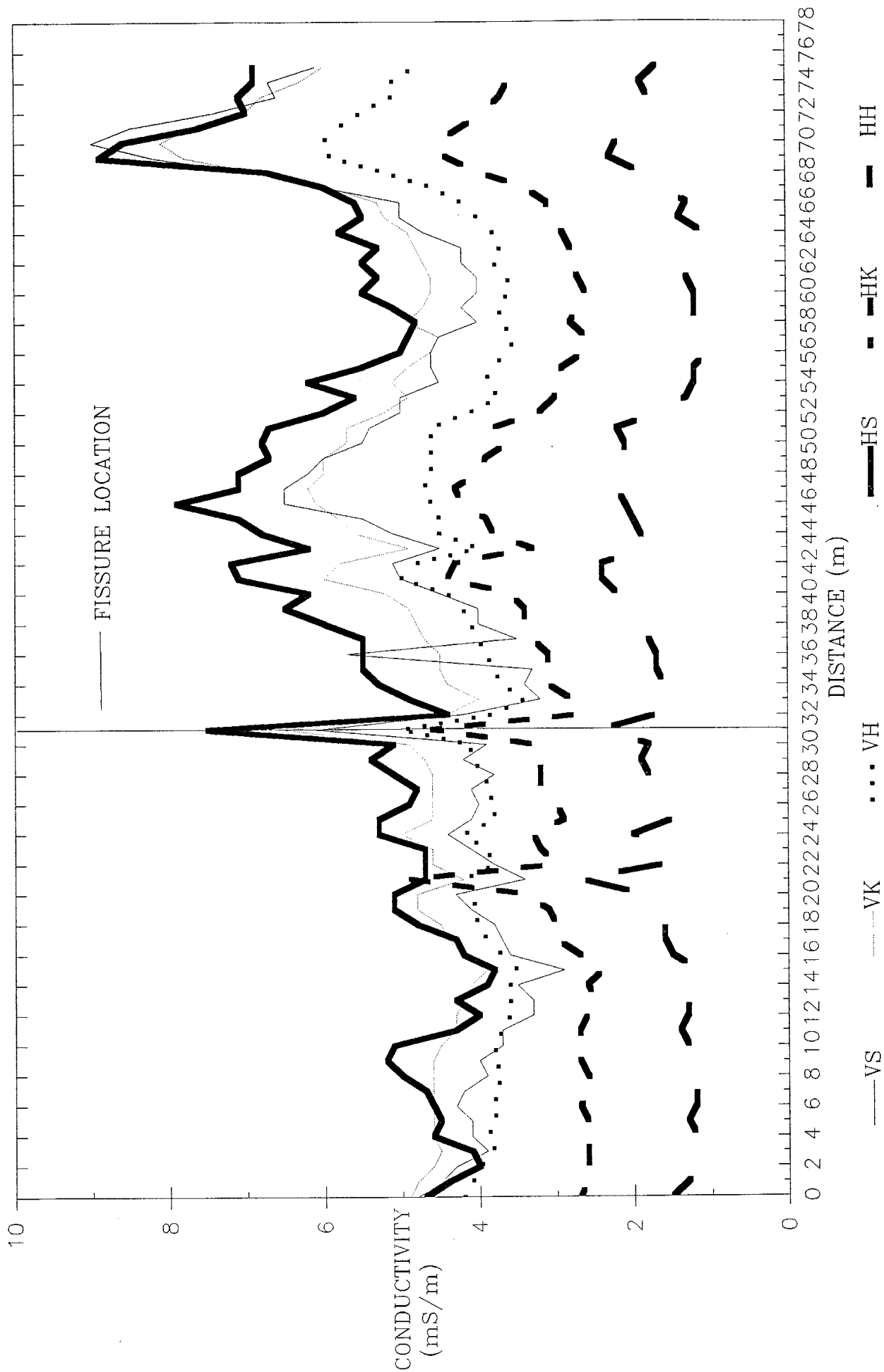


Figure 25. Conductivity vs distance measured with the EM-38 at three heights (surface, knee, and hip) at two configurations (vertical and horizontal modes)

EM31
 DISTANCE VS CONDUCTIVITY OVER THE SAN MARCIAL FISSURE
 TRANSECT D1--D2
 COILS PERPENDICULAR TO FISSURE

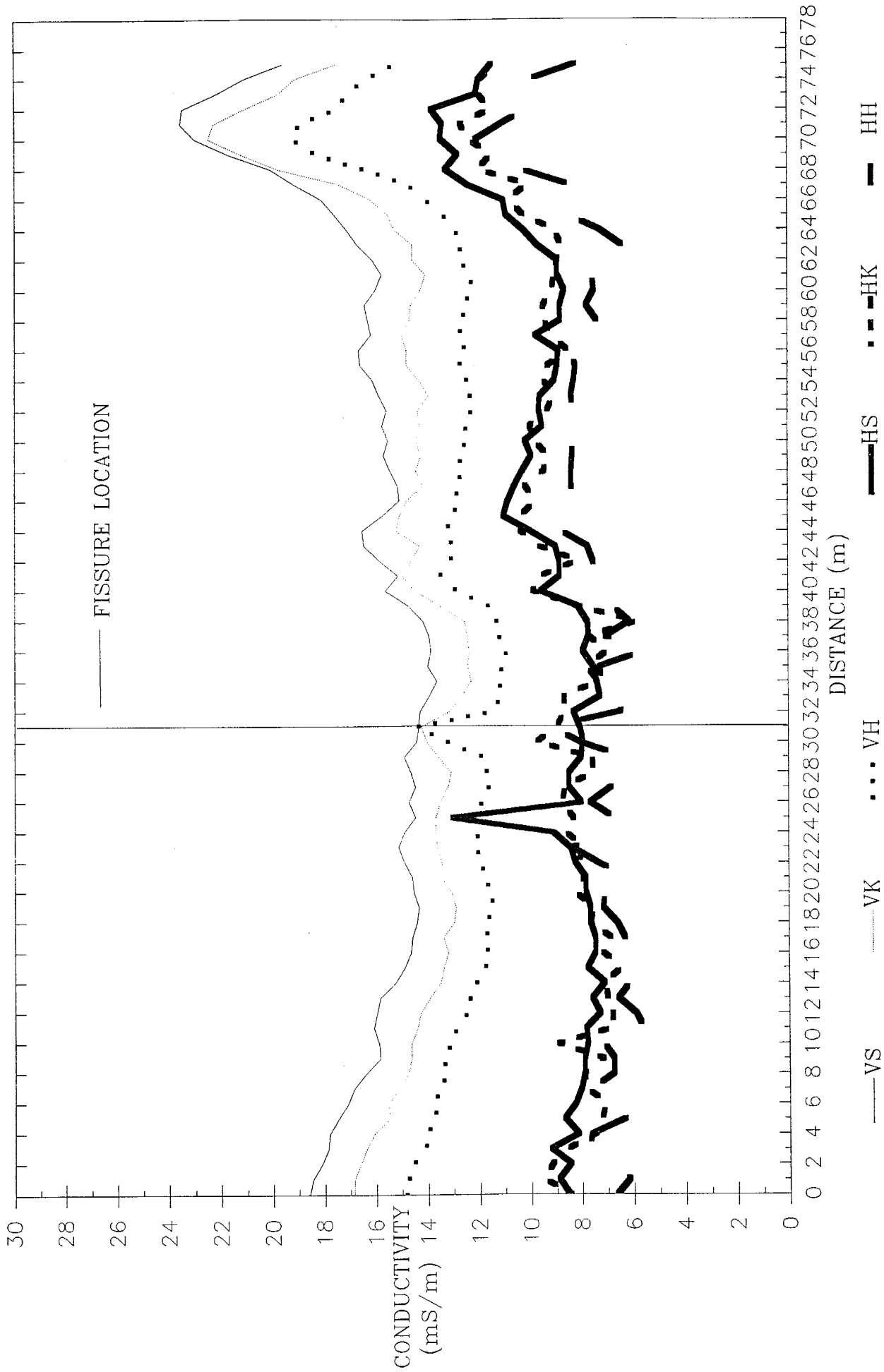


Figure 26. Conductivity vs distance measured with the EM-31 at three heights (surface, knee, and hip) at two configurations (vertical and horizontal modes)

EM38

DISTANCE VS CONDUCTIVITY OVER THE SAN MARCIAL FISSURE
TRANSECT E1-E2
COILS PERPENDICULAR TO FISSURE

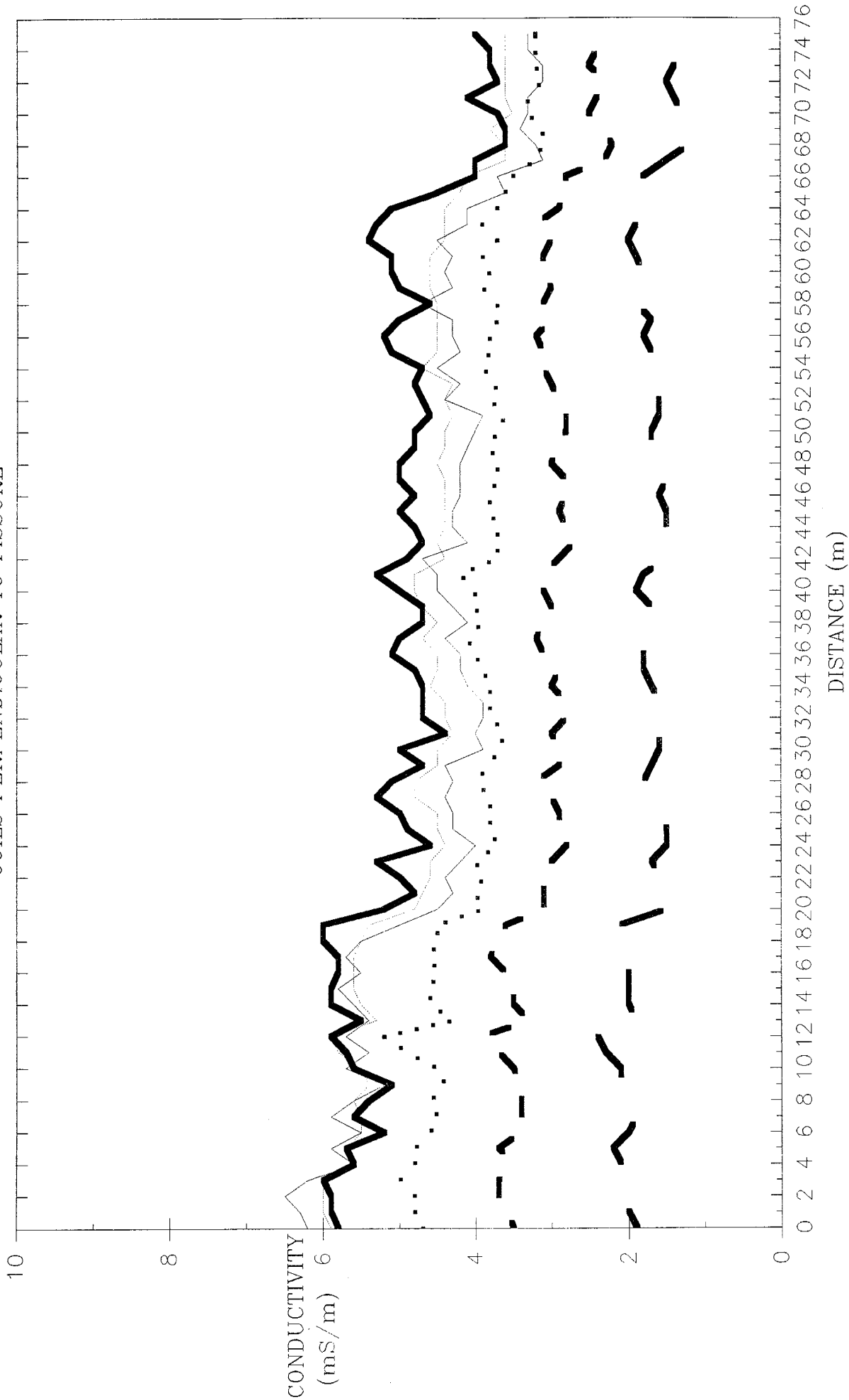


Figure 27. Conductivity vs distance measured with the EM-38 at three heights (surface, knee, and hip) at two configurations (vertical and horizontal modes)

EM31
 DISTANCE VS CONDUCTIVITY OVER THE SAN MARCIAL FISSURE
 TRANSECT E1-E2
 COILS PERPENDICULAR TO FISSURE

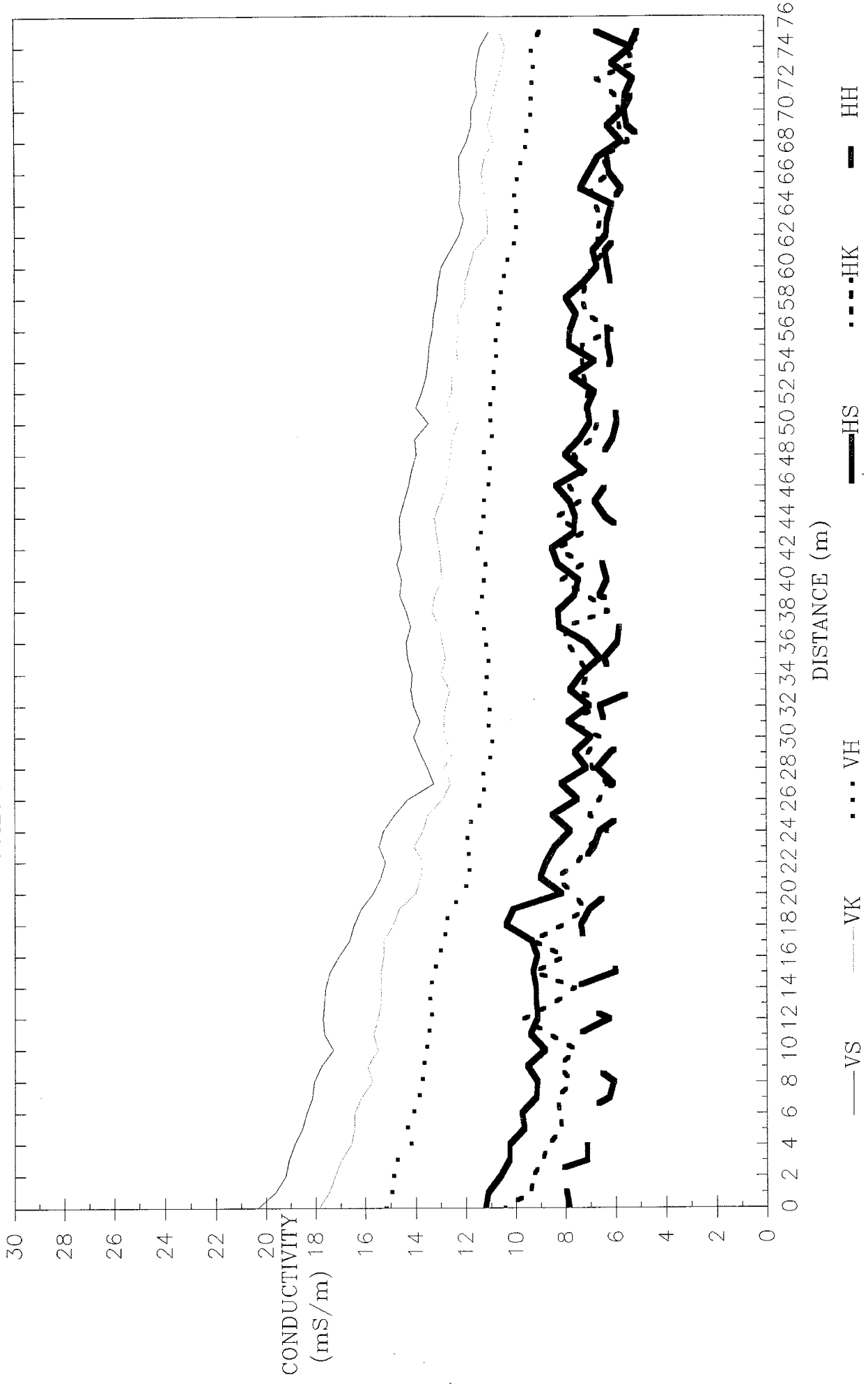


Figure 28. Conductivity vs distance measured with the EM-31 at three heights (surface, knee, and hip) at two configurations (vertical and horizontal modes)

EM38
 DISTANCE VS CONDUCTIVITY OVER SAN MARCIAL FISSURE
 TRANSECT F1-F2
 COILS PERPENDICULAR TO FISSURE

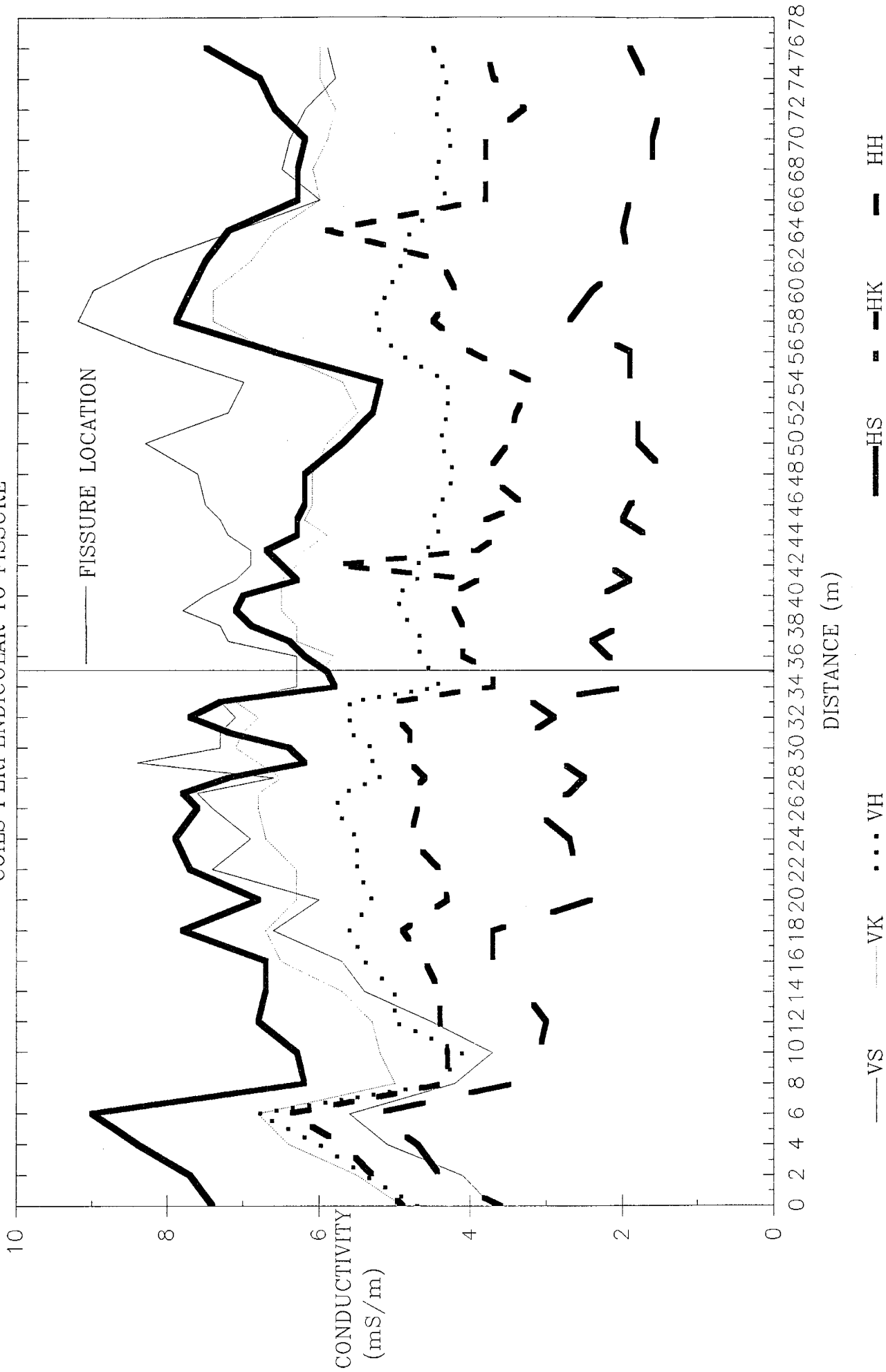


Figure 29. Conductivity vs distance measured with the EM-38 at three heights (surface, knee, and hip) at two configurations (vertical and horizontal modes)

EM31
 DISTANCE VS CONDUCTIVITY OVER SAN MARCIAL FISSURE
 TRANSECT F1-F2
 COILS PERPENDICULAR TO FISSURE

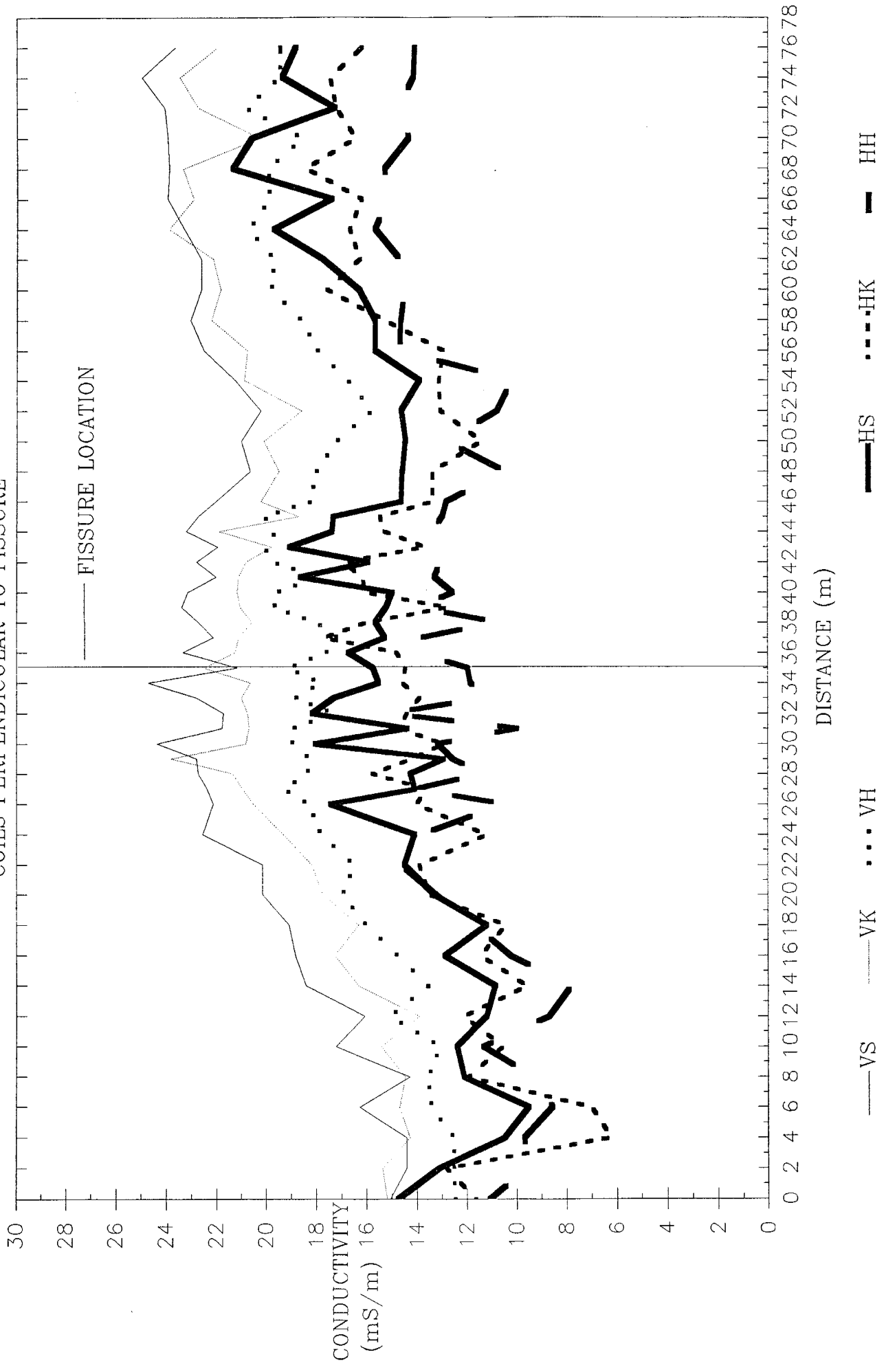


Figure 30. Conductivity vs distance measured with the EM-31 at three heights (surface, knee, and hip) at two configurations (vertical and horizontal modes)

EM38

DISTANCE VS CONDUCTIVITY OVER THE SAN MARCIAL FISSURE
TRANSECT G1-G2
COILS PERPENDICULAR TO FISSURE

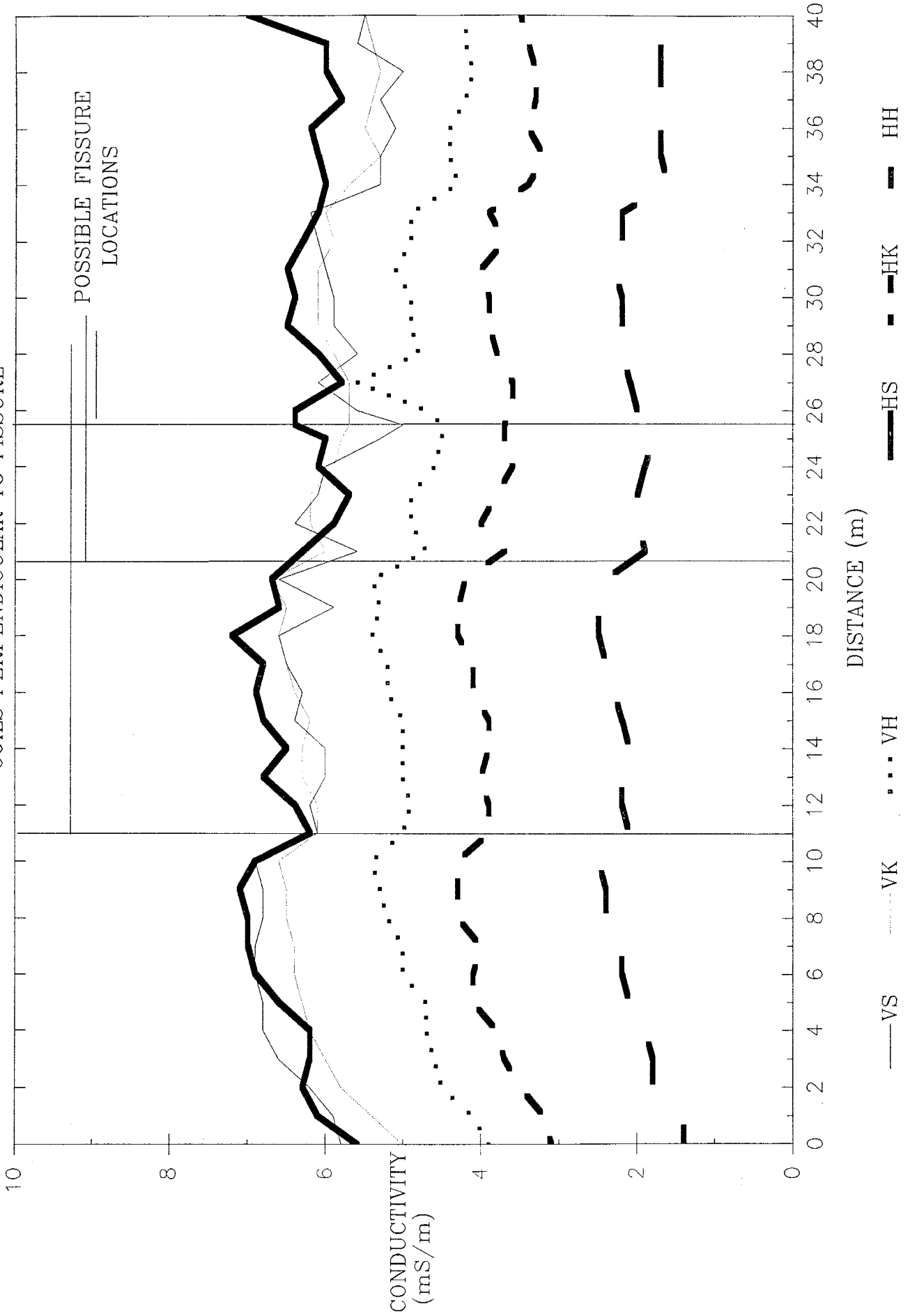


Figure 31. Conductivity vs distance measured with the EM-38 at three heights (surface, knee, and hip) at two configurations (vertical and horizontal modes)

EM31
 DISTANCE VS CONDUCTIVITY OVER THE SAN MARCIAL FISSURE
 TRANSECT G1-G2
 COILS PERPENDICULAR TO FISSURE

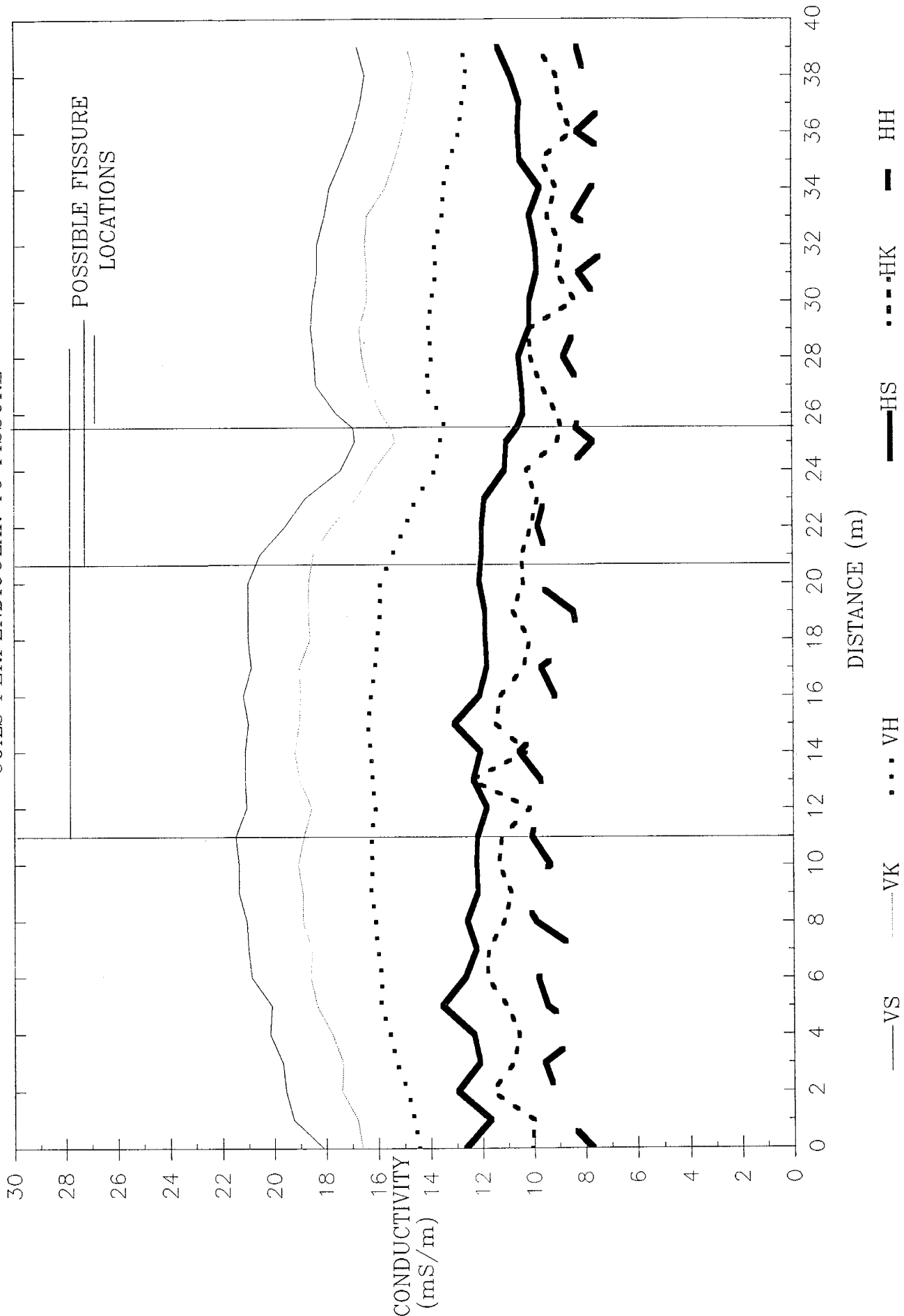
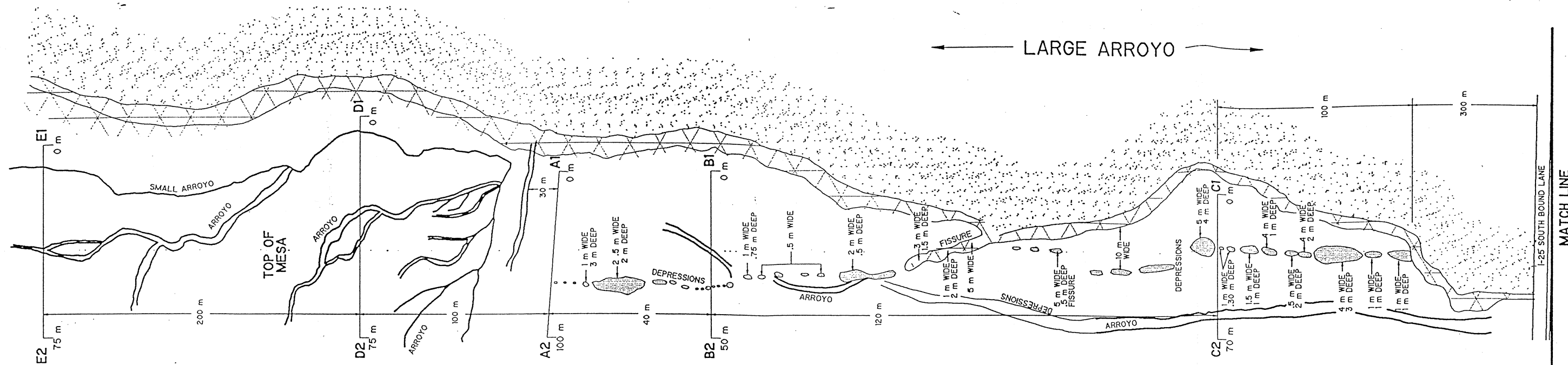
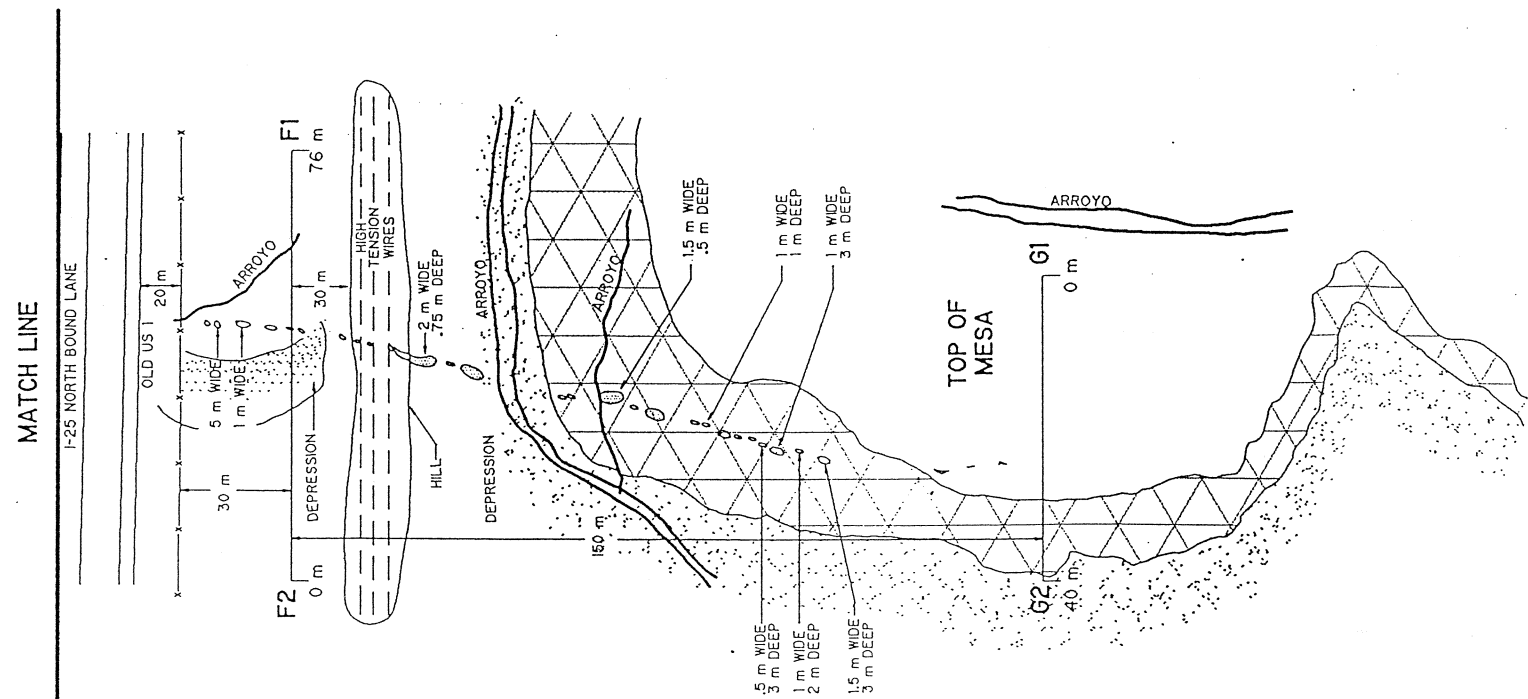


Figure 32. Conductivity vs distance measured with the EM-31 at three heights (surface, knee, and hip) at two configurations (vertical and horizontal modes)



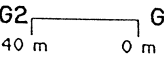

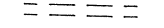
WEST OF I-25



EAST OF I-25



LEGEND:

-  FISSURE LOCATION
-  SLOPE OF HILL
-  TRANSECTS WHERE EM MEASUREMENTS WERE TAKEN
-  BARB WIRE FENCE
-  HIGH TENSION WIRES

SAN MARCIAL FISSURE
SITE LOCATION MAP